The Dissertation Committee for Jung-Hwan Kwon Certifies that this is the approved version of the following dissertation:

Bioavailability of Endocrine Disrupting Chemicals (EDCs): Liposome-water Partitioning and Lipid Membrane Permeation

Committee:

Howard M. Liljestrand, Co-Supervisor

Lynn E. Katz, Co-Supervisor

Kerry A. Kinney

Mary Jo Kirisits

Keith P. Johnston

Bioavailability of Endocrine Disrupting Chemicals (EDCs): Liposome-water Partitioning and Lipid Membrane Permeation

by

Jung-Hwan Kwon, B.S.; M.S.

Dissertation

Presented to the Faculty of the Graduate School of

The University of Texas at Austin

in Partial Fulfillment

of the Requirements

for the Degree of

Doctor of Philosophy

The University of Texas at Austin

August, 2006

Dedication

To my parents and parent-in-laws

Acknowledgements

First, I would like to thank my co-advisors, Dr. Howard Liljestrand and Dr. Lynn Katz for their inspiration, advice and patience throughout four years of my doctoral study. Without their support, this dissertation would not come out. Furthermore, I could learn from them what a good research advisor should be. I also thank my other committee members, Dr. Kerry Kinney, Dr. Mary Jo Kirisits, and Dr. Keith Johnston. Their constructive suggestions and comments significantly improved the quality of this dissertation. I also appreciate the help by Dr. Hiroshi Yamamoto for shipping me his equilibrium dialysis reactors and advising laboratory details and Dr. Beate Escher for sharing valuable discussion about the scientific and regulatory merits of the research and offering me a postdoc position in her institution.

Members of Dr. Katz research group, Dr. Chen, Adriano, Julian, Mara, Shannon, Andrew, and Ram, were always helpful in many ways during my experimental works. Wayne Fontenot, Charles Prego and Jianling Wang helped me building custom-made lab equipments and using analytical instruments.

I greatly thank my friends and neighbors, Jae-Hak and Kyung-Hwa, Takkan and Kyoko, Cheol-Kyu and Yeo-Jung, and Soondong for their kindness and friendship during our stay in Austin. Finally, I thank my wife Heajin and my son Joon-Young for their support, sacrifice, and hope we shared.

Bioavailability of Endocrine Disrupting Chemicals (EDCs): Liposome-water Partitioning and Lipid Membrane Permeation

Publication No._____

Jung-Hwan Kwon, Ph.D.

The University of Texas at Austin, 2006

Co-Supervisors: Howard M. Liljestrand, Lynn E. Katz

The bioavailability of endocrine disrupting chemicals (EDCs) is a function of a number of parameters including the ability of the chemical to partition into organic tissue and reach receptor sites within an organism. In this dissertation, equilibrium partition coefficients between water and lipid membrane vesicles and artificial lipid membrane permeability were investigated for evaluating bioavailability of aqueous pollutants. Structurally diverse endocrine disrupting chemicals were chosen as model compounds for partitioning experiments and simple hydrophobic organic chemicals were used for the evaluation of a parallel artificial membrane device developed to mimic bioconcentration rates in fish.

Hydrophobic interactions represented by octanol/water partition coefficients (K_{OW}s) were not appropriate for estimating lipid membrane/water partition coefficients (K_{lipw}s) for the selected EDCs having a relatively large molar liquid volume (MLV) and containing polar functional groups. Correlations that include MLV and polar surface area (PSA) reduce the predicted value of log K_{lipw}, suggesting that lipid membranes are less

favorable than 1-octanol for a hydrophobic solute because of the changes in membrane fluidity and the amount of cholesterol in the lipid bilayers. These results suggested that K_{OW} alone has limited potential for estimating K_{lipw}, and MLV or PSA may be used as additional descriptors for developing quantitative structure-activity relationships (QSARs). The poor correlations between K_{OW} and K_{lipw} observed in this research may be due to the highly organized structure of lipid bilayers. Measured thermodynamic constants demonstrated that the entropy contribution becomes more dominant for more organized liposomes having saturated lipid tails. This implies that entropy-driven partitioning process makes K_{lipw} different from K_{OW} especially for more saturated lipid bilayer membranes.

In the parallel artificial membrane system developed, a membrane filter-supported lipid bilayer separates two aqueous phases that represent the external and internal aqueous environments of fish. The thickness of the aqueous mass transfer boundary layer was carefully adjusted to mimic bioconcentration rate parameters in small fish. For the selected twenty-three simple aromatic hydrocarbons, literature absorption/elimination rates fall within the range predicted from measured membrane permeabilities and elimination rates of the selected chemicals using a diffusion mass transfer model. A simple equilibrium binding model for EDCs to estrogen receptors was applied to potentially link the developed artificial membrane system to existing toxicity assays and to better utilize in vitro toxicity data.

Table of Contents

List of Tables

List of Figures

Chapter 1: Introduction

1.1. INTRODUCTION

The presence of endocrine disrupting chemicals (EDCs) in natural water has been of significant concern for decades. One of the major sources of EDCs to public waterways is effluent from municipal wastewater treatment plants (Birkett and Lester, 2003). Indeed, several studies have identified reproductive abnormalities in fish in waters that receive wastewater treatment plant discharges (Barnhoorn et al., 2004; Rodgers-Gray et al., 2001; Routledge et al., 1998). In spite of surging concern about the release of EDCs into aquatic environments, much still remains uncertain regarding the fate of EDCs and their adverse impacts on humans and ecosystems. To fill this gap, further evaluation is required for the fate of and risks associated with suspected EDCs as a function of concentration and background solution composition. Concentration dependent dose-response relationships should be developed considering both transport to receptor sites and toxicity.

It is generally acknowledged that uptake and release of xenobiotic organic pollutants are mainly transported by passive diffusion processes through a series of cellular membranes made of lipid bilayers. In addition, lipid bilayer membranes are major storage compartments in an organism in addition to the storage lipids not forming bilayers. Thus, it is important to know "how much" of a particular EDC will be concentrated in organisms and "how fast" it will permeate through biological barriers to reach target sites (Figure 1.1).

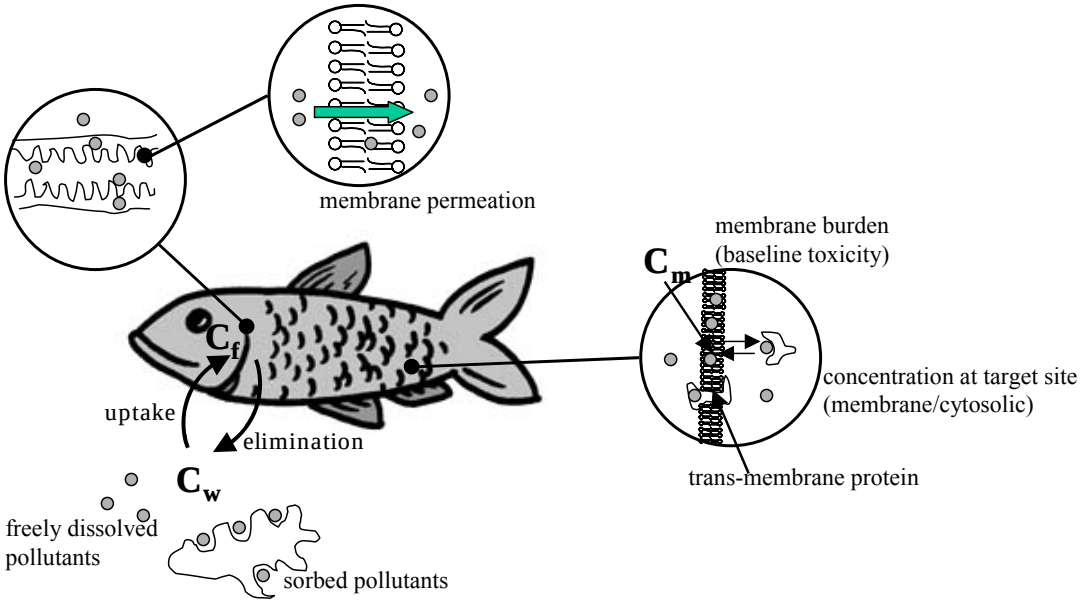

Figure 1.1: System description. Importance of partitioning and lipid membrane permeation.

Traditionally, bioconcentration and acute toxicity of xenobiotic chemicals have been evaluated using animal tests. However, simpler model systems have been used for screening purposes because animal tests are expensive and time consuming. For example, organic solvents, such as 1-octanol, have been widely used for evaluating equilibrium bioconcentration (Davies and Dobbs, 1984; Mackay, 1982; Neely et al., 1974; Oliver and Niimi, 1985; Veith et al., 1980) and several passive sampling devices have been used for evaluating bioconcentration kinetics and time-weighted exposure concentrations (Huckins, 1990, 1993; Södergren, 1987; Vrana et al., 2001). Although they have been successful for the evaluation of the environmental fate of certain persistent organic chemicals (e.g., PCBs and organochlorine pesticides), serious theoretical limitations have been proposed (Opperhuizen et al., 1988; van Wezel et al., 1996; Woodrow and Dorsey, 1997). More recently, systems more closely resembling actual biological membranes, adopting the lipid bilayer concept, have been studied to investigate equilibrium

partitioning (Escher and Schwarzenbach, 1996; Escher et al., 2000; Gobas et al., 1988; Liu et al., 2001; Smejtek et al., 1996; Vaes et al., 1997; van Wezel et al., 1996) and biological membrane permeation (Kansy et al., 1998; Sugano et al., 2003; Wohnsland and Faller, 2001; Zhu et al., 2002). Bioavailability of EDCs in aquatic organisms and potentially at target sites can be estimated from equilibrium partition coefficients between water and lipid membranes (K_{lipw}) and rate parameters of lipid membrane permeation. The primary focus of this study is to provide a theoretical basis for predicting K_{lipw} from known physico-chemical properties and to propose a better screening tool using an abiotic physical model that mimics passive uptake/elimination in fish.

1.2. RESEARCH HYPOTHESES

During the initial review of previous research conducted in this area, a number of questions evolved. Research conducted to answer these questions will improve predictions of equilibrium partition coefficients between water and lipid membranes and quantify uptake/elimination kinetics in abiotic lipid membrane systems. The questions are

(A) How can we relate a lipid membrane water partition coefficient (K_{lipw}) to the commonly used 1-octanol-water partition coefficient (K_{OW})?

Although K_{lipw} correlates well with K_{OW} for relatively small and structurally homogeneous chemicals (Gobas et al., 1988; Escher et al., 2000; Smejtek et al., 1996; Vaes et al., 1997; van Wezel et al., 1996), a recent study showed that K_{lipw} does not correlate well with K_{OW} for relatively big and structurally diverse endocrine disrupting chemicals (EDCs) (Yamamoto and Liljestrand, 2004). If molecular size and structural diversity are important contributors to partitioning, then these partition coefficients can

be better correlated by including additional parameters reflecting the effects of molecular size and structural diversity from a larger set of EDCs. If this hypothesis is valid, a theoretically based investigation is required to understand these phenomena and to ultimately develop a quantitative structure activity relationship. Therefore, a follow-up question is

(A-1) Is the discrepancy between K_{OW} and K_{lipw} due to the so-called "bilayer effects" including conformational changes of a solute, immobilization of a solute and perturbations of the lipid bilayer structure? If so, how is this effect incorporated into thermodynamically based predictions of partitioning?

The conventional approach to determine enthalpy and entropy change for a phase transfer reaction is to use the van't Hoff isochore (e.g., Opperhuizen et al., 1988; Whimly and White, 1993). Measuring K_{lipw} at different temperatures with different membrane compositions will reveal any significant dependence of K_{lipw} on the characteristics of synthetic lipid membrane vesicles. Moreover, these results may provide a theoretical basis for incorporating the effects of solute size on K_{lipw} and the bioconcentration factor.

(B) Can we develop an abiotic system that mimics passive uptake and elimination processes for aquatic organisms?

Parallel artificial membrane permeability assay (PAMPA) has become popular in screening the bioavailability of orally administered drugs because it conceptually mimics passive transcellular transport through intestinal cell membranes (e.g., Avdeef, 2005; Kansy et al., 1998; Zhu et al., 2003). If uptake/elimination of hydrophobic pollutants is

governed by passive tanscellular diffusion, as often described in diffusion mass transfer models (e.g., Gobas et al., 1986; Sijm and van der Linde, 1995), a modification of PAMPA can be used for the evaluation of bioconcentration rate parameters. The major advantages of the system are mimicking permeation of a hydrophobic solute through lipid bilayers and easy accessibility for both donor and acceptor compartments, which serve as the external and the internal environment of an organism, respectively.

(B-1) Can we apply this physical model to develop a more reliable tool for assessing estrogenic potential of aquatic pollutants?

Many in vitro assays have been developed to evaluate estrogenic potential of putative EDCs and effluents from wastewater treatment plants (e.g., Koda et al., 2001; Routledge and Sumpter, 1996; Soto et al., 1995). However, most of these assays detect the potential impacts at a cellular level in an artificial condition. They do not address the available free concentration of the EDCs nor transport to the receptor site. Therefore, more reliable prediction of ecological risks associated with EDCs could be made by linking existing in vitro toxicity assays to a physical system that can control available free EDC concentrations and mass transport mechanisms.

Therefore, four research hypotheses were derived from the questions above, as follows:

1. Poor correlations between K_{lipw} and K_{OW} are expected if structurally diverse EDCs are investigated. These quantitative structure-activity relationships (QSARs) may be improved by introducing the effects of solute size and polar interactions.

2. The discrepancy between K_{lipw} and K_{OW} can be explained by the thermodynamics of solute transfer from water to lipid bilayers.
3. A parallel artificial membrane system can reasonably mimic bioconcentration rate parameters for moderately hydrophobic and non-metabolizable chemicals because bioconcentration is dominated by passive diffusion through a series of lipid membranes.
4. An existing in vitro assay for the detection of estrogenicity can be improved by combining it with an abiotic system that models passive uptake/elimination and controls available free concentration.

1.3. SPECIFIC OBJECTIVES

As described above, the primary emphases of this research are on predicting equilibrium partitioning of selected EDCs into synthetic lipid membrane vesicles and quantifying the rate of lipid membrane permeation in an artificial system. Consequently, specific objectives are stated as follows:

1. To obtain equilibrium partition coefficients between water and various synthetic lipid membrane vesicles for structurally diverse EDCs to evaluate the effects of hydrophobicity, molecular size, and polar interactions.
2. To develop empirical relationships between K_{lipw} and K_{OW} using additional parameters reflecting the effects of molecular size and polar interactions.
3. To evaluate the effects of lipid components on the partitioning.
4. To obtain equilibrium partition coefficients at different temperatures in order to calculate thermodynamic constants of partitioning, the enthalpy change (ΔH) and the entropy change (ΔS).

5. To evaluate the effects of the physical characteristics of different lipid membrane vesicles on the thermodynamic constants to provide a theoretical basis for the discrepancy between K_{lipw} and K_{OW}.
6. To evaluate literature data on bioconcentration rate parameters in small fish to provide a theoretical basis for the development of a parallel artificial lipid membrane system using a diffusion based mass transfer model.
7. To optimize an artificial membrane system by controlling mass transfer resistances.
8. To determine membrane permeabilities and elimination rate constants using the artificial membrane system and compare those with literature uptake/elimination rate constants in small fish.
9. To evaluate an estrogen receptor binding assay using freely available concentration with a proposed equilibrium binding model to provide an example that demonstrates the utility of assessing the internal exposure using an artificial membrane system for receptor-mediated toxicants.

1.4. STRUCTURE OF THIS DISSERTATION

In this dissertation, background information and a literature review are provided in Chapter 2. The review includes a brief overview of endocrine disrupting chemicals (EDCs) with in vitro screening methods for the detection of estrogenicity, concepts of equilibrium partitioning for hydrophobic organic chemicals between water and model biological phases, and a review of bioconcentration models and currently available in vitro techniques for evaluating bioavailability.

The next four chapters are dedicated to the experimental results and discussion of each topic and are written in a manuscript format for a journal article. Chapter 3 discusses

possible mechanistic insights to the non-linear relationship between log K_{OW} and bio-partitioning of moderately hydrophobic endocrine disruptors. In order to investigate the theoretical basis for biopartitioning, effects of liposome compositions on partitioning thermodynamics are described in Chapter 4. Chapter 5 presents a possible parallel artificial lipid membrane system for use as an environmental exposure assessment tool. For this purpose, artificial membrane permeability and elimination rate constants are compared with literature uptake/elimination rate constants in small fish. In Chapter 6, the potential applicability of the artificial membrane system is discussed by applying an equilibrium binding model using freely available concentration for a competitive estrogen receptor binding assay. This provides an insight for improving toxicity screening using in vitro assays for receptor-mediated or reactive toxicants.

Finally, conclusions and recommendations for future research are provided in Chapter 7. Appendices are provided to present more detailed information than is summarized in the main body of each chapter. A bibliography is provided at the end.

Chapter 2: Literature Review

2.1. INTRODUCTION

The overall goals of this research are to provide a theoretical understanding of the observed non-linear relationship between 1-octanol/water partitioning and biomembrane/water partitioning for EDCs and to link an abiotic exposure device to existing in vitro assays of detecting estrogenic potential. To make this process worthwhile, it is important to understand the current state of knowledge concerning the research area.

Since the environmental pollutants of concern in this study are EDCs, a brief overview of their properties is provided in Section 2.2. In vitro screening methods for the

detection of estrogenicity is also provided in that section. Partitioning concepts related to hydrophobic organic chemicals between water and model biological phases are provided in Section 2.3 to set the stage for the experimental plan and thermodynamic modeling conducted as part of this research. Finally, a review of bioconcentration models and currently available in vitro techniques for evaluating bioavailability are provided in Section 2.4.

2.2. ENDOCRINE DISRUPTING CHEMICALS (EDCS)

2.2.1. Definition of EDCs

Endocrine disrupting chemicals (EDCs) are defined as "exogenous substances that interfere with synthesis, secretion, transport, binding, action, or elimination of natural hormones in the body that are responsible for the maintenance of homeostasis, reproduction, development, and/or behavior" (US EPA, 1997). Endocrine disruption occurs when EDCs interact with hormone receptors. Figure 2.1 shows two types of processes involved in endocrine disruption. Both agonists and antagonists bind to the receptor and make subtle changes to the receptor conformation that may (agonist) or may not (antagonist) activate a response.

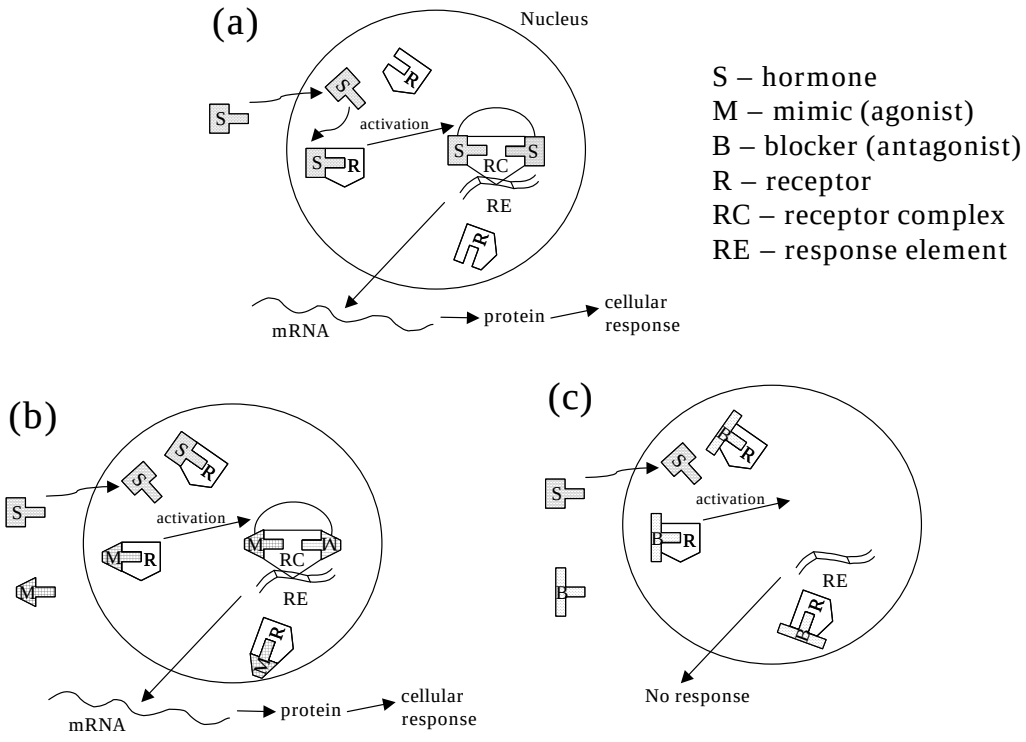

Figure 2.1: Interference of hormone action. (a) natural response; (b) agonist; (c) antagonist.

A wide variety of chemicals are now suspected as potential EDCs, including steroids, phytoestrogens, surfactants, polyaromatic compounds, pesticides, organo oxygenated compounds and organotin compounds (Birkett and Lester, 2003). Table 2.1 provides a selective list of representative EDCs and their chemical structures.

Table 2.1: Potential endocrine disrupting chemicals

Groups	Chemical structures
Steroids 17β-Estradiol (E2) Estrone (E1) Ethinylestradiol (EE2) Diethylstilbestrol (DES), etc.	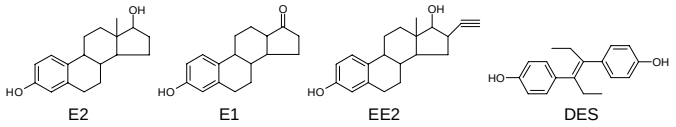
Phytoestrogens Genistein (GEN) Naringenin (NAR) Coumestrol (COU), etc.	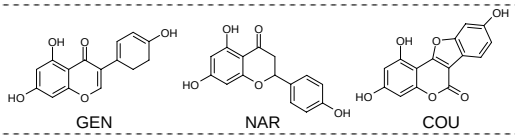
Surfactants Nonylphenol (NP) Nonylphenol ethoxylates (NPnE) Octylphenol (OP) Octylphenol ethoxylates (OPnE), etc.	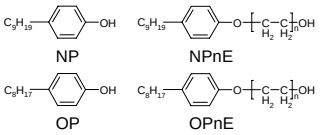
Polyaromatic compounds Polychlorinate biphenyls (PCBs) Polycyclic aromatic hydrocarbons (PAHs) Polybrominate diphenyl ethers (PBDEs), etc.	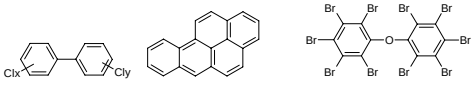
Pesticides Lindane (LIN) *p,p*'-DDT Dieldrin (DIEL) Atrazine (ATZ), etc.	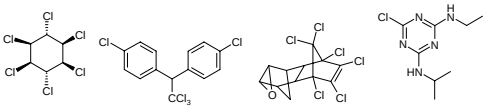
Organo oxygenated compounds Bisphenol A (BPA) Polychlorinated dibenzodioxins (PCDDs) Polychlorinated dibenzofurans (PCDFs) Benzylbutyl phthalate (BBP) Diethylhexyl phthalate (DEHP), etc.	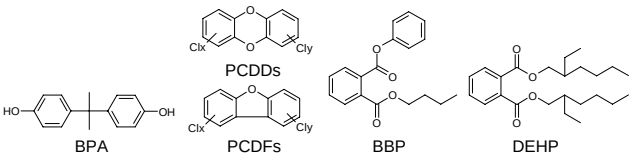
Organo tin compounds Tributyltin (TBT), etc.	

2.2.2. Occurrence and fate of EDCs

The first synthetic estrogen, diethylstilbestrol (DES), used for miscarriage prevention in the 1950s and 1960s, was discontinued because it was found to cause reproductive malfunction in male offspring (Colburn et al., 1996). Many pesticides, such as DDT, and extremely hydrophobic chlorinated aromatic chemicals, such as polychlorinated biphenyls (PCBs), are also known to disrupt the endocrine system. One of the most well-known examples of an endocrine disrupting chemical is DDT. DDT was shown to cause eggshell thinning and other reproductive failures in fish-eating birds (Ratcliffe, 1967) as well as developmental abnormalities in reptiles (Guillette et al., 1994). While PCBs and polychlorinated dibenzodioxins/furans (PCDD/Fs) are found in almost all environmental media, they are found in higher concentrations in higher trophic level organisms due to their extreme hydrophobicity and persistence in the environment. Endocrine disrupting effects caused by these chemicals have been reported in literature (e.g., Giesy et al., 1994; Murk et al., 1996; Subramanian et al., 1987). More recently, treated effluent from sewage treatment plants (STPs) has been found to be estrogenic (e.g., Aerni et al., 2001; Nakada et al., 2004) and increased vitellogenin levels have been reported in male fish caught near STPs (e.g., Nolan et al., 2001; Routledge et al., 1998). The main causative chemicals are natural estrogens and breakdown products from surfactants (e.g., Barnhoorn et al., 2004; Nolan et al., 2001; Routledge et al., 1998; Rodgers-Gray et al., 2001). In addition, many industrial chemicals are suspected EDCs including bisphenol A (e.g., Steinmetz et al., 1997), phthalate esters (Zacharewski et al., 1998), organotin compounds (Alzieu, 1991), etc. Table 2.2 summarizes sources, occurrence in the environment, and (suspected) effects in human and wildlife of various classes of endocrine disrupting compounds.

Table 2.2: Summary of sources, occurrence, and suspected effects of EDCs

EDC classes		Sources*	Environmental occurrence	Observed effects in human and wildlife
Steroids	Natural hormones	- foods - mammalian excretion - agricultural uses	Effluent (e.g., Nakada et al., 2004; Aerni et al., 2004) Surface water (e.g., Kuch and Ballschmitter, 2001) Groundwater (e.g., Hanselman et al., 2003)	Increased vitellogenin in male fish/intersex (e.g., Routledge et al., 1998; Nolan et al., 2001;)
	Synthetic hormones	- oral contraception		Reproductive malformation of the male offspring in human (e.g., Gupta, 2000)
Phytoestrogens		- plant-derived	Surface water: (e.g., Kawanishi et al., 2004)	
Surfactants		- break-down product from detergents - other industrial uses	Effluent (e.g., Ahel et al., 1993; Nakada et al., 2004) Surface water (e.g., Ahel et al., 1993; Snyder et al., 1999; Kuch and Balschmitter, 2001; Shao et al., 2004) Groundwater (e.g., Rudel et al., 1998) Drinking water (e.g., Shao et al., 2005) Sediment (e.g., Lye et al., 1999) Fish (e.g., Shao et al., 2005; Lye et al., 1999) Air (e.g., Dachs et al., 1999)	Increased vitellogenin in male fish/intersex (e.g., Barnhoorn et al., 2004; Rodgers-Gray et al., 2001)
Polyaromatic compounds	PAHs	- combustions	Persistent, found in almost all environmental media (e.g., de Wit, 2002; Lee et al., 2004; Muir et al., 1999)	Reduced hatching in birds (e.g., Murk et al., 1996)
	PCBs	- industrial uses		Reduced testosterone levels in Dall's porpoises (Subramanian et al., 1987)
	PBDEs	- flame retardants		
Pesticides	DDT, DDE	- banned	Persistent, found in almost all environmental media (e.g., Muir et al., 1999)	Feminization, egg shell thinning in birds (e.g., Ratcliffe, 1967) Developmental abnormalities in alligators (e.g., Guillette, 1994) Reduced testosterone levels in Dall's porpoises (Subramanian et al., 1987)
	Others	- agricultural uses		
Organo oxygen compounds	PCDD/Fs	- combustions - industrial byproducts	Persistent, found in all environmental media (e.g., Czuczwa and Hites, 1984)	Reproductive failure in fish eating birds (e.g., Giesy et al., 1994)
	Bisphenol A	- plastic additives	Effluent (e.g., Kuch and Ballschmitter, 2001; Rudel et al., 1998) Surface water (e.g., Kuch and Ballschmitter, 2001) Groundwater (e.g., Rudel et al., 1998) Drinking water (e.g., Kuch and Ballschmitter, 2001) Sediment (Khim et al., 1999)	In vivo and in vitro evidences only (e.g., Steinmetz et al., 1997)
	Phthalate esters	- plastic additives	Found in almost all environmental media (e.g., Staples et al., 1997)	In vitro evidences, conflict in vivo effects (e.g., Zacharewski et al., 1998)
Organotin comopounds		- antifouling agents	Seawater/sediment: (e.g., Konstantinou and Albanis, 2004; Pereira et al., 1999)	Reduced oyster reproduction (e.g., Alziee, 1991)

* Birkett and Lester, 2003

2.2.3. In vitro assays for the detection of estrogenicity

Several in vitro assays have been developed for potentially identifying EDCs and assessing effluent waters for their endocrine disrupting potential. These in vitro assays are simpler, require less time and care, and are more economical than conventional in vivo experiments using laboratory animals. In vitro assays monitor ligand-like actions at various stages of the molecular signaling cascade, including ligand/estrogen receptor (ER) binding, ER complex binding to estrogen response element (ERE), association with co-activators, target gene expression, and corresponding enzymatic activity (Figure 2.2). Assays for estrogenicity differ with respect to the step within the molecular signaling cascade that is targeted and the sensitivity of the method. Table 2.3 summarizes some popular in vitro assays for detecting estrogenic and antiestrogenic chemicals. As can be seen from this table, all the necessary steps in Figure 2.2 are utilized as endpoints of measuring (anti-)estrogenic potential.

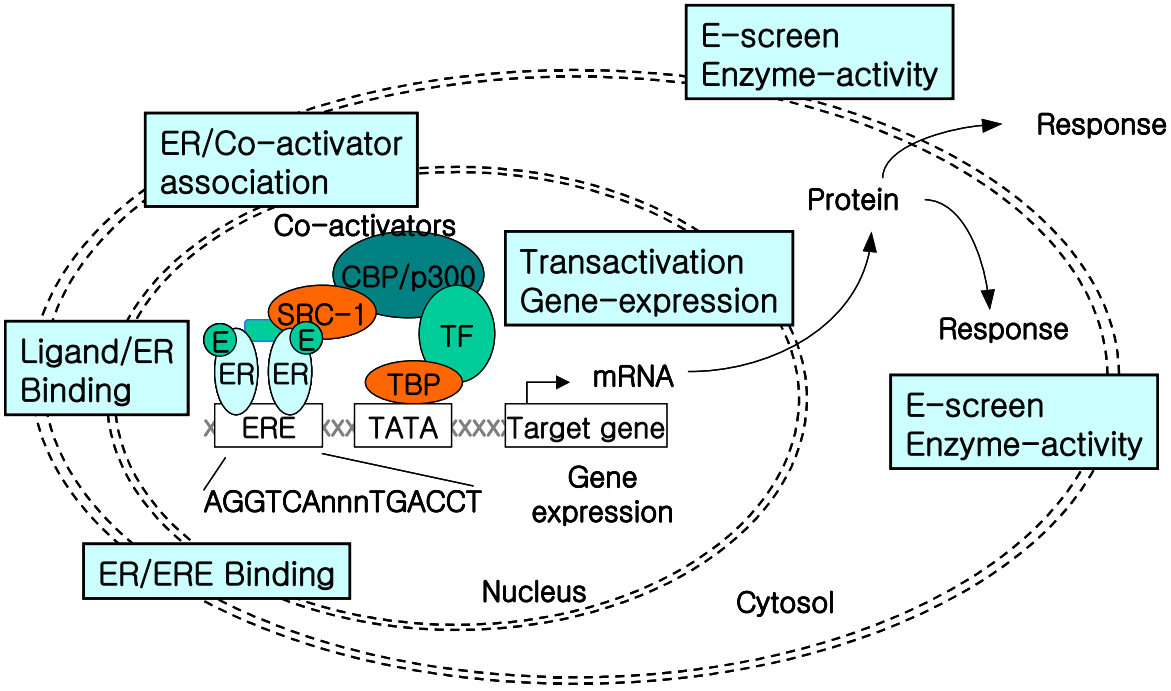

Figure 2.2: Molecular mechanism of estrogen receptor (ER) mediated action. CBP/p300, co-activator protein; E, ER-ligand; ERE, estrogen responsive element; RNA pol, RNA polymerase; SRC-1, co-activator protein; TATA, TATA box; TBP, TATA binding protein; TF, general transcription factor (From Mueller, 2002).

Table 2.3: Some popular in vitro assays for detecting estrogenic and antiestrogenic chemicals

In vitro assay	Endpoint	Advantages	Limitations	Reference
Ligand-binding	Binding affinity to ERα or ERβ	Simple; high-throughput; ER binding is fundamental step.	Cannot distinguish between agonists and antagonists; Serum binding protein absent	e.g. Koda et al., 2001; Murdock et al., 1990
ER-binding to ERE	Binding affinity to various ERE	Simple; various ERE can be used	Low sensitivity	e.g. Nikov et al., 2000
Two-hybrid assay	Ligand-dependent association of ERα or ERβ with co-activators	Analysis of molecular interactions; measures estrogens and antiestrogens	Artificial system	e.g. Nishikawa et al., 1999
Reporter-gene expression	Expression of ER regulated genes	Wide variety of cell-line origins can be used	Could be restricted to some cell lines; may be susceptible to mechanisms that do not involve the ER; compounds might not have consistent tissue- or species-specific responses	e.g. Pons et al., 1990; Chen et al., 1995
Recombinant receptor-reporter gene construct	Recombinant gene expression	Direct cell exposure; internal control reporter gene to monitor toxicity; cab use transfected mammalian or yeast cell	No standardized assay system generally available; yeast cell walls can affect the uptake of xenoestrogens	e.g. Routledge and Sumpter, 1996
Cell proliferation	Proliferation of ERα-positive cells	Measure physiological endpoint of estrogen action; can distinguish between agonist and antagonist	Only a few cell lines are estrogen responsive; 4-6 d incubation period	e.g. Soto et al., 1995

2.3. PARTITIONING OF HYDROPHOBIC ORGANIC CHEMICALS BETWEEN WATER AND MODEL BIOLOGICAL PHASES

Understanding partitioning behavior into biological organic phases is of critical importance because many pollutants are transported from the environment to an organism via passive diffusion and are stored in the organic phases within cells, such as plasma membranes. Due to the difficulty associated with measuring partitioning in biological samples, simpler model systems have been widely used as surrogates for biological organic phases. This section reviews some of the most popular model systems and their thermodynamic bases.

2.3.1. 1-Octanol/water partition coefficient (K_{OW})

Bulk organic solvent-water partition coefficients have been used to model biological partitioning since the end of the 19th century (Meyer, 1899). Among various solvents, 1-octanol is considered to be suitable for representing biological systems in drug design work due to its reasonable polarity and the accumulation of data for comparison with drug testing (Smith et al., 1975). The 1-octanol-water partition coefficient (K_{OW}) has also been successfully used to evaluate bioconcentration of xenobiotics (Davies and Dobbs, 1984; Mackay, 1982; Neely et al., 1974; Oliver and Niimi, 1985; Veith et al., 1980), sorption coefficients for partitioning of contaminants to soils/sediment organic matter (Briggs, 1981; Chiou et al., 1983; Karickhoff et al., 1979) and non-specific toxicity such as narcosis through linear free energy relationships (LFERs) (Hansch and Leo, 1995). Table 2.4 shows some examples of LFERs using K_{OW}.

Table 2.4: Examples of estimating bioconcentration, sorption coefficients, and aquatic toxicity from K_{OW} through linear free energy relationships (LFERs).

	Relationship	Source
Bioconcentration:		
Whole body BCF of fish	$\log BCF = 0.542 \log K_{OW} + 0.124$ (n=8)	Neely et al., 1974
	$\log BCF = 0.76 \log K_{OW} - 0.23$ (n=84, r^2=0.90)	Veith et al., 1980
	$\log BCF = \log K_{OW} - 1.32$ (n=51, r^2=0.95)	Mackay, 1982
	$\log BCF = 0.597 \log K_{OW} + 0.188$ (n=31, r=0.748)	Davies and Dobbs, 1984
	$\log BCF = 0.98 \log K_{OW} - 1.30$ (hydrocarbons only, n=20, r=0.898)	
	$\log BCF = 0.96 \log K_{OW} - 0.56$ (n=16, r^2=95)	Oliver and Niimi, 1985
Uptake/elimination rate constant	$\log k_1 = 0.337 \log K_{OW} - 0.373$	Hawker and Connell, 1985
	$\log k_2 = -0.663 \log K_{OW} + 0.947$	
	$k_1 = 0.048\ K_{OW}/(0.00142 K_{OW} + 12.01)$	Hawker and Connell, 1988
	$k_2 = 1/(0.00142 K_{OW} + 12.01)$	
	$\log k_1 = 0.122 \log K_{OW} + 2.192$	Tolls and Sijm, 1995
	$\log k_2 = -0.791 \log K_{OW} + 2.972$	
Sorption:		
Soil organic matter adsorption	$\log K_{om} = 0.52 \log K_{OW} + 0.41$ (n=105, r=0.95)	Briggs, 1981
	$\log K_{oc} = 0.904 \log K_{OW} - 0.543$	Chiou et al., 1983
	$\log K_{oc} = 1.00 \log K_{OW} - 0.21$	Karickhoff et al., 1979
Sorption to surfactant micelle	$\log K_{micw} = 0.72 \log K_{OW}$ + constant	Pramauro et al., 1988
Sorption to lipid membranes	$\log K_{MW} = 1.19 \log K_{OW} - 0.645$ (n=25, r=0.96)	Gobas et al., 1988
	$\log K_{lipw} = 0.78 \log K_{OW} + 1.12$ (n=20, r^2=0.92)	Escher et al., 2000
		Smejtek et al., 1996
Toxicity:		
Acute toxicity	$\log(1/C) = 0.84 \log K_{OW} + 1.22$ (n=105, r^2=0.88)	Hansch and Leo, 1995

2.3.2. Surfactant micelle-water partition coefficient

Surfactants form highly organized self-aggregates ("micelles") above a certain concentration called the "critical micelle concentration." The sorption coefficient onto/into micelles (K_{micw}) has been estimated by several researchers because micelles may be more realistic physical models for soil partitioning than bulk organic solvents (e.g., Dulfer et al., 1995; Guha et al., 1998; Woodrow and Dorsey, 1997). Although earlier studies found that there are linear relationships between log K_{micw} and log K_{OW} (e.g., Pramauro et al., 1988), more recent studies proposed non-linearity between these log K's (Dulfer et al., 1995).

2.3.3. Lipid membrane-water partition coefficient (K_{lipw})

Synthetic lipid membrane vesicles, more often called "liposomes", can be manufactured from lipid molecules (Mueller et al., 1962). The bilayer structure of liposomes is thought to be a better representation of real biological membranes composed of lipid bilayer and membrane proteins (Singer and Nicholson, 1972). For this reason, partition coefficients between water and synthetic membrane vesicles (K_{lipw}) are often used for evaluating bioconcentration and biological membrane permeation (Escher and Schwarzenbach, 1996; Escher et al., 2000; Gobas et al., 1988; Liu et al., 2001; Smejtek et al., 1996; Vaes et al., 1997; van Wezel et al., 1996). Although partitioning between water and octanol is theoretically different from partitioning between water and synthetic membrane vesicles (detailed discussion in the next section), many studies have shown linear relationships between log K_{OW} and log K_{lipw} for moderately hydrophobic organic chemicals of environmental concern as summarized in Table 2.4.

2.3.4. Thermodynamics of partitioning phenomena

A thorough review of the thermodynamics of partitioning can be found in Katz and Diamond (1974) and Gobas et al. (1988). In brief, the logarithm of the partition coefficient between water and an organic phase is related to the free energy of solute transfer from water to the organic phase (ΔG_{ST}). ΔG_{ST} can be divided into two components: the free energy of solution in water ($\Delta G_{S,W}$) and the free energy of solution in the organic phase ($\Delta G_{S,O}$). Further division of these two terms, as depicted in Figure 2.3, into the free energy of cavity creation and free energy of interaction between solute and solvent leads to the following expression.

$$\Delta G_{ST} = \Delta G_{S,O} - \Delta G_{S,W} = \left(\Delta G_{C,O} + \Delta G_{I,O}\right) - \left(\Delta G_{C,W} + \Delta G_{I,W}\right) = \left(\Delta G_{C,O} - \Delta G_{C,W}\right) + \left(\Delta G_{I,O} - \Delta G_{I,W}\right) \quad (2.1)$$

The free energy of cavity creation depends on the size of the solute, and the free energy of interaction is determined by van der Waals interactions, hydrogen bonding, other specific interactions. The partition coefficient between water and organic phases is linearly dependent on the molar liquid volume (MLV) if the ($\Delta G_{C,O} - \Delta G_{C,W}$) term in Eq. 2.1 is linearly proportional to MLV and the solutes are chemically similar (Gobas et al., 1988). Linear relationships between K_{OW} and molar liquid volume (MLV) have been observed for homologous series of chemicals, such as polychlorinated benzenes and polychlorinated biphenyls (e.g., Miller et al., 1985). In addition, an empirical Collander type equation is expected between K_{OW} and partition coefficients between water and other organic phases when MLV is linearly proportional to the logarithm of the partition coefficients.

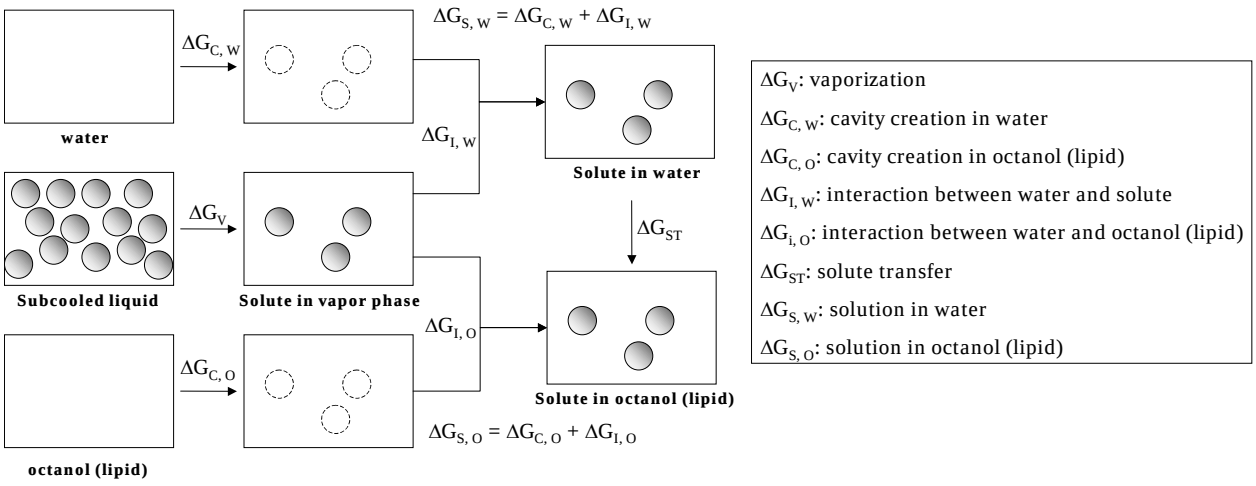

Figure 2.3: Thermodynamic cycle of dissolving a solute.

However, investigations of the thermodynamic quantities (the enthalpy change (ΔH) and the entropy change (ΔS)) of solute transfer using van't Hoff isochores clearly revealed that partitioning between water and octanol is significantly different from

partitioning between water and fish (Opperhuizen et al., 1988), between water and lipid membranes (van Wezel et al., 1996), and between water and surfactant micelles (Woodrow and Dorsey, 1997). Whereas octanol-water partitioning is driven by negative enthalpy changes and positive entropy changes, biopartitioning is more likely driven by positive entropy only and is not favorable in terms of enthalpy change (Opperhuizen et al., 1988). A critical process determining these differences in Figure 2.3 would be cavity creation if the free energy of interaction does not significantly depend on different organic phases. The enthalpy required to create cavities in lipid membranes would be much greater than required in octanol. It is thought that the positive ΔH associated with cavity creation is fully compensated by the negative ΔH of interaction (i.e. ΔH_{ST} is negative) in octanol-water partitioning but not fully compensated by the negative ΔH of interaction (i.e. ΔH_{ST} is positive) in lipid membrane-water partitioning. Several researchers have shown that using more organized lipid membranes resulted in more positive ΔH_{ST} values (Rowe et al., 1998). For example, ΔH_{ST} is usually positive for gel phase lipid bilayers (Katz and Diamond, 1974; van Wezel et al., 1996; Yang et al., 2000) but is usually negative for liquid crystalline phase lipid bilayers (Takegami et al., 2003; Wenk et al., 1996). Partitioning experiments between water and fish storage lipids (e.g., triolein, which does not form bilayers) showed negative ΔH values (van Wezel and Opperhuizen, 1995).

2.4. BIOCONCENTRATION MODELS AND IN VITRO TECHNIQUES FOR EVALUATING BIOAVAILABILITY

2.4.1. Bioconcentration models

Bioconcentration in aquatic organisms involves uptake of a chemical from water via the respiratory surface of the organism (e.g., gills and skin) and the loss or elimination

of that chemical from the organism (Gobas and Morrison, 2000). Uptake from water is the predominant route of uptake for most organic micropollutants except extremely hydrophobic organic chemicals, for which uptake from contaminated food contributes significantly to the total bioaccumulation (Opperhuizen, 1991; Randall et al., 1998). Elimination occurs predominantly via gills for chemicals not readily metabolized. For moderately hydrophobic and non-readily metabolizable chemicals (e.g., chlorobenzenes), it is commonly assumed that chemical uptake across the gill dominates all other routes of uptake and chemical exchange across the gill occurs by simple passive diffusion. In the simplest model, bioconcentration has been described using linear two-compartment first-order kinetics represented by the following equation:

$$\frac{dC_f}{dt} = k_a C_w - k_e C_f = k_a \left(C_w - C_a \right) \tag{2.2}$$

where C_f is the fish's whole-body concentration of solute (μg/g), C_w is the freely dissolved concentration of solute in water (μg/ml), k_a (cm^3/g-s) and k_e (s^{-1}) are first-order absorption and elimination rate constants, respectively, and C_a is the freely dissolved solute concentration in the fish's aqueous phase (=C_f/*BCF*).

A number of expressions for the uptake rate constant (cm^3/g-s) or chemical's overall permeability (cm/s) have been proposed as summarized in Table 2.5. Among the models described, the stagnant diffusion mass transfer model is most frequently used due to its theoretical simplicity. Mathematical description of this model is provided in the next section.

Table 2.5: Several types of bioconcentration models.

Models*	Assumptions	Reference
Steady-state uptake through multiple diffusion layers	Molecules have to pass through stagnant diffusion barriers made of water and lipid bilayers.	Gobas et al., 1986 Sijm and van der Linde, 1995
Passive uptake with flow limitation	Mass transport could be limited not only by aqueous and epithelial diffusion but also by gill ventilation and blood flow. Several limiting cases could be derived from this assumption.	Erickson and McKim, 1990 Erickson et al., 2006a Hayton and Barron, 1990
Diffusion uptake with forced convection	Gill's uptake rate could be given as the solution of the partial differential equation that models the steady-state chemical diffusion from a laminar flow liquid through the permeable walls of a flat channel.	Barber et al., 1991
Prediction from oxygen consumption	Chemical uptake via fish's gill is proportional to the fish's ventilation volume.	Neely, 1979 Yang et al., 2000

*Model classifications from Barber (2003).

2.4.2. Diffusion mass transfer model

Assuming that uptake through the gill is controlled by a series of diffusion barriers made of water and lipid membranes, one can express the uptake rate constant (k_a) in Equation 2.2 as:

$$k_a = P\frac{A}{W} \tag{2.3}$$

where P is overall permeability (cm/s), A is gill surface area (cm^2) and W is the fish weight (g). Aqueous permeability (P_{aq}) and membrane permeability (P_m) are given by:

$$P_{aq} = \frac{D_w}{\delta_w} \tag{2.4}$$

$$P_m = \frac{K_m D_m}{\delta_m} \tag{2.5}$$

where D_w and D_m are aqueous and membrane diffusivities (cm^2/s), respectively, δ_w and δ_m are the aqueous and membrane diffusion film thickness, respectively, and K_m is the lipid membrane-water partition coefficient. Combining Equation 2.4 and 2.5 to get the

overall permeability, P, and plugging this into Equation 2.3 yields the following expression for k_a.

$$k_a = \frac{1}{\frac{\delta_w}{D_w} + \frac{\delta_m}{K_m D_m}} \frac{A}{W} \tag{2.6}$$

Since the elimination rate constant (k_e) equals k_a/BCF and partitioning to the lipid compartment in fish dominates over partitioning to other parts of the whole fish, k_e is given as

$$k_e = \frac{k_a}{(1-\alpha) + \alpha K_m} = \frac{1}{\frac{\delta_w}{D_w} + \frac{\delta_m}{K_m D_m}} \frac{1}{(1-\alpha) + \alpha K_m} \frac{A}{W} \tag{2.7}$$

where α is the lipid content in whole body.

If K_{OW} could be used as a surrogate for K_m in Equation 2.6 and 2.7, k_a and k_e could be predicted in the general forms of $\alpha K_{OW}/(a+bK_{OW})$ and $1/(a+bK_{OW})$, as suggested by Hawker and Connell (1988).

2.4.3. In vitro techniques for evaluating bioavailability

Due to difficulties in analyzing biological samples for aquatic exposure assessment, time-weighted concentrations of organic pollutants have been measured using abiotic passive sampling devices. These devices often use membranes containing organic phases or porous organic solid phases. Table 2.6 shows some representative examples of biomimetic passive sampling devices. Semipermeable membrane devices are the most popular among these. Studies showed that these devices can be used, not only to measure time-weighted concentrations in water (Huckins et al., 1990, 1993), but also to evaluate bioconcentration kinetics and critical body burden (Verbruggen et al., 2000).

Table 2.6: Examples of abiotic devices for aquatic exposure assessment

Abiotic device	Content/membrane	Target chemicals	Reference
Dialysis membrane bags	Hexane/dialysis membrane Polydimethylsiloxane/dialysis membrane	Lipophillic Hydrophobic persistent organics	Södergren, 1987 Vrana et al., 2001
Semipermeable membrane devices (SPMD)	Trolein/polyethylene	Lipophillic	Huckins et al., 1990, 1993
Empore discs	Filter with C18 resin (without membrane)	Lipophillic	Freidig et al., 1998
Solid phase microextraction (SPME)	Various solid phases (without membrane)	Various chemicals	Verbruggen et al., 2000

More recently, a high-throughput parallel artificial membrane permeability assay (PAMPA) has been developed to estimate human intestinal absorption of orally administered drugs (Kansy et al., 1998; Sugano et al., 2003; Wohnsland and Faller, 2001; Zhu et al., 2002). PAMPA uses microporous filter-supported lipid bilayers exhibiting similar membrane properties to the black lipid bilayer (Thompson et al., 1980; 1982). Because most drugs are thought to permeate intestinal barriers via passive paracellular diffusion, permeability of a drug to microporous filter-supported lipid bilayers is a measure of the prediction of drug absorption potential. Measured permeabilities from a 96-well plate platform correlate well with % absorption of orally administered drugs that passively permeate intestinal aqueous and lipid barriers (Sugano et al., 2003; Zhu et al., 2002). The parallel artificial membrane system used in PAMPA may have great potential for water quality assessment purposes because this physical model is closer to an actual biological membrane compared to most existing passive sampling devices (Table 2.6), and it is thought that same passive paracellular diffusion processes govern both human intestinal absorption and accumulation of hydrophobic organic chemicals (HOCs) from

water to aquatic organisms. In addition, this system allows easy access to both sides of the aqueous solution that serve as the external aqueous environment and the internal aqueous solution. In addition to the simple abiotic systems described in Table 2.6, many researchers have developed tools for evaluating absorption/elimination of chemicals using intestinal cell monolayers (e.g., Vasiluk et al., 2005), isolated gill membranes (e.g., Barron, 1989; Sijm et al., 1993), and perfused organs (e.g., James et al., 2001; Kleinow et al., 1998).

Chapter 3: Partitioning of Moderately Hydrophobic Endocrine Disruptors between Water and Synthetic Membrane Vesicles

The partition coefficient between water and lipid membrane vesicles (K_{lipw}) has been used as an alternative to the 1-octanol-water partition coefficient (K_{OW}) between water and organic solvent, because it more closely represents actual biological membranes. Despite theoretical differences, log K_{lipw} correlates well with log K_{OW} for conventional nonpolar organic pollutants. In the present study, K_{lipw} values of 11 structurally diverse endocrine-disrupting chemicals (EDCs) were measured for three different types of lipid membrane vesicles from dipalmitoylphosphatidylcholine (DPPC), DPPC/cholesterol, and palmitoyloleoylphosphatidylcholine. Correlation analyses were conducted to evaluate the effects of hydrophobicity, molar liquid volume (MLV), and polar surface area (PSA) for 20 EDCs, including nine EDCs from a previous study. Correlations that include MLV and PSA reduce the predicted value of log K_{lipw}, suggesting that lipid membranes are less favorable than 1-octanol for a hydrophobic solute because of the changes in membrane fluidity and the amount of cholesterol in the lipid bilayer. Therefore, lipid components should be chosen carefully to evaluate bioconcentration of these compounds.

3.1. INTRODUCTION

To assess possible harmful effects of organic micropollutants on both humans and wildlife, it is necessary to evaluate the fate and distribution of these pollutants. Understanding partitioning behavior in biological organic phases is of critical importance because many pollutants are transported from the environment to an organism via passive diffusion and are then stored in the organic phases within cells, such as plasma membranes. Because of the difficulty associated with measuring partitioning in biological

samples, organic solvents, such as 1-octanol, have been widely used as a surrogate for biological organic phases (see, e.g., Davies and Dobbs, 1984; Hansch and Leo, 1995; Neely et al., 1974). The 1-octanol-water partition coefficient (K_{OW}) has been used successfully to evaluate the bioconcentration of xenobiotics (see, e.g., Davies and Dobbs, 1984; Neely et al., 1974) and nonspecific toxicity such as narcosis (see, e.g., Hansch and Leo, 1995) through linear free-energy relationships. However, recent studies have shown that the thermodynamics of partitioning between water and 1-octanol are significantly different from those between water and fish (Opperhuizen et al., 1988) and between water and lipid membranes (van Wezel et al., 1996; Wimley and White, 1993). The highly organized structure of biological membranes is thought to be the main cause of disparities between partitioning coefficients measured using 1-octanol versus lipid membranes. For this reason, partition coefficients between water and synthetic membrane vesicles, called liposomes, are often used for evaluating bioconcentration or biological membrane permeation (see, e.g., Diamond and Katz, 1974; Dulfer and Govers, 1995; Escher and Schwarzenbach, 1996; Escher et al., 2000; Gobas et al., 1988; Liu et al., 2001; Smejtek et al. 1996; Vaes et al., 1997; van Wezel et al., 1996; Yamamoto and Liljestrand, 2004).

Although partitioning between water and 1-octanol is thermodynamically different from partitioning between water and synthetic membrane systems, many studies have shown linear relationships between the log K_{OW} and the logarithm of lipid membrane-water partition coefficient (log K_{lipw}) for moderately hydrophobic organic chemicals of environmental concern having values of log K_{OW} between 1 and 5.5 (Gobas et al., 1988; Escher et al., 2000; Smejtek et al., 1996; Vaes et al., 1997; van Wezel et al., 1996). For more hydrophobic chemicals, the linear relationship is not applicable (Dulfer and Govers, 1995; Gobas et al., 1988). Gobas et al. (1988) observed that the linear

correlation breaks down for chemicals with log K_{OW} values of greater than 5.5, corresponding to molar volumes of greater than 230 cm^3/mol using dimyristoylphosphatidylcholine (DMPC) membrane vesicles. They also observed that logarithms of the species' activity coefficients in 1-octanol are linearly related to their molar volume, whereas those in DMPC membranes exhibit a parabolic relationship with the molar volume of solutes. Similarly, Dulfer and Govers (1995) found parabolic relationships between log K_{OW} and log K_{lipw} for highly hydrophobic PCBs ($5.0<\log K_{OW}<8.5$) using small unilamellar vesicles of DMPC, dipalmitoylphosphatidylcholine (DPPC), distearoylphosphatidylcholine (DSPC), and diarachidoylphosphatidylcholine (DAPC). However, the effects of the molar volume of moderately hydrophobic chemicals could not be elucidated, because the molar volumes of the solutes were proportional to their log K_{OW} in the aforementioned studies. Yamamoto and Liljestrand (2004) showed that only moderate/weak linear relationships exist for structurally diverse endocrine disrupting chemicals (EDCs) having log K_{OW} values between two and six using three different types of liposomes, DPPC, DPPC/cholesterol (60:40 wt %), and palmitoyloleoylphosphatidylcholine (POPC). The poor linear correlation likely results from the fact that the molar volumes of all the selected compounds were greater than the critical molar volume of 230 cm^3/mol proposed by Gobas et al. (1988). Unlike the work of Dulfer and Govers (1995), the molar volumes were not linearly related with log K_{OW} values, so it should be possible to differentiate the effect of molar volume from log K_{OW}. In this regard, regressions developed using a combination of moderately hydrophobic EDCs and nonpolar hydrophobic organic molecules provide this range of behavior, because log K_{OW} values typical of moderately hydrophobic EDCs are much smaller than those of nonpolar hydrophobic organics with equivalent molecular weight or molar volume. All the EDCs used in this study contain polar functional groups, such as phenolic

groups, that may contribute to log K_{lipw} because of hydrogen bonding and other polar interactions.

Several research groups have also shown that polar surface area (PSA) is an important contributor to partitioning correlations. Typically, PSA is negatively correlated with the permeability of drugs in humans (see, e.g., Palm et al., 1997; Veber et al., 2002; Zhu et al., 2002) either by lowering the partition coefficient or by lowering the diffusivity in the lipid membranes. Thus, both molar volume and PSA should be evaluated for their impact on partitioning of EDCs.

In this study, log K_{lipw} values were measured using the same three types of synthetic lipid membrane vesicles as in Yamamoto and Liljestrand (2004) for 11 additional EDCs to evaluate partitioning of EDCs into biological media. Relationships between log K_{lipw} and log K_{OW} were evaluated for all 20 EDCs, including those from the study by Yamamoto and Liljestrand (2004). Effects of the membrane fluidity and of cholesterol in the lipid membranes on log K_{lipw} were evaluated for the selected chemicals, because cholesterol content varies significantly in biological membranes. Effects of molar volume, PSA, and molecular geometry were examined. Relative contributions of the selected molecular descriptors were compared with respect to the characteristics of the lipid membranes.

3.2. MATERIALS AND METHODS

3.2.1. Chemicals

Three synthetic estrogens (diethylstilbestrol, hexestrol, and dienestrol), one natural hormone (progesterone), five industrial estrogenic chemicals (4,4'-dihydroxybenzophenone, benzyl-4-hydroxybenzoate, butyl-4-hydroxybenzoate, 4-phenylphenol, diethylphthalate), and two breakdown products of alkylphenol ethoxylates

(4-*sec*-butylphenol, 4-*tert*-amylphenol) were chosen. All are known to bind human estrogen receptor α (Blair et al., 2000). All the chosen EDCs either have a phenolic group or are a phthalate ester. Diethylstilbestrol (99%), hexestrol (98%), dienestrol (98%), and diethylphthalate (99.5%) were purchased from Sigma Chemical (St. Louis, MO, USA). Progesterone (98%), 4-*sec*-butylphenol (98%), 4-*tert*-amylphenol (99%), 4,4'-dihydroxybenzophenone (99%), benzyl-4-hydroxybenzoate (99%), and cholesterol (99%) were obtained from Aldrich Chemical (Milwaukee, WI, USA). 4-phenylphenol (98%) and butyl-4-hydroxybenzoate (99%) were purchased from Fluka Chemical (Milwaukee, WI, USA). Since palmitoyl (C16:0) and oleoyl (C18:1 9-*cis*) are the two most abundant components of fatty chains (Gennis, 1989; Jain, 1988), dipalmitoyl-phosphatidylcholine (DPPC, C16:0, C16:0) and palmitoyl-oleoyl-phosphatidylcholine (POPC, C18:1, C16:0) were chosen as representative liposome components. Cholesterol was selected as a model sterol due to its ubiquitous presence. The model liposome with cholesterol consists of DPPC containing 40% cholesterol by mass or 56% by mole fraction. This high level of cholesterol may reflect plasma membranes having extremely low permeability, because typical plasma membranes contain about 30 to 50% cholesterol by mole fraction (Jain, 1988). Chloroform solutions of model lipid components, DPPC and POPC were purchased from Avanti Polar Lipids (Albaster, AL, USA).

3.2.2. Preparation of liposome suspensions

Large unilamellar vesicle suspensions of DPPC, DPPC/cholesterol (60:40 w/w), and POPC were prepared using the thin film hydration technique (Mueller et al., 1983) followed by rapid extrusion processes (Hope et al., 1985) as described previously (Yamamoto and Liljestrand, 2004). In short, chloroform solution of the lipid was evaporated under a gentle nitrogen stream, and the thin film of the residue was dissolved in dilution water (buffered at pH 7.0 and ionic strength of 0.02 M, using KH_2PO_4, NaOH,

and NaCl) to make the liposome suspension. Then, the suspension was extruded several times through a polycarbonate membrane to reduce polydiversity of vesicles. The diameter of vesicles was mostly between 0.4 to 1.2 μm after extrusion.

3.2.3. Determination of K_{lipw}

Partition coefficients of the selected chemicals were determined by the equilibrium dialysis technique described in detail by Escher and Schwarzenbach (1996). Two identical amber glass vials, which served as donor and acceptor cells, were connected to each other by a Teflon® joint and were separated by regenerated cellulose dialysis membrane (Por7 MWCO 10,000, purchased from Spectrum Scientific, Rancho Dominguez, CA, USA). Solution containing EDCs was used to fill the donor cells. Aqueous buffer and liposome suspensions were filled in the acceptor cells of reference and sample reactors, respectively. The reference reactors were used to monitor losses over time and to validate the initial concentration. The pH of dilution water (pH 7.0) was lower than the log of the ionization constant (pK_a) for all the selected chemicals, as shown in Figure 3.1. Thus, negligibly small amounts of the ionized form of each compound were present. Sodium azide (0.02%) was added to prevent microbial activity. The equilibrium dialysis reactors were mixed using a tumbler in the dark at room temperature (22°C) for 7 d and at least four replicates were analyzed to determine the aqueous concentrations of reference cells and at least three sample reactors. Previous studies (Yamamoto and Liljestrand, 2004) and preliminary experiments showed that mass transfer is limited by permeation through the dialysis membrane and apparent equilibrium was attained after 7 d. The aqueous concentration of the selected chemicals was measured using a Waters 2690 high-performance liquid chromatography system equipped with a Waters 996 photodiode-array detector (Milford, MA, USA) for both sides of the reference reactors (C_{ref}, mg/L) and the side without lipid vesicle suspension in the sample

reactors (C_w, mg/L). The concentration of the lipid membrane vesicles (m, kg-lipid/L) was calculated from the total organic carbon concentration, as measured using a Dohrmann Apollo 9000 (Tekmar-Dohrmann, Cincinnati, OH, USA) total organic carbon analyzer, multiplied by the stoichiometric ratio of each lipid component (g lipid/g C). The partition coefficients of the selected chemicals (K_{lipw}) were calculated as described by Escher and Schwarzenbach (1996):

$$K_{lipw}\left(\mathrm{L/kg-lipid}\right) = \frac{C_{ref} - C_w}{C_w m} \tag{3.1}$$

The initial concentration of the donor cell (C_o) was set between 0.7 mg/L and 5.0 mg/L for all the selected chemicals, considering aqueous solubilities and method detection limits. Mass recovery (R) calculated from Equation 3.2 was between 89% and 105% for all species, except for an 82.5% recovery for dienestrol (see Appendix A):

$$R = (C_o - C_{ref,\,donor} - C_{ref,\,acceptor}) \times 100\ (\%) \tag{3.2}$$

The liposome concentrations ranged from 18 to 1,800 mg-lipid/L and were based on a goal of achieving a C_w of approximately 50% of C_{ref}. The C_w attained for all batches actually ranged between 10 and 95% of C_{ref}.

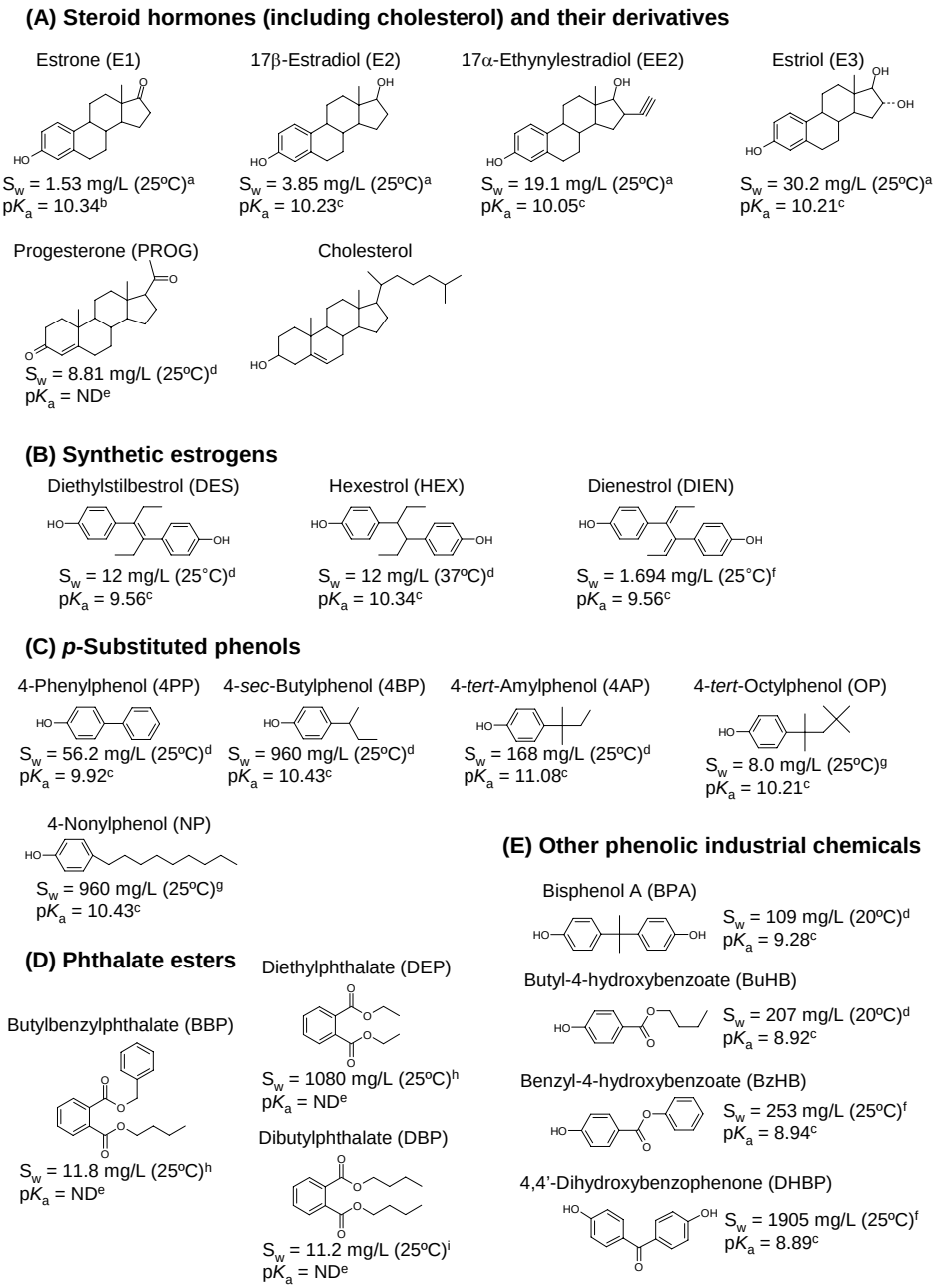

Figure 3.1: Chemical structures, aqueous solubilities, and acid dissociation constants of the selected chemicals. a, from Yalkowski (1999); b, from Perrin et al. (1977); c, estimated from phenol using the fragmentation method (Perrin et al., 1977); d, from Yalkowski and Dannelfelser (1992); e, not defined; f, estimated from log K_{OW} using log S_w = 0.796 – 0.854 log K_{OW} – 0.00728 MW + 0.580 for phenols (Ahel and Giger, 1993); g, from Ahel and Giger (1993); h, from Ellington and Floyd (1996); i, from Howard et al. (1985).

3.2.4. Correlation analyses and evaluation of the models

The molar liquid volume of each chemical was calculated using the LeBas method (Reid et al., 1977), and PSA values were calculated by a simple fragmentation method proposed by Ertl et al. (2000) (Table 3.1). To evaluate the model performance, Akaike information criterion (*AIC*) for small sample size was used (for details see Burnham and Anderson, 2002). The best model in this criterion is the one minimizing *AIC*. When errors are normally distributed, small-sample Akaike information criterion (AIC_c) for a least-square method is given as:

$$AIC_c = n\{\ln(2\pi) + \ln(RSS/n) + 1\} + 2K + \frac{2K(K+1)}{n-K-1} \quad (3.3)$$

where n is the sample size, *RSS* is the sum of the squares of residuals in a least square method, and K is the number of parameters. Least-square regression analyses were performed by SPSS Windows (Ver 12.0; SPSS, Chicago, IL, USA).

3.3. RESULTS

3.3.1. Liposome-water partition coefficients

Table 3-1 summarizes the values of log K_{OW}, MLV, PSA, and the partition coefficients between water and synthetic lipid membrane vesicles (K_{lipw}) of all the selected chemicals determined using the three different lipid compositions–DPPC, DPPC/cholesterol (60:40 % by weight), and POPC–in the present study as well as that of Yamamoto and Liljestrand (2004). The K_{lipw} values for diethylphthalate with DPPC liposomes and for 4-*sec*-butylphenol, 4,4'-dihydroxybenzophenone, diethylphthalate with DPPC/cholesterol liposomes could not be determined, because little difference was found between the concentration in the reference reactor (C_{ref}) and the concentration in the sample reactor (C_w). For all the selected chemicals, K_{lipw} values increased in the order DPPC/cholesterol, DPPC, and POPC, except for 4-phenylphenol, for which $K_{lipw,}$

$_{DPPC/cholesterol}$ is only slightly greater than $K_{lipw,DPPC}$. The $K_{lipw,DPPC/cholesterol}$ values for moderately hydrophobic EDCs were within one order of magnitude, except for the most hydrophilic estriol and the two most hydrophobic alkylphenols, nonylphenol and *p-tert*-octylphenol. The log K_{lipw} values for three relatively hydrophilic chemicals (diethylphthalate, 4,4'-dihydroxybenzophenone, and 4-*sec*-butylphenol), for which log K_{lipw} values could not be determined because of the limitation in the experimental method, are thought to be 1.5 or less, considering the experimental limits.

Table 3.1: Octanol-water partition coefficients (K_{OW}), molar liquid volumes (MLV), polar surface areas (PSA), and lipid membrane-water partition coefficients (K_{lipw}) of selected endocrine disruptors; DPPC = dipalmitoylphosphatidylcholine, POPC = palmitoyloleoylphosphatidylcholine.

Chemicals	log K_{OW}	Molar Liquid Volume[a] (cm^3/mol)	Polar Surface Area[b] ($Å^2$)	$K_{lipw, DPPC}$	$K_{lipw, DPPC/cholesterol}$	$K_{lipw, POPC}$
17β-Estradiol[c]	4.01[d]	355.0	40.46	$2.94 (\pm0.24)\times10^2$	$1.94 (\pm0.50)\times10^2$	$6.15 (\pm0.88)\times10^3$
Estrone[c]	3.13[d]	347.6	37.30	$4.13 (\pm0.32)\times10^2$	$2.82 (\pm2.31)\times10^2$	$8.36 (\pm0.24)\times10^3$
Estriol[c]	2.45[d]	377.2	60.68	$1.99 (\pm1.59)\times10$	$1.47 (\pm0.89)\times10$	$9.09 (\pm4.91)\times10$
17α-Ethynylestradiol[c]	3.67[d]	384.6	40.46	$5.62 (\pm1.31)\times10^2$	$1.65 (\pm0.69)\times10^2$	$1.57 (\pm0.03)\times10^4$
4-Nonylphenol[c]	5.76[d]	303.2	20.23	$6.87 (\pm0.92)\times10^4$	$6.88 (\pm3.91)\times10^3$	$3.18 (\pm0.62)\times10^5$
4-*tert*-Octylphenol[c]	5.85[e]	281.0	20.23	$3.48 (\pm1.29)\times10^5$	$1.38 (\pm0.39)\times10^5$	$4.04 (\pm0.35)\times10^5$
Bisphenol A[c]	3.32[d]	266.0	40.46	$1.79 (\pm0.99)\times10^3$	$1.78 (\pm1.23)\times10^2$	$2.91 (\pm0.30)\times10^4$
Butylbenzylphthalate[c]	4.91[d]	365.4	52.61	$5.74 (\pm1.18)\times10^2$	$1.25 (\pm0.94)\times10^2$	$4.75 (\pm1.06)\times10^4$
Dibutylphthalate[c]	4.57[d]	347.2	52.61	$9.29 (\pm4.05)\times10^3$	$1.03 (\pm0.45)\times10^2$	$1.55 (\pm0.43)\times10^4$
Diethylstilbestrol	5.07[d]	325.5	40.46	$1.66 (\pm0.15)\times10^4$	$1.67 (\pm0.83)\times10^2$	$9.61 (\pm1.18)\times10^4$
Hexestrol	5.60[f]	332.6	40.46	$9.23 (\pm2.38)\times10^3$	$1.28 (\pm0.48)\times10^2$	$3.82 (\pm0.49)\times10^4$
Dienestrol	5.43[f]	317.8	40.46	$1.63 (\pm0.41)\times10^4$	$1.45 (\pm0.12)\times10^2$	$2.84 (\pm0.40)\times10^5$
4-*sec*-Butylphenol	3.08[d]	192.2	20.23	$6.63 (\pm3.78)\times10$	-	$1.45 (\pm0.07)\times10^3$
4-*tert*-Amylphenol	3.91[f]	214.4	20.23	$3.04 (\pm0.56)\times10^2$	$3.32 (\pm1.66)\times10$	$4.01 (\pm0.33)\times10^3$
4-Phenylphenol	3.20[d]	192.0	20.23	$4.47 (\pm0.34)\times10^2$	$4.77 (\pm0.13)\times10^2$	$4.87 (\pm0.23)\times10^3$
Butyl-4-hydroxybenzoate	3.57[d]	229.0	46.53	$2.99 (\pm0.57)\times10^2$	$1.80 (\pm0.52)\times10^2$	$3.49 (\pm0.27)\times10^3$
Benzyl-4-hydroxybenzoate	3.21[f]	214.0	46.53	$4.67 (\pm0.53)\times10^2$	$2.63 (\pm0.40)\times10^2$	$6.93 (\pm0.86)\times10^3$
4,4'-Dihydroxybenzophenone	2.19[f]	206.8	57.53	$5.44 (\pm1.31)\times10$	-	$5.05 (\pm0.11)\times10^2$
Diethylphthalate	2.42[g]	254.0	52.61	-	-	$5.93 (\pm2.20)\times10$
Progesterone	3.87[d]	406.6	34.14	$2.53 (\pm1.19)\times10^2$	$1.19 (\pm0.75)\times10^2$	$1.89 (\pm0.49)\times10^3$

Values in parentheses are standard deviations.
[a]Calculated using LeBas method (Reid et al., 1977).
[b]Calculated using the atomic contributors (Ertl et al., 2000).
[c]Yamamoto and Liljestrand (2004). [d]Hansch et al. (1995).
[e]Estimated from phenol using the fragment method (Hansch et al., 1979).
[f]Estimated using KOWWIN software (US Environmental Protection Agency, 2000).
[g]Ellington and Floyd (1996).

3.3.2. Correlation between log K_{lipw} and log K_{OW}

As illustrated in Figure 3-2, log K_{lipw} values did not correlate well with reported log K_{OW} values. Correlation coefficients (r^2) for DPPC and POPC liposomes were approximately 0.78, whereas that for DPPC/cholesterol liposomes was only 0.37. These relationships are much weaker than those obtained by other studies using relatively smaller and structurally less diverse chemicals, for which r^2 values were typically are 0.9 or greater (Escher and Schwarzenbach, 1996; Gobas et al., 1988; Smejtek et al., 1996; Vaes et al., 1997; van Wezel et al., 1996). The linear correlation is weakest for the liposomes containing a high amount of cholesterol (40% by mass or 56% by mole fraction). The slopes in Figure 3.2a and 3.2c were not statistically different as determined by a *t* test, even at the 70% confidence interval. This indicates that selectivity in liposome-water systems is similar to that in octanol-water system regardless of lipid saturation, whereas a higher affinity is shown for unsaturated versus saturated liposomes. Figure 3-2b shows that log $K_{lipw,DPPC/cholesterol}$ was increased only with increasing hydrophobicity when log K_{OW} was 3.0 or less and 5.5 or greater, implying an invariance to the increase in hydrophobicity for moderately hydrophobic chemicals.

Examination of the types of compounds that deviate from the trends shown in Figure 3.2 are revealing. The two most hydrophobic alkylphenols, 4-nonylphenol and 4-*tert*-octylphenol, fall above the regression lines for all types of liposomes, whereas the two hydrophobic phthalate esters, benzylbutylphthalate and dibutylphthalate, fall below the regression lines for all cases. In addition, variation in log K_{lipw} values for steroid hormones, except for the most hydrophilic estriol, was not as great as the variation in their hydrophobicity. If only the five *p*-substituted phenols (4-*sec*-butylphenol, 4-*tert*-amylphenol, 4-phenylphenol, 4-nonylphenol, and 4-*tert*-octylphenol) from Figure 3.2 are

regressed, a much stronger linear relationship can be developed between log K_{OW} and log K_{lipw}, as shown in the literature using structurally similar and relatively small (MLV < 230 cm^3/mole) chemicals (Escher and Schwarzenbach, 1996; Gobas et al., 1988; Smejtek et al., 1996; Vaes et al., 1997; van Wezel et al., 1996):

$$\log K_{lipw,\ DPPC} = 1.15 \log K_{OW} - 1.57 \qquad n = 5,\ r^2 = 0.93 \text{ (at 22°C)} \qquad (3.4)$$

$$\log K_{lipw,\ DPPC/cholesterol} = 0.94 \log K_{OW} - 1.12 \qquad n = 4,\ r^2 = 0.66 \text{ (at 22°C)} \qquad (3.5)$$

$$\log K_{lipw,\ POPC} = 0.84 \log K_{OW} + 0.67 \qquad n = 5,\ r^2 = 0.96 \text{ (at 22°C)} \qquad (3.6)$$

The 4-phenylphenol had higher log K_{lipw} values compared with those predicted by linear regression for all three lipid-compositions, whereas 4-*sec*-butylphenol and 4-*tert*-amylphenol were slightly below the regression lines, suggesting that branching has a significant effect.

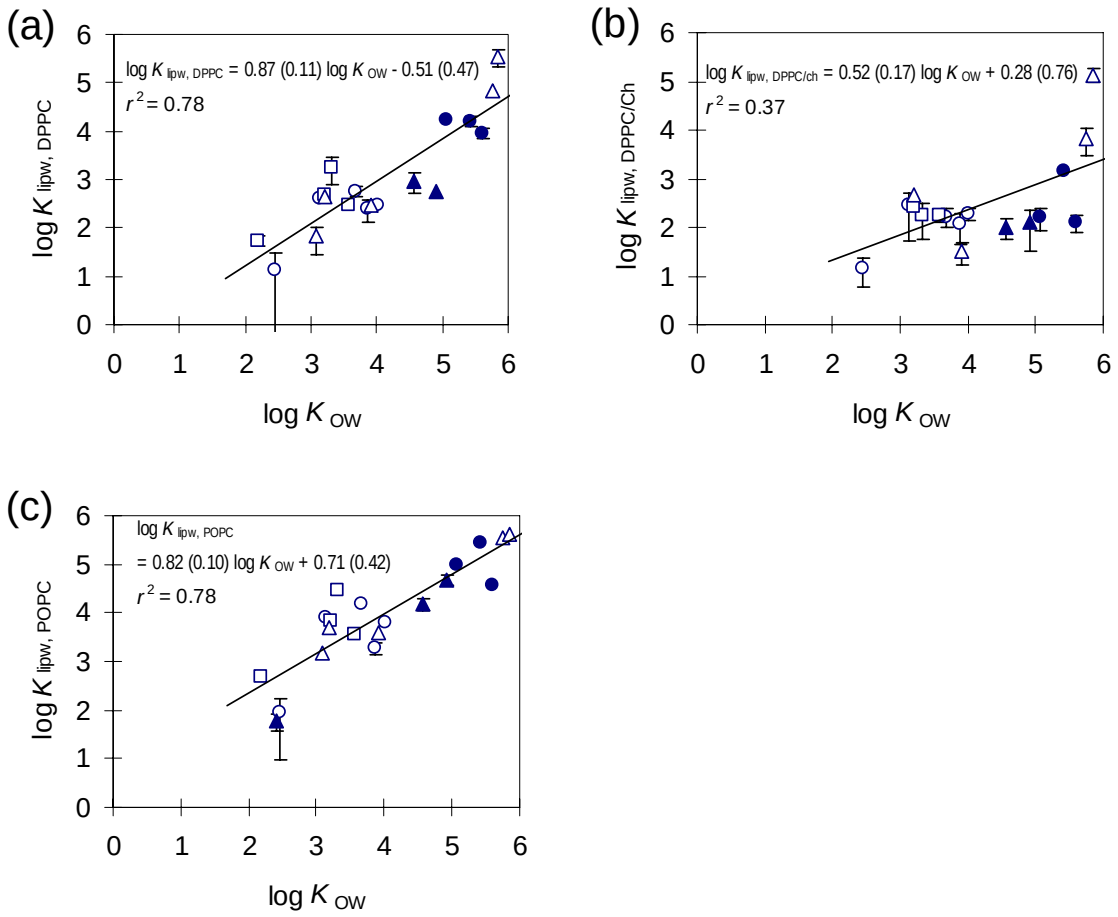

Figure 3.2: Relationship between reported octanol-water partition coefficients and liposome-water partition coefficient measured from (a) dipalmytoylphosphatidylcholine (DPPC), (b) dipalmytoylphosphatidylcholine/cholesterol (60:40 wt %), and (c) palmytoyloleoylphosphatidylcholine (POPC) with linear regression lines and equations. Values in parenthesis denote standard errors of the regression. Data are shown for steroid hormones and their derivatives (○), synthetic estrogens (●), p-substituted phenols (△), phthalate esters (▲), and other phenolic chemicals (□). Error bar denotes standard deviation, not shown when it is smaller than the symbol.

3.3.3. Effects of MLV and PSA

The free energy of solute transfer between an organic phase and water is determined by the free energy of cavity formation and solute-solvent interactions in the two phases. Gobas et al. (1988) suggested that the free energy of cavity formation would be dominant when a series of chemicals are relatively large and have similar solute-solvent interactions. They derived the following equation when the free energy of cavity formation follows a parabolic relationship with respect to MLV in the lipid membranes and is linearly proportional to MLV in 1-octanol:

$$\log K_{lipw} = (a + b\ \text{MLV}) \log K_{OW} + c \qquad (3.7)$$

where a and b are empirical constants related to differences in the free energy of cavity formation due to solute size and c is assumed to be a constant if differences in solute-solvent interactions among chemicals are negligible. Due to the relatively large molecular size of the selected EDCs, ranging from 190 to 400 cm^3/mole (Table 3.1), the free energy of cavity formation would be dominant, if their solute-solvent interactions are not significantly different. Using Equation 3.7, best-fit parameters and correlation coefficients (r^2) were obtained from the values presented in Table 3.1:

$$\log K_{lipw,\ DPPC} = (1.23\ (\pm 0.21) - 0.00097\ (\pm 0.00049)\ \text{MLV}) \log K_{OW} - 0.77\ (\pm 0.46)$$
$$n = 19,\ r^2 = 0.82\ (\text{at } 22°C) \qquad (3.8)$$

$$\log K_{lipw,\ DPPC/cholesterol} = (0.94\ (\pm 0.30) - 0.00122\ (\pm 0.00073)\ \text{MLV}) \log K_{OW} - 0.57\ (\pm 0.44) \qquad n = 17,\ r^2 = 0.47\ (\text{at } 22°C) \qquad (3.9)$$

$$\log K_{lipw,\ POPC} = (1.01\ (\pm 0.22) - 0.00051\ (\pm 0.00051)\ \text{MLV}) \log K_{OW} - 0.12\ (\pm 0.72)$$
$$n = 20,\ r^2 = 0.79\ (\text{at } 22°C) \qquad (3.10)$$

In all three equations, $\log K_{lipw}$ decreases with increasing MLV for compounds with the same hydrophobicity. This suggests that the additional free energy of cavity

formation in the lipid membranes per unit volume increases with increasing cavity size, because the (a + b MLV) term represents the ratio of free energy required for the formation of cavities in two organic phases (Gobas et al., 1988). Correlation coefficients increased slightly by including the effects of MLV, as seen by comparing Equation 3.8 to 3.10 with the respective equations in Figure 3.2. The correlations including MLV effects also show increasing b values with decreasing membrane fluidity (i.e., in the order of POPC<DPPC<DPPC/cholesterol), although this general trend is not statistically significant.

Effects of PSA were evaluated by multiple linear regression using log K_{OW} and PSA as independent variables, and the results are as follows:

$$\log K_{lipw,\ DPPC} = 0.82\ (\pm\ 0.12)\ \log K_{OW} - 0.014\ (\pm\ 0.010)\ PSA + 0.22\ (\pm\ 0.70)$$
$$n = 19,\ r^2 = 0.80\ (\text{at } 22°C) \qquad (3.11)$$

$$\log K_{lipw,\ DPPC/cholesterol} = 0.40\ (\pm\ 0.16)\ \log K_{OW} - 0.032\ (\pm\ 0.014)\ PSA + 1.99\ (\pm\ 1.01)$$
$$n = 17,\ r^2 = 0.54\ (\text{at } 22°C) \qquad (3.12)$$

$$\log K_{lipw,\ POPC} = 0.78\ (\pm\ 0.11)\ \log K_{OW} - 0.009\ (\pm\ 0.010)\ PSA + 1.23\ (\pm\ 0.68)$$
$$n = 20,\ r^2 = 0.79\ (\text{at } 22°C) \qquad (3.13)$$

As shown in Equations 3.11 to 3.13, log K_{lipw} is negatively correlated with PSA, with slight improvement in r^2 values as compared with those without including PSA. As was the case for MLV, the coefficient for PSA increases with decreasing membrane fluidity, but again, this trend is not statistically significant. This implies that transferring a molecule having hydrogen bonding capacity into a more structurally ordered lipid membrane generally requires more free energy than transferring the same molecule into less structurally ordered membranes.

3.4. DISCUSSION

3.4.1. Relationship between log K_{lipw} and log K_{OW}

Weak/moderate relationships between log K_{lipw} and log K_{OW} for selected EDCs (Figure 3.2) strengthen the suggestion that log K_{OW} has only limited potential for prediction of bioconcentration of endocrine disruptors (Yamamoto and Liljestrand, 2004). Unlike dissolution of organic solutes in a solvent like octanol, which is a homogeneous distribution, the dissolution in liposomes distributed with respect to diameter and local sterol content is not a homogeneous distribution. Solute partitioning would be more favored in regions with more favorable cavity formation. Effects of molar volume become more apparent when the molar volume of a solute is not directly related to its hydrophobicity. Most of the previous studies on conventional water pollutants have found that molar volume of solutes was related linearly with their log K_{OW} (Escher and Schwarzenbach, 1996; Gobas et al., 1988; Smejtek et al., 1996; Vaes et al., 1997; van Wezel et al., 1996). Thus, steric effects could be masked from their regression analyses. Weakest correlation between log K_{lipw} and log K_{OW} occurred for liposomes containing a high amount of cholesterol (56% by mole fraction). The amount of cholesterol used in the present study would be an extreme case, because cholesterol content may vary from about 12% by mole in the endoplasmic reticulum to between 30 and 50% by mole fraction in plasma membranes (Jain, 1988). Whereas the compounds chosen do not reflect the full range of chemical structure for EDCs, further investigation is needed to determine the effects of cholesterol on the bioconcentration of moderately hydrophobic EDCs.

3.4.2. Effects of the membrane fluidity on K_{lipw}

Effects of lipid components on the partition coefficients can be interpreted by the fluidity of the membrane. Because of the carbon-carbon double bond in the unsaturated hydrophobic tails of POPC, the average distance between phospholipid molecules is greater than that of saturated lipid molecules, such as DPPC (Jain, 1988). This less dense distribution of lipid molecules provides more cavities for sorption, lowering hydrophobic interaction and increasing membrane fluidity. The observed trend of higher K_{lipw} values for unsaturated lipid components compared with those for saturated lipids is in agreement with that in previous studies (Cantor, 2001; Liu et al., 2001; Yamamoto and Liljestrand, 2004).

The presence of cholesterol in the lipid bilayer makes the lipid membrane more rigid (Jain, 1988) by filling the free spaces in the hydrophobic tail region (Figure 3.3). Higher cholesterol contents in the lipid membranes also lower the partition coefficient between water and lipid membranes (Cantor, 2001; Lagerquist et al., 2001; Liu et al., 2001; Yamamoto and Liljestrand, 2004). Moreover, the decrease in log K_{lipw} on addition of cholesterol to the lipid membrane generally was greater for more hydrophobic chemicals, as in Figure 3.4. The Δlog K_{lipw} values, defined as the differences between log $K_{lipw,\ DPPC}$ and log $K_{lipw,\ DPPC/cholesterol}$, ranged from 0 (4-phenylphenol) to 2.0 (diethylstilbestrol). For 4-nonylphenol and 4-*tert*-octylphenol, the effects of cholesterol were not as great as for other hydrophobic chemicals such as diethylstilbestrol and hexestrol, which have Δlog K_{lipw} values of 2.00 and 1.86, respectively. This tendency is consistent with the findings of Liu et al. (2001) and Lagerquist et al. (2001), who found that log K_{lipw} for hydrophobic drugs with lipid membranes containing 40% by mole fraction cholesterol were less than those from lipid membranes without cholesterol by 0.5 log units, whereas these drops were negligible for more hydrophilic drugs. As a result of

this general tendency, log $K_{lipw,\ DPPC/cholesterol}$ did not correlate with log K_{OW} especially for moderately hydrophobic EDCs, as shown in Figure 3.2. The binding locations of a solute into the lipid bilayer can be divided into three regions: Near the polar head groups, hydrophobic tails with a high conformational order, and center of the bilayer. In general, more hydrophobic chemicals are believed to partition closer to the bilayer center (e.g., Scheidt et al., 2004). A decrease in log K_{lipw} on the addition of cholesterol may be explained by two mechanisms. First, a solute competes for the same binding site with cholesterol, and second, cholesterol restricts the motion of fatty acyl chains by occupying free spaces in the outer parts of them and, thus, reducing the membrane fluidity. As described in Figure 3.3, the effects of cholesterol would be greatest for chemicals entering the ordered hydrophobic tail region. Moderately hydrophobic EDCs with relatively high molar volume could be affected by both mechanisms, because they may partition into ordered hydrophobic tails and compete with cholesterol. Therefore, no increase in log $K_{lipw,\ DPPC/cholesterol}$ for these chemicals with increasing hydrophobicity could be explained by significant competition with cholesterol. For example, Jacobsohn et al. (1994) and Golden et al. (1998) have shown that the binding location of 17-β-estradiol moves toward the outer part of the bilayer by the addition of cholesterol. Conversely, $\Delta\log K_{lipw}$ could be smaller for 4-nonylphenol and 4-*tert*-octylphenol if they do not compete with cholesterol.

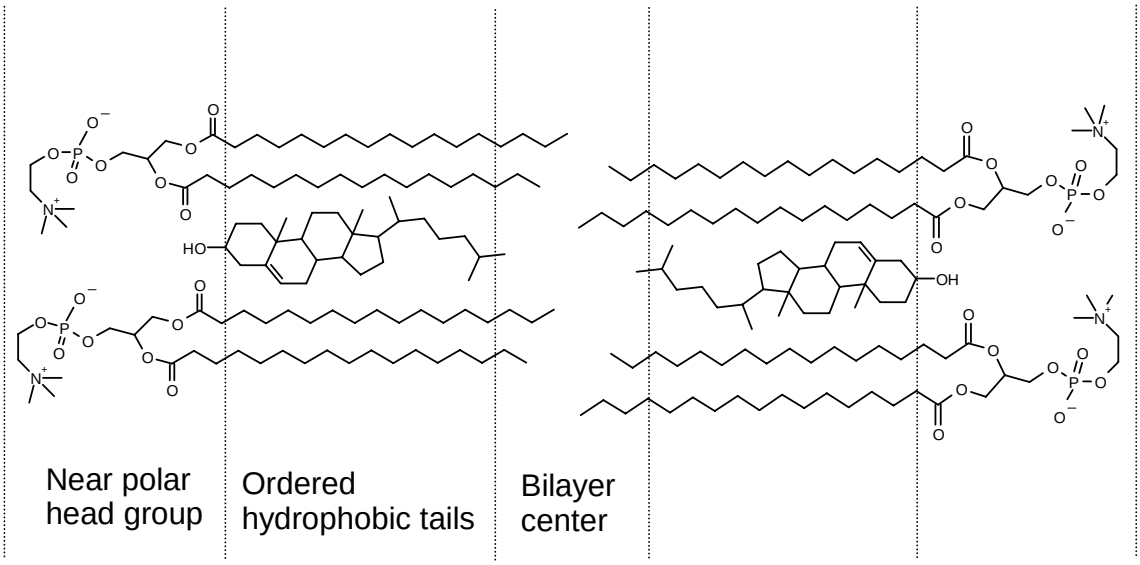

Figure 3.3: Cholesterol molecule in the dipalmytoylphostatidylcholine (DPPC) lipid bilayer and three zones of the lipid bilayer.

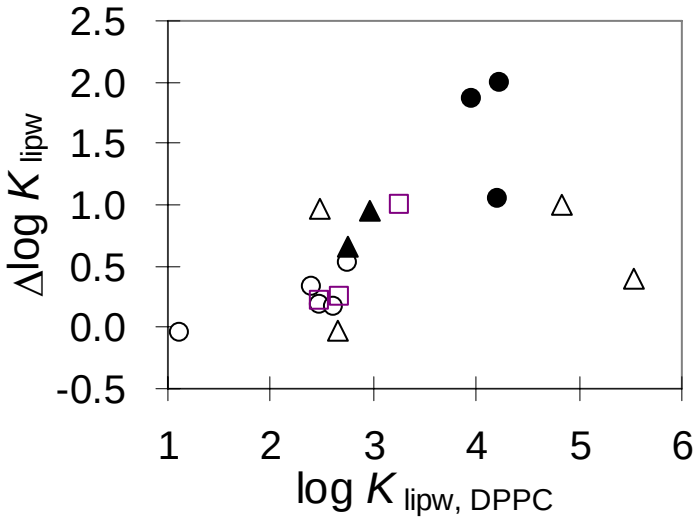

Figure 3.4: Effects of cholesterol on the drop in log K_{lipw} from dipalmytoylphostatidylcholine (DPPC) liposomes. $\Delta\log K_{lipw}$ is calculated from $\log K_{lipw,\ DPPC} - \log K_{lipw,\ DPPC/cholesterol}$. Data are shown for steroid hormones and their derivatives (○), synthetic estrogens (●), *p*-substituted phenols (△), phthalate esters (▲), and other phenolic chemicals (□).

3.4.3. Effects of MLV and PSA

Although it has been observed that linear correlations between log K_{lipw} and log K_{OW} breaks down for chemicals with higher molar volume (Dulfer and Govers, 1995; Gobas et al., 1988), the effects of MLV could not be separated from hydrophobicity, because they were strongly correlated. However, Equations 3.8 to 3.10 showed independent contribution of MLV from hydrophobicity, because collinearity between MLV and log K_{OW} was very low for the chemicals selected in the present study.

Studies have shown that human intestinal absorption of drugs (see, e.g., Clark, 1999; Veber et al., 2002; Zhu et al., 2002)) and blood-brain barrier partition coefficient (see, e.g., Feher et al., 2000) correlate negatively with PSA. Polar surface area, defined as the surface area contributed by oxygen or nitrogen atoms or hydrogen atoms attached to oxygen or nitrogen atoms, is related to the chemical's capacity to form hydrogen bonds (Clark, 1999). Equations 3.11 to 3.13 suggest that more energy is required to transport a molecule having greater hydrogen bonding capacity into the lipid membranes than into the bulk organic solvent 1-octanol. The negative contribution of PSA is also consistent with the findings of Vaes et al. (1998) that log $K_{lipw,\ DMPC}$ correlated negatively with quantum mechanical descriptors representing greater hydrogen-bonding interaction. As for MLV, the coefficient for PSA increased with decreasing membrane fluidity, but again, this trend is not statistically significant. This implies that transferring a molecule having hydrogen-bonding capacity into a more structurally ordered lipid membrane requires more free energy than into less structurally ordered membranes. However, there would be compensating effects of PSA if a molecule associates with polar head groups via specific polar interactions (see, e.g., Niu and Litman, 2002).

3.4.4. Effects of molecular geometry

In addition to hydrophobicity, molecular size, and polar interactions, molecular geometry may affect the relationship between log K_{lipw} and log K_{OW}. As shown in Figure 3.1, the chemical structures of the synthetic estrogens, diethylstilbestrol, hexestrol, and dienestrol, are very similar. Their differences in PSA and MLV are negligible. However, the measured log K_{lipw} values for hexestrol with each of the three different liposomes are significantly lower than those for diethylstilbestrol and dienestrol. The flat structures of diethylstilbestrol and dienestrol, due to the delocalization of π electrons, make these molecules easily accommodated in the structured hydrophobic tail region of the membrane bilayer. Conversely, conformational restriction is expected when hexestrol enters membranes, because rotation along the carbon-carbon single bond in the middle of the compound requires a large free volume. This also would be consistent with the observed higher log K_{lipw} for 4-phenylphenol being higher than predicted by the regression line as a result of its flat structure. Although the carbon-carbon single bond contributes more in hydrophobicity to the log K_{OW} estimated by atomic fragmentation methods compared with a carbon-carbon double bond (Meylan and Howard, 1995), a more careful approach is required when estimating log K_{lipw} from molecular structure.

3.4.5. Statistical evaluation of the models

The standardized regression coefficients were calculated to evaluate the importance of the two variables, log K_{OW} and MLV × log K_{OW} or log K_{OW} and PSA (Table 3.2). As can be seen in Equations 3.11 to 3.13, the importance of MLV was greatest for estimating log $K_{lipw,\ DPPC/cholesterol}$ and comparable to the significance of log K_{OW}. Similarly, for Equations 3.11 thtough 3.13, the contribution of PSA was almost the same as that of log K_{OW} for predicting log $K_{lipw,\ DPPC/cholesterol}$, whereas PSA effects were very small for predicting log $K_{lipw,\ DPPC}$ and log $K_{lipw,\ POPC}$. Because improvements in

correlation coefficients obtained by incorporating additional model parameters do not imply that a model is superior, a small-sample Akaike information criterion (AIC_c) was used to provide a standard criterion for model performance. The AIC_c values obtained using the MLV containing model were lower for DPPC and DPPC/cholesterol liposomes than those obtained using solely log K_{OW} suggesting that adding MLV to these systems is justified, especially for DPPC liposomes. The AIC analysis also showed that PSA effects were greatest for the most structurally rigid lipid membrane, DPPC/cholesterol liposomes. Adding either MLV or PSA effects did not improve the predictive model for the most flexible lipid membrane, POPC liposomes, in terms of AIC_c. As indicated above, the effects of an additional descriptor, MLV or PSA, were more significant for the more structurally organized lipid membranes.

Table 3.2: Standardized regression coefficients[a] from multiple linear regressions.

Variables in the model		log $K_{lipw, DPPC}$	log $K_{lipw, DPPC/cholesterol}$	log $K_{lipw, POPC}$
log K_{OW} and Molar Liquid Volume (MLV) eq. 3.8-3.10	log K_{OW}	1.232	1.198	1.015
	MLV×log K_{OW}	-0.411	-0.719	-0.153
log K_{OW} and Polar Surface Area (PSA) eq. 3.11-3.13	log K_{OW}	0.831	0.472	0.840
	PSA	-0.162	-0.430	-0.117

[a]Regression coefficients on autoscaled variables, indicating the change in the standard units of the dependent variable for each increase of one standard unit in the independent variable, controlling for all other independent variables.

3.4.6. Implication of the study

For certain EDCs in the present study, K_{lipw} varied almost two orders of magnitude because of the changes in lipid composition of the membrane vesicles. This may reflect the interspecies variation of lipid-normalized bioconcentration factor (LBCF) as well as differences in LBCFs among different organs. Effects of lipid components on LBCFs may be evaluated by further research. The equilibrium partition coefficient between aqueous buffer and the lipid compartment with a specific lipid composition could be a significant parameter determining internal distribution of hydrophobic pollutants in the body of aquatic organisms as well as other physiological processes. Potential improvement of empirical quantitative structure-activity relationships could be achieved by additional descriptors, such as MLV and PSA.

Chapter 4: Partitioning Thermodynamics of the Selected Endocrine Disruptors between Water and Synthetic Membrane Vesicles: Effects of Membrane Compositions

The thermodynamics of partitioning of selected endocrine disrupting compounds between water and synthetic membrane vesicles were investigated. For most chemicals investigated, partitioning is dominated by the enthalpy change for unsaturated lipid membrane vesicles, whereas it is dominated by the entropy contribution for saturated lipid membrane vesicles. The contribution of entropy terms becomes more important compared to the enthalpy term with increased branching of *p*-substituted phenols in determining the free energy change. These results indicate that the thermal energy required for and the entropy gain associated with the creation of cavity in the lipid bilayer is of critical importance in differentiating the process from 1-octanol/water partitioning. In addition, partitioning thermodynamics are significantly influenced by cholesterol content in the lipid membranes. Results of the present study and studies in the literature suggest that partitioning processes significantly depend on the physical state of the lipid membranes and log K_{OW}-based quantitative structure-activity relationships may be theoretically applicable only for the case that the bioconcentration is dominated by the equilibrium partitioning between water and unsaturated fatty acid components or storage lipids.

4.1. INTRODUCTION

It has been generally acknowledged that hydrophobic organic pollutants accumulate in lipid compartments of the body. For this reason, bioconcentration of xenobiotic chemicals has been estimated from equilibrium partition coefficients between

water and surrogate organic phases, such as 1-octanol/water partition coefficient (K_{OW}) (e.g., Davies and Dobbs, 1984; Hansch and Leo, 1995; Neely et al., 1974). Although K_{OW} is proven to be a good parameter for the estimation of biopartitioning especially for non-polar organic chemicals, many researchers have indicated that the 1-octanol/water partition coefficient has only limited potential for estimating bioconcentration for a wide range of organic chemicals in phytoplanktons (Swackhamer and Skoglund, 1993) and in fish (Opperhuizen et al., 1988). Moreover, recent studies have shown that K_{OW} does not correlate well with the partition coefficient between water and lipid membrane vesicles (K_{lipw}), theoretically better surrogates for biological membranes, for structurally diverse organic chemicals (Kwon et al., 2006a; Yamamoto and Liljestrand, 2004).

Most of the quantitative structure-activity relationships (QSARs) between K_{OW} and bioconcentration factors (or K_{lipw}) rely on the assumption that the free energy change of a solute transfer from water to 1-octanol ($\Delta G_{w\rightarrow o}$) is linearly related to that from water to biological lipid phases ($\Delta G_{w\rightarrow l}$) (Hansch and Leo, 1995). However, Opperhuizen et al. (1988) showed that the partitioning of chlorinated benzenes between water and fish is thermodynamically different from that between water and 1-octanol. Whereas the former is characterized by a positive enthalpy change and is driven by the entropy change, the latter is driven by a large negative enthalpy change. Similarly, Woodrow and Dorsey (1997) reported that the free energy of solute transfer is dominated by the entropy change for surfactant micelle/water partitioning, although the enthalpy change (ΔH) is slightly negative. However, van Wezel and Opperhuizen (1995) showed that ΔH of partitioning between water and fish storage lipids was negative and thus the partitioning process is driven by enthalpy change as is the case with K_{OW}. Because storage lipids do not form highly organized structures, such as bilayers or micelles, it may be deduced that the

higher organization of lipid molecules in biological membranes discriminates the partitioning thermodynamics in water/lipid membranes system.

In spite of the large variation in body lipid components, bioconcentration factors (BCFs) in aquatic animals are typically normalized by total lipid contents (e.g., Bertelsen et al., 1998; Geyer et al., 1985). There have been a few studies to relate bioaccumulation with lipid compositions (Bergen et al., 2001; Ewald and Larsson, 1994). Ewald and Larsson (1994) observed significantly less accumulation in fish species containing high phospholipids contents using 2,2',4,4'-tetrachlorobiphenyl as a model compound, indicating that it is more soluble in non-membrane lipids. However, there are large gaps between measured BCFs at an organism level and equilibrium partition coefficients between water and different lipid components even when biopartitioning is dominated by chemical equilibrium between water and biological organic phases of an organism. Fish have various types of fatty acids in their membranes. In addition, fatty acid composition is significantly different from one species to another as well as from one organ to another within an individual (Henderson and Tocher, 1987). Biopartitioning is also affected by temperature (e.g., Hazel, 1995; Robertson and Hazel, 1995) and diet (e.g., Castell et al., 1994). Thus, a better characterization of the roles of fatty acid components in the membranes is needed for development of more reliable QSARs.

Consequently, we evaluated the enthalpy change (ΔH) and entropy change (ΔS) of partitioning between water and lipid membrane vesicles formed from two surrogate phospholipids, dipalmitoylphosphatidylcholine (DPPC, C16:0, 16:0) and palmitoyloleoylphosphatidylcholine (POPC, C18:1, 16:0), each of which serves a representative saturated and unsaturated lipid, respectively. Sixteen structurally diverse endocrine disrupting chemicals (EDCs) were investigated for evaluating the effects of saturation in lipid tails. The effects of lipid components were further evaluated using

additional liposomes comprised of dimyristoylphosphatidylcholine (DMPC), distearylphosphatidylcholine (DSPC), and dioleoylphosphatidylcholine (DOPC) for 17β-estradiol, diethylstilbestrol, bisphenol A and nonylphenol. In addition, the effects of cholesterol, a common membrane strengthening agent, on the partitioning thermodynamics in saturated and unsaturated liposomes were investigated by varying cholesterol contents.

4.2. MATERIALS AND METHODS

4.2.1. Chemicals

Sixteen moderately hydrophobic endocrine disrupting chemicals were selected to investigate thermodynamics of partitioning between water and synthetic lipid membrane vesicles, including natural hormones (17β-estradiol, estrone), synthetic estrogens (ethynylestradiol, diethylstilbestrol, meso-hexestrol, and dienestrol), break-down products of alkylphenol ethoxylates (4-n-nonylphenol, 4-tert-octylphenol, 4-*sec*-butylphenol, and 4-*tert*-amylphenol) and industrial estrogenic compounds (bisphenol A, benzyl-4-hydroxybenzoate, butyl-4-hydroxybenzoate, 4-phenylphenol, dibutylphthalate, benzylbutylphthalate). Diethylstilbestrol (99%), meso-hexestrol (98%), dienestrol (98%), and diethylphthalte (99.5%) were purchased from Sigma Chemical Co. (St. Louis, MO, USA). 4- *sec*-butylphenol (98%), 4-*tert*-amylphenol (99%), 4,4'-dihydroxybenzophenone (99%), and benzyl-4-hydroxybenzoate (99%) were obtained from Aldrich Chemical Co. (Milwaukee, WI, USA). 4-Phenylphenol (98%) and butyl-4-hydroxybenzoate (99%) were purchased from Fluka Chemical Co. (Milwaukee, WI, USA). Dipalmytoylphosphatidylcholine (DPPC, C16:0, 16:0) and palmytoyloleoylphsphatidylcholine (POPC, C18:1, 16:0) were chosen as model saturated

and unsaturated lipid membrane phases due to their abundance in biological membranes. Dimyristoylphosphatidylcholine (DMPC, C12:0, 12:0), distearylphosphatidylcholine (DSPC, C18:0, 18:0), and dioleoylphosphatidylcholine (DOPC, C18:1, 18:1) were also chosen for further investigation for 17β-estradiol, diethylstilbestrol, bisphenol A and nonylphenol. DPPC and DOPC liposomes with varying cholesterol contents were used to evaluate the effects of cholesterol in lipid membranes on the thermodynamics. Chloroform solutions of model lipid components, DOPC, POPC, DMPC, DPPC and DSPC were purchased from Avanti Polar Lipids (Albaster, AL, USA). Cholesterol was purchased from Aldrich Chemical Co. (Milwaukee, WI, USA).

4.2.2. Preparation of liposome suspensions

Large unilamella vesicle suspensions of selected lipid components were prepared using the thin film hydration technique (Mueller et al., 1983) followed by rapid extrusion processes (Hope et al., 1985), as described previously (Kwon et al., 2006a). The chloroform solution of the lipid was evaporated under a gentle nitrogen stream and the thin residue film was dissolved in dilution water (buffered at pH 7.0 and ionic strength of 0.02 M, using KH_2PO_4, NaOH, and NaCl) to make the liposome suspension. The suspension was further extruded through a polycarbonate membrane several times to reduce vesicle polydiversity.

4.2.3. Determination of K_{lipw} using equilibrium dialysis technique

Partition coefficients of the selected chemicals were determined by the equilibrium dialysis technique described in literature (Escher and Schwarzenbach, 1996; Kwon et al., 2006a). Two 2 mL amber vials were separated by a dialysis membrane (MWCO 10,000). Solution containing EDCs was used to fill one cell and lipid vesicle suspension (concentration of lipid, m) was used to fill the other. Equilibrium partition

coefficients were determined by analyzing the remaining aqueous EDC concentrations in the vial without lipid vesicles in the sample reactors (C_w, mg/L) and both sides of the reference reactors (C_{ref}, mg/L) that initially contained buffer solution instead of lipid suspensions. Chemical analyses were performed after 14 day incubation (28 day incubation at 11°C). Preliminary studies showed that apparent equilibrium was obtained after 14 days (28 days at 11°C) using a custom-made tumbling device. The aqueous concentrations of the selected chemicals were measured using a Waters 2690 high-performance liquid chromatography system equipped with a Waters 996 photodiode array detector (Milford, MA, USA). The partition coefficient (K_{lipw}) was calculated using

$$K_{lipw}\left(\mathrm{L/kg-lipid}\right)=\frac{C_{ref}-C_w}{C_w m} \quad (4.1)$$

4.2.4. Determination of thermodynamic functions of a solute transfer

For the evaluation of partitioning thermodynamics, K_{lipw} values were obtained at 11, 22, 30, and 37°C. The enthalpy change ($\Delta H_{w\to l}$) and the entropy change ($\Delta S_{w\to l}$) of solute transfer from water to lipid membrane vesicles were obtained from the slope and the intercept of the regression, log K_{lipw} vs. $1/T$, using van't Hoff relationship:

$$\log K_{lipw}=-\frac{\Delta H_{w\to l}}{2.303R}\frac{1}{T}+\frac{\Delta S_{w\to l}}{2.303R} \quad (4.2)$$

where R is gas constant (8.314 J/mole-K) and T is temperature (K). $\Delta H_{w\to l}$ and $\Delta S_{w\to l}$ represent the change in enthalpy and entropy, respectively, when one mole of a solute is transferred from 1 L aqueous solution to 1 kg lipid membrane vesicles at infinite dilution.

4.3. RESULTS AND DISCUSSION

4.3.1. Effects of membrane compositions

Table 4.1 shows K_{lipw} values between water and POPC vesicles ($K_{lipw,POPC}$) and between water and DPPC vesicles ($K_{lipw,DPPC}$) at 11, 22, 30 and 37°C. For most endocrine disrupting chemicals investigated, $K_{lipw,POPC}$ decreases with increasing temperature whereas $K_{lipw,DPPC}$ increases with increasing temperature. Enthalpy change (ΔH) and entropic contribution ($T\Delta S$) at 22°C in the partitioning process calculated using Equation 4.2 are shown in Table 4.2 with r^2 values of the regression. As can be seen from Table 4.2, solute transfer from water to POPC liposomes is generally driven by thermal energy gain. Entropy contribution is greater for the two phthalates. However, their entropic contribution in partitioning between water and POPC liposomes is significantly smaller than that between water and DPPC liposomes. Conversely, solute transfer from water to DPPC vesicles is generally endothermic (i.e. $\Delta H>0$), but driven by large entropy gain. Estrone and *p*-*tert*-octylphenol have negative enthalpy changes in both cases, indicating the processes are exothermic. There are negligible changes in enthalpy and entropy for *p*-*tert*-octylphenol between saturated and unsaturated lipids. However, the enthalpy contribution on the partitioning of estrone into DPPC liposomes is much smaller than into POPC liposome, whereas entropy gain is higher for DPPC liposomes. Thus, partitioning into saturated liposomes requires more thermal energy and the overall process is more likely to be driven by the entropy change compared to partitioning into unsaturated analogues, except for *p*-*tert*-octylphenol. The initial concentration of *p*-*tert*-alkylphenol of 1.0~1.8 mg/L was comparable to the typical liposome concentrations (3.0~10.0 mg/L), whereas that of *n*-nonylphenol was ~0.4 mg/L. At these relative concentrations, the infinite dilution assumption may not be applicable and alteration of the membrane

fluidity may be possible as sorbed non-ionic surfactants in lipid membranes may increase membrane fluidity (Edwards and Almgren, 1992).

Table 4.1: Liposome-water partition coefficients for 16 EDCs obtained at 4 different temperatures using palmitoyloleoylphosphatidylcholine (POPC) and dipalmitoylphosphatidylcholine (DPPC) liposomes.

Chemicals	K_{lipw} ($\times 10^3$ L/kg liposomes)							
	POPC liposomes				DPPC liposomes			
	11°C	22°C	30°C	37°C	11°C	22°C	30°C	37°C
Estrone	6.58 (0.76)	5.65 (1.03)	4.15 (1.17)	1.22 (0.21)	0.69 (0.24)	0.70 (0.14)	0.55 (0.14)	0.44 (0.07)
17β-Estradiol	2.13 (0.25)	1.63 (0.67)	1.43	1.41	0.15 (0.04)	0.17 (0.04)	0.21	0.25
Ethynylestradiol	5.95 (1.74)	5.12 (0.09)	3.96 (0.26)	2.76 (0.37)	0.45 (0.05)	0.34 (0.12)	0.52 (0.02)	0.82 (0.01)
Diethylstilbestrol	77.1	57.9 (3.6)	55.4 (10.6)	35.3 (3.8)	8.42 (0.73)	14.9 (3.3)	14.4 (1.7)	24.6 (2.9)
meso-Hexestrol	36.8	30.4 (10.2)	25.1	10.5 (1.6)	4.37 (0.49)	4.96 (0.97)	5.74 (1.32)	5.54 (0.58)
Dienestrol	201	117	94.4 (5.5)	64.5 (25.9)	18.5 (2.3)	11.3 (0.9)	19.3	17.8 (0.3)
4-*n*-Nonylphenol	966 (319)	664 (35)	442 (114)	304 (130)	512 (143)	617 (199)	543 (75)	885 (406)
4-*tert*-Octylphenol	630 (40)	275 (55)	219	145 (75)	482 (20)	409	256 (119)	132 (16)
4-*tert*-Amylphenol	3.73 (0.05)	3.81 (0.18)	3.46 (0.22)	2.18 (0.36)	0.35 (0.04)	0.43 (0.06)	0.66 (0.09)	1.20 (0.79)
4-*sec*-Butylphenol	2.73 (0.22)	1.95 (0.23)	1.96 (0.13)	1.30 (0.10)	0.22 (0.03)	0.18 (0.02)	0.29 (0.02)	0.42 (0.02)
4-Phenylphenol	7.48 (0.87)	5.41(0.16)	3.87	2.25 (0.52)	0.64 (0.01)	0.53 (0.01)	0.66 (0.01)	1.17 (0.04)
Bisphenol A	12.0	7.59	6.78 (0.18)	3.17 (0.32)	1.10 (0.02)	0.79 (0.06)	1.38 (0.16)	1.67 (0.08)
Dibutylphthalate	3.96 (0.33)	6.11 (0.28)	4.28 (0.17)	3.18 (2.26)	0.43 (0.03)	0.46 (0.04)	0.86 (0.07)	1.19 (0.38)
Benzylbutylphthalate	12.8 (0.9)	18.3	12.1 (4.3)	15.1 (4.8)	2.01 (0.16)	4.19 (0.11)	4.80 (2.37)	4.56 (0.15)
Butyl-4-hydroxybenzoate	3.73 (0.09)	3.08 (0.04)	3.09 (0.11)	1.20 (0.30)	0.36 (0.05)	0.39 (0.03)	0.39 (0.03)	1.03 (0.11)
Benzyl-4-hydroxybenzoate	8.29 (0.74)	6.96 (0.04)	6.32	3.21 (0.07)	0.70 (0.04)	0.60 (0.02)	0.66 (0.05)	1.20 (0.05)

Values in parentheses are standard deviation of triplicate analyses. Average values are used when duplicates are used without standard deviation

Excluding *p-tert*-nonylphenol, the results are generally consistent with those reported in the literature, which show that partitioning into gel phase liposomes is typically driven by entropy change (Ávila and Martinez, 2003; van Wezel et al., 1996) whereas partitioning into liquid-crystalline phase liposomes is driven by enthalpy change (Seelig and Ganz, 1993; van Wezel et al., 1996; Wenk et al., 1996; Wimley and White, 1993). Partitioning into mixed lipid such as egg-phosphatidylcholine has been reported to be driven by either enthalpy change (Takegami et al., 2003) or entropy change (Yang et al., 2000b).

Experimental partition coefficients at four temperatures (five for DMPC liposomes) using five different types of liposomes are shown in Figure 4.1 for the selected endocrine disruptors, 17β-estradiol, bisphenol A, diethylstilbestrol, and nonylphenol. For these two model lipid membranes, the thermodynamics of partitioning strongly depends on lipid saturation. Partition coefficients for nonylphenol are not significantly different with respect to lipid compositions (Fig. 4.1d). For the selected chemicals, the partitioning process is dominated by the enthalpy gain for unsaturated DOPC liposomes, whereas it is dominated by the entropy change for saturated DSPC liposomes, except for bisphenol A. In addition, the partition coefficient between water and DMPC liposomes generally increases with increasing temperature below the main transition temperature (T_m = 23°C; *29*), but decreases with increasing temperature above T_m, except for *n*-nonylphenol. Although DMPC is a saturated lipid, its physical state (liquid crystalline phase) is closer to that of unsaturated liposomes at temperatures above T_m. Thus, the physical state of the lipid membrane is critical in determining the partitioning behavior of these hydrophobic organic chemicals.

Table 4.2: Enthalpies (ΔH) and entropies (ΔS) of partitioning between water and synthetic membrane vesicles.

	$K_{lipw, POPC}$			$K_{lipw, DPPC}$		
Chemicals	ΔH (kJ/mole)	$T\Delta S$* (kJ/mole)	r^2	ΔH (kJ/mole)	$T\Delta S$* (kJ/mole)	r^2
Estrone	-42.6 (18.8)	-22.1 (18.6)	0.72	-12.5 (4.8)	3.3 (4.7)	0.78
17β-Estradiol	-12.2 (2.3)	-6.1 (2.3)	0.93	14.4 (2.0)	27.2 (2.0)	0.96
Ethynylestradiol	-21.0 (4.8)	-0.3 (4.8)	0.91	16.4 (12.5)	31.6 (12.4)	0.46
Diethylstilbestrol	-19.7 (5.3)	7.2 (5.3)	0.87	27.0 (6.8)	50.3 (6.7)	0.89
meso-Hexestrol	-31.7 (12.5)	-6.7 (12.4)	0.76	7.5 (2.0)	28.4 (2.0)	0.88
Dienestrol	-30.9 (2.4)	-2.1 (2.4)	0.99	2.0 (11.6)	25.8 (11.5)	0.02
4-*n*-Nonylphenol	-13.1 (8.8)	19.3 (8.8)	0.98	12.2 (7.4)	44.8 (7.4)	0.57
4-*tert*-Octylphenol	-40.0 (4.5)	-8.9 (4.5)	0.98	-35.3 (10.1)	-4.2 (10.0)	0.86
4-*tert*-Amylphenol	-13.8 (7.6)	6.1 (7.6)	0.62	33.8 (8.4)	49.2 (8.4)	0.89
4-*sec*-Butylphenol	-17.7 (3.0)	1.0 (3.0)	0.79	18.8 (5.0)	32.3 (5.0)	0.59
4-Phenylphenol	-32.5 (5.9)	-11.7 (5.9)	0.94	15.1 (11.6)	31.1 (11.5)	0.46
Bisphenol A	-28.9 (5.6)	-6.9 (5.5)	0.93	13.7 (11.5)	30.9 (11.4)	0.41
Dibutylphthalate	-6.5 (11.7)	14.1 (11.6)	0.13	30.2 (8.3)	45.9 (8.2)	0.87
Benzylbutylphthalate	1.4 (8.6)	24.9 (8.5)	0.01	23.7 (8.6)	43.7 (8.6)	0.79
Butyl-4-hydroxybenzoate	-26.8 (14.1)	-7.3 (14.0)	0.64	23.8 (15.6)	38.8 (15.4)	0.54
Benzyl-4-hydroxybenzoate	-23.6 (9.6)	-2.1 (9.5)	0.75	12.3 (11.4)	28.5 (11.3)	0.37

*Entropy contribution ($T\Delta S$) to the free energy change (ΔG) calculated at 22°C. Values in parentheses are standard errors of the regression.

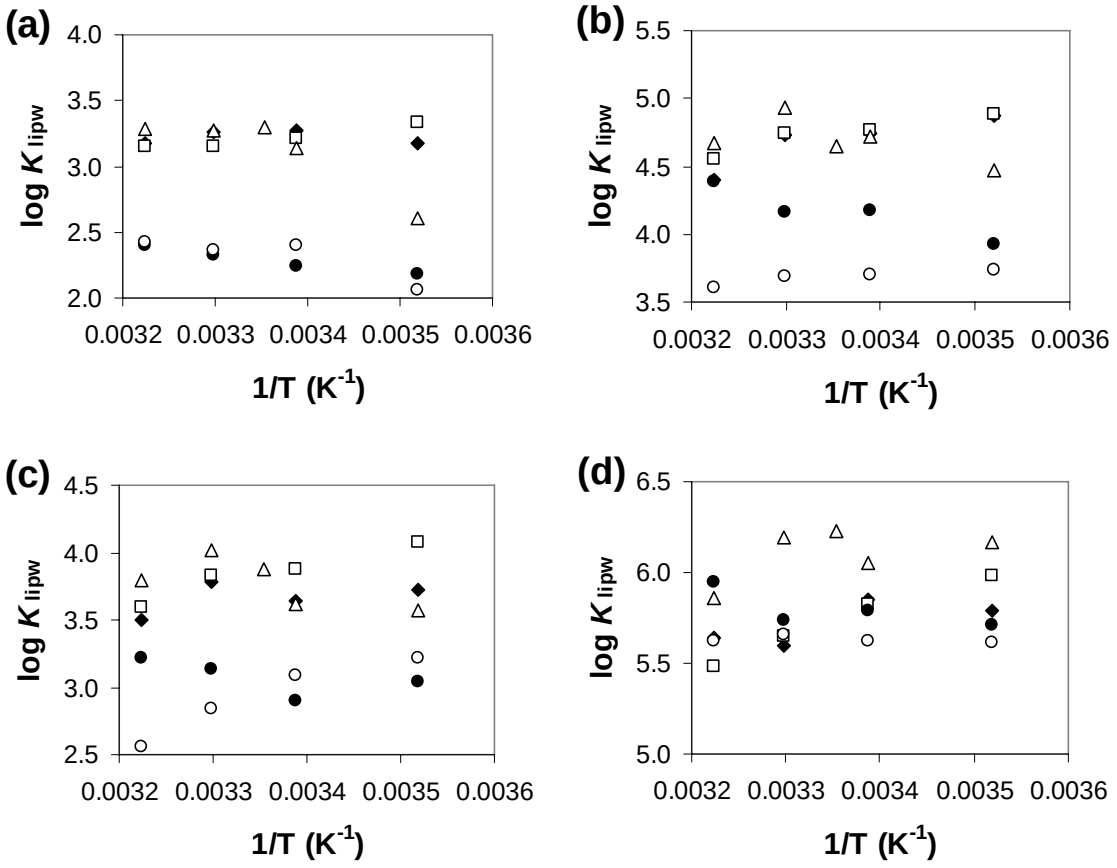

Figure 4.1: Effects of temperature on partitioning between water and various synthetic lipid membrane vesicles for (a) 17β-estradiol, (b) diethylstilbestrol, (c) bisphenol A, and (d) *p*-*n*-nonylphenol. Error bars denote standard deviations. (closed diamond: DOPC, open square: POPC, open triangle: DMPC, closed circle: DPPC, open circle: DSPC)

Partitioning of moderately hydrophobic organic chemicals between water and synthetic membrane vesicles is conceptually divided into two sequential processes, evaporating a solute from water and dissolving it to the organic phase. Dissolution in each solution can be further divided into two processes including the creation of a cavity for a solute and the formation of a new interaction between the solute and solvent molecules (Gobas et al., 1988; Katz and Diamond, 1974). The logarithm of the partition coefficient between water and an organic phase is related to the free energy of solute transfer from water to the organic phase (ΔG). It can be estimated from theoretical free energy changes including cavity creation and free energy of interaction between solute and solvent, as follows:

$$\Delta G = \Delta G_{s,org} - \Delta G_{s,w} = (\Delta G_{c,org} + \Delta G_{i,org}) - (\Delta G_{c,w} + \Delta G_{i,w}) = (\Delta G_{c,org} - \Delta G_{c,w}) + (\Delta G_{i,org} - \Delta G_{i,w}) \quad (4.3)$$

where subscript c denotes energy required for creating a cavity for a solute, i denotes interaction energy, and org and w represent the organic phase and water, respectively. As summarized in Figure 4.2, thermodynamic constants are affected differently by each process. Loss of a solute from water could be accompanied by a significant increase in entropy because water molecules near a hydrophobic solute are strictly organized (Tanford, 1980). Negative ΔH is expected by filling a cavity in water. Creation of a cavity in lipid bilayers requires more heat than in other organic phases because of their highly organized structure, whereas thermal energy gain due to newly formed van der Waals interaction would not be significantly different from that for other organic phases. The average distance between lipid components would be increased by introducing a sufficiently large molecule in the bilayers. This would result in positive ΔH and positive ΔS. Noticeable differences in partitioning thermodynamics in Table 4.2 for DPPC and POPC liposomes could attribute to $\Delta G_{c,org}$ because all other terms are not significantly

affected by the physical characteristics of lipid bilayers. More thermal energy would be required to move neighboring phosphatidylcholine molecules apart, and this would result in a corresponding increase in entropy. As can be seen in Table 4.2, the overall partitioning process is greatly affected by cavity creation and $\Delta G_{c,org}$ results in more positive enthalpy and entropy changes in DPPC liposomes compared with those for POPC liposomes. This also distinguishes partitioning into biological membranes from that into 1-octanol or natural organic matter that is dominated by the solute's activity in aqueous solution (Chiou et al., 1983).

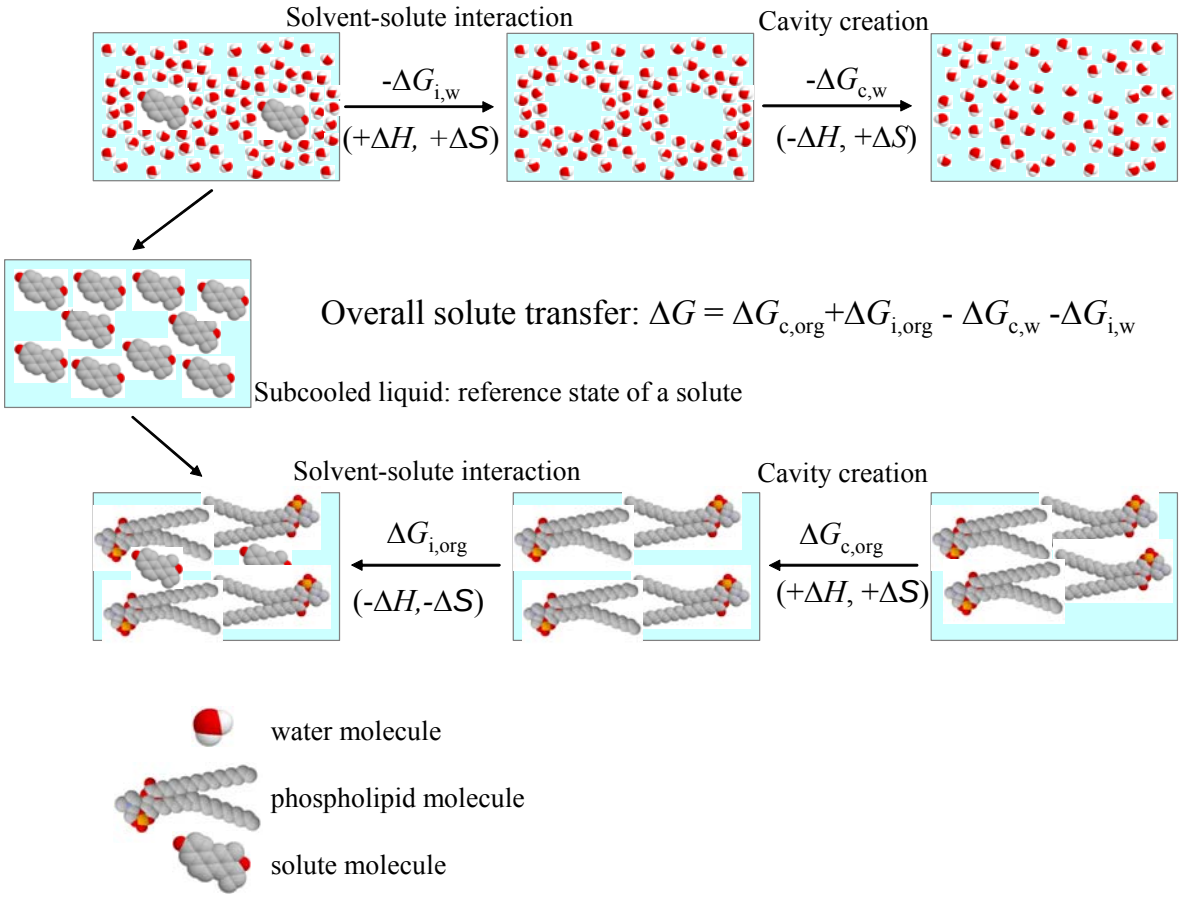

Figure 4.2: Thermodynamic cycle for solute transfer.

4.3.2. Effects of molecular geometry

As depicted in Figure 4.2, partitioning of a chemical with a greater molar volume in lipid bilayers would be driven by more positive entropy change and by less negative enthalpy change when all other interactions are similar. Three moderately hydrophobic *p*-substituted phenols (4-*tert*-amylphenol, 4-*sec*-butylphenol, and 4-phenylphenol) are structurally similar and have similar hydrophobicity. As previously reported, K_{lipw} values for 4-phenylphenol are greater than expected from the linear regression lines whereas the other two branched *p*-substituted phenols have values less than predicted from linear regressions for moderately hydrophobic EDCs, possibly due to the flat structure of 4-phenylphenol (Kwon et al., 2006a). Partitioning enthalpy and entropy values follow the order 4-*tert*-amylphenol > 4-*sec*-butylphenol > 4-phenylphenol for partitioning into both POPC and DPPC liposomes (Table 4.2), although this trend is not statistically significant. Enthalpy contribution decreases and entropy contribution increases in the partitioning process with increased branching in *p*-substitution of these phenols. This is consistent with the proposed enthalpy and entropy changes in Figure 4.2 when $\Delta G_{c,org}$ is the most significant term in determining K_{lipw}.

4.3.3. Effects of cholesterol in the membrane

Figure 4.3 shows changes in log K_{lipw} with cholesterol content and temperature for diethylstilbestrol, meso-hexestrol, and *p*-*tert*-octylphenol. The partition coefficient decreases much more for the two synthetic estrogens, diethylstilbestrol and meso-hexestrol, with increasing cholesterol contents in lipid membranes. In contrast, only a slight decrease in the partition coefficient is observed for *p*-*tert*-octylphenol at room

temperature (Kwon et al., 2006a; Yamamoto and Liljestrand, 2004). The partition coefficients for diethylstilbestrol and meso-hexestrol between water and DOPC liposomes increased with decreasing temperature regardless of the amounts of cholesterol in the membrane (Fig. 4.3a,c). The slopes and the intercepts of these regressions are not statistically different, although log K_{lipw} values are consistently lower with increasing amount of cholesterol in DOPC membranes over the temperature range investigated. Thus, the observed decrease in log K_{lipw} for diethylstilbestrol and meso-hexestrol may be due to less negative enthalpy, more positive entropy, or both.

In contrast, cholesterol has a much different effect on the partitioning between water and saturated liposomes, DPPC, than observed using unsaturated liposomes. Partitioning of diethylstilbestrol into DPPC liposomes is endothermic as observed for other EDCs into DPPC. However, adding a small amount of cholesterol (15% by mole fraction) into DPPC dramatically changed the partitioning thermodynamics for diethylstilbestrol to an exothermic process strongly driven by enthalpy change (Fig. 4.3b). The small amount of cholesterol may increase membrane fluidity of the gel phase liposome by separating phospholipids molecules, a process that does not happen in unsaturated liposomes which have cavities for cholesterol (New, 1990). The effects of small cholesterol contents in saturated lipid membrane is not apparent for meso-hexestrol, possibly as a result of meso-hexestrol requiring a larger space than diethylstilbestrol because this molecule can freely rotate along the central C-C single bond. Adding more cholesterol in the membrane gradually decreases fluidity, and the thermodynamic trends become consistent with that for pure DPPC liposomes. At high fractions of cholesterol in the phospholipids, K_{lipw} values for for diethylstilbestrol and meso-hexestrol drop by almost two orders of magnitude, which may be due to competition with cholesterol (Jacobsohn et al., 1994; Kwon et al., 2006a). Effects of cholesterol in saturated liposomes

in this study are not consistent with the findings from Rowe et al. (1998), which showed that the existence of cholesterol in multilamellar DPPC liposomes makes both the enthalpy and entropy contributions significantly more positive for *n*-alcohols. This may be a result of the larger solute size of the species used in the present study.

Effects of cholesterol on the partitioning of *p-tert*-octylphenol are negligibly small compared with synthetic estrogens even though their hydrophobicities are not significantly different. As proposed previously, the more hydrophobic alkylphenol may partition into the center of the bilayer, and the energy required to create a cavity may not be significantly affected by the amount of cholesterol or membrane fluidity (Kwon et al., 2006a). Another possibility is alteration of the membrane fluidity caused by sorbed alkylphenols as indicated above.

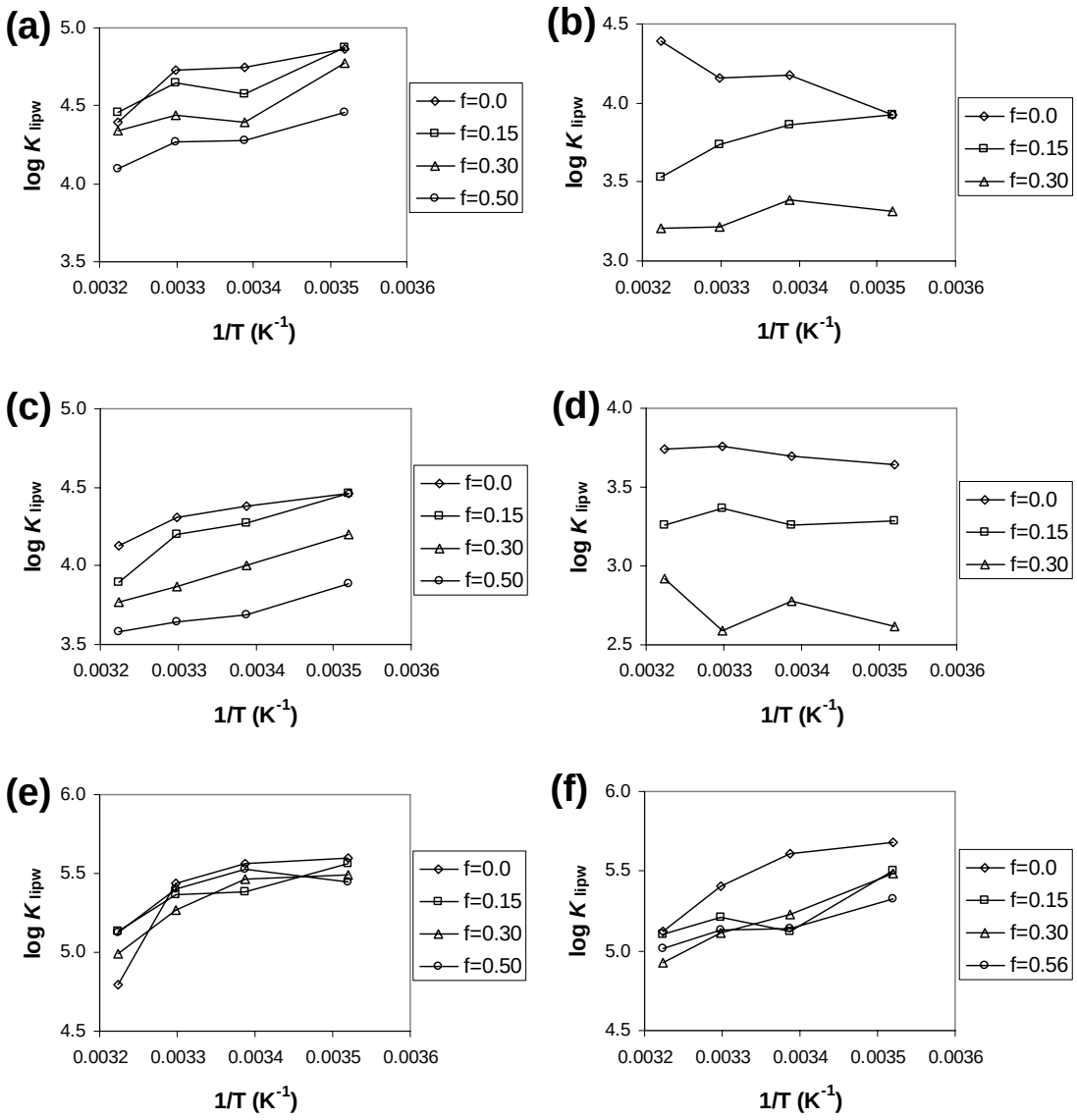

Figure 4.3: Effects of cholesterol on partitioning thermodynamics between water and membrane vesicles for (a) diethylstilbestrol using dioleoylphosphatidylcholine (DOPC) liposomes, (b) diethylstilbestrol using dipalmitoylphosphatidylcholine (DPPC) liposomes, (c) meso-hexestrol using DOPC liposomes, (d) meso-hexestrol using DPPC liposomes, (e) *p-tert*-octylphenol using DOPC liposomes, and (f) *p-tert*-octylphenol using DPPC liposomes. f denotes mole fraction of cholesterol in the membranes.

4.3.4. Implication for bioconcentration assessment

Table 4.3 typical trends in thermodynamic constants of partitioning between water (or buffer) and different organic phases for some environmental contaminants and pharmaceuticals. Although the literature values are somewhat chemical-specific, different organic phases are categorized into two groups in terms of thermodynamics, highly-ordered membrane phases (i.e. gel phase membrane lipids and surfactant micelles) and less ordered organic phases including bulk solvents, non-membrane lipids, and membrane lipids above the main transition temperature, as they are in this study. The driving forces for partitioning into saturated lipid membranes can be differentiated from those for more fluidic surrogate phases. The existence of saturated lipid components below their main transition temperature partly explains the endothermic nature of biopartitioning in fish (Opperhuizen et al., 1988) and phytoplankton (Koelmans and Jiménez, 1994), although they are simplified models for actual plasma membranes. However, partitioning into saturated lipid tails does not fully support the observed temperature dependency in guppies (Opperhuizen et al., 1988), and thus there may be many other factors affecting the overall bioconcentration in fish at the organism level even if bioconcentration is dominated by equilibrium partitioning processes. Fish contain large amount of poly-unsaturated fatty acids in their plasma membrane (Henderson and Tocher, 1987) and significant amounts of storage lipids, such as triolein, which do not form organized bilayers. As reported by Van Wezel and Opperhuizen (1995), partitioning into storage lipids is driven by enthalpy change. Thus, there should be some compensating effects of unsaturated fatty acids and storage lipids in overall bioconcentration. Existence of sterols and membrane proteins can make the plasma membrane more rigid and this can cause the overall biopartitioning to be driven by entropy change. In addition, fish lipid composition changes in response to environmental temperature. It has been observed that warm-

acclimated fish contain more cholesterol in their plasma membrane than cold-acclimated fish to control the permeability of the membrane (e.g., Hazel, 1995; Robertson and Hazel, 1995). Increased amounts of cholesterol at warmer temperature may reduce the equilibrium partition coefficient. This would be opposite to the results observed in fish bioconcentration (Opperhuizen et al., 1988).

Bioconcentration in fish often correlates well with a simple partition coefficient, such as log K_{OW}. It has been reported that log K_{OW} correlates better with the partition coefficient between water and storage lipids than membrane lipids/water partition coefficient (Jabusch and Swackhamer, 2005). Furthermore, log K_{OW} generally correlates better with log K_{lipw} for more fluidic lipid membranes than that for less fluidic membranes (Kwon et al., 2006a; Yamamoto and Liljestrand, 2004). Because the key assumption in most relationships is that the free energy change of partitioning in one process is linearly related to that in another, log K_{OW}-based QSAR for bioconcentration may be theoretically applicable only for cases dominated by unsaturated fatty acid components or storage lipids.

Table 4.3: Trends in ΔH and ΔS for chemicals between water and different organic phases.

Organic phases		Chemicals	ΔH	ΔS	Reference
1-octanol		CBs	-	+	Opperhuizen et al., 1988
		benzocaine	-	+	Ávila and Martinez, 2003
		CBs	-	n.d.	Bahadur et al., 1997
		CBs, PAHs, PCNs, PCBs	-	n.d.	Lei et al., 2000
		mefloquine/quinine	-/+	-/+	Go and Ngiam, 1997
		dipyridamole	+	+	Betageri and Dipali, 1993
Fish storage lipids		CBs	-	+	van Wezel and Opperhuizen, 1995
Surfactant micelles (SDS)		Various water pollutants	-/+	+	Woodrow and Dorsey, 1997
Lipid bilayer membranes	DPPC (16:0, 16:0)	benzocaine	+	+	Ávila and Martinez, 2003
		CBs	+ (< T_m) - (> T_m)	+	van Wezel et al., 1996
		dipyridamole	+	+	Betageri and Dipali, 1993
		EDCs	+	+	this study
	DPPC with cholesterol	EDCs	+	+	this study
	DSPC (18:0, 18:0)	EDCs	+/-	+	this study
	DMPC (12:0, 12:0)	Benzocaine	- (>T_m)	-	Ávila and Martinez, 2003
		small non-electrolytes	+	+	Katz and Diamond, 1974
		mefloquine/quinine	- (>T_m) + (<T_m)	- (>T_m) + (<T_m)	Go and Ngiam, 1997
		dipyridamole	+	+	Betageri and Dipali, 1993
		EDCs	- (>T_m) + (<T_m)	+	this study
	POPC (18:1, 16:0)	pharmaceuticals	-	+	Wenk et al., 1996
		pharmaceuticals	-	+/-	Seelig and Ganz, 1993
		EDCs	-	+/-	this study
	DOPC (18:1, 18:1)	EDCs	-	+/-	this study
	DOPC with cholesterol	EDCs	-	+/-	this study
	EPC (mixture)	phosphonium homologues	+	+	Yang et al., 2000b
		phenothiazine drugs	-	+	Takegami et al., 2003
Living organisms	Phytoplankton	CBs	+	+	Koelmans and Jiménez, 1993
	Fish	CBs	+	+	Opperhuizen et al., 1988

CBs=chlorobenzenes, DMPC=dimyristoylphosphatidylcholine, DOPC=dioleoylphosphatidylcholine, DPPC=dipalmytoylphosphatidylcholine, DSPC=distearylphosphatidylcholine, EDCs=endocrine disrupting chemicals, EPC=egg-yolk phosphatidylcholine, PAHs=polyaromatic hydrocarbons, PCBs=polychlorinated biphenyls, PCNs=polychlorinated naphthalenes, POPC=palmytotyloleoylphosphatidylcholine, SDS=sodium dodecylsulfate, T_m=main transition temperature

Chapter 5: Use of a Parallel Artificial Membrane System to Evaluate Passive Absorption and Elimination in Small Fish

A parallel artificial lipid membrane system was developed to mimic passive mass transfer of hydrophobic organic chemicals in fish. In this physical model system, a membrane filter-supported lipid bilayer separates two aqueous phases that represent the external and internal aqueous environments of fish. To predict bioconcentration kinetics in small fish using this system, literature absorption and elimination rates were analyzed using an allometric diffusion model to quantify the mass transfer resistances in the aqueous and lipid phases of fish. The impact of the aqueous phase mass transfer resistance was controlled by adjusting stirring intensity to mimic bioconcentration rates in small fish. Twenty-three simple aromatic hydrocarbons were chosen as model compounds for purposes of evaluation. For most of the selected chemicals, literature absorption/elimination rates fall into the range predicted from measured membrane permeabilities and elimination rates of the selected chemicals determined using the diffusion model system.

5.1. INTRODUCTION

Bioconcentration of hydrophobic organic chemicals (HOCs) by fish from water has been modeled by employing physico-chemical partitioning between water and lipid tissues and diffusion through a series of aqueous and lipid barriers (Barber et al., 1988; Chaisuksant and Connell, 1997; Gobas et al., 1986; Sijm and van der Linde, 1995). Without active transport or metabolic transformation, uptake and elimination of HOCs are often evaluated by simple first-order rate expressions assuming that a fish can be represented as a single compartment. In this sense, many abiotic devices are available for evaluating bioconcentration equilibrium or uptake/elimination rates of HOCs (see, e.g. Huckins et al., 1990, 1993; Verbruggen et al., 2000; Verweij et al., 2004). Furthermore, this simplistic approach has been used to assess the toxicity of accumulative water pollutants as well as the time-averaged aqueous concentration (Petty et al., 2000; Verbruggen et al., 2000).

More recently, a high-throughput parallel artificial membrane permeability assay (PAMPA) has been developed to estimate human intestinal absorption of orally administered drugs (Kansy et al., 1998; Sugano et al., 2003; Wohnsland and Faller, 2001; Zhu et al., 2002). This type of device also has potential for assessing bioconcentration in fish. The greatest advantage of PAMPA is that the microporous filter-supported bilayers have similar properties to actual biological membranes (Thompson et al., 1982). Measured permeability correlates well with percent absorption of orally administered drugs that passively permeate intestinal aqueous and lipid barriers (Sugano et al., 2003; Zhu et al., 2002). This implies that PAMPA has the potential for evaluating uptake and elimination rates in fish, where uptake and elimination are governed by passive paracellular diffusion. Furthermore, this system allows easy access to both the external

aqueous environment and the internal aqueous solution of a fish, thereby allowing the development of a monitoring system that combines passive transport processes to target sites and adverse toxic effects that occur at cellular/molecular levels. The first step is to construct an artificial membrane system analogous to the membrane systems present in aquatic organisms with respect to absorption and elimination characteristics.

Thus, the goal of this research was to develop a parallel artificial membrane system that mimics passive mass transfer of hydrophobic organic chemicals in fish. The artificial membrane system developed was tuned to mimic bioconcentration rates in small fish by adjusting the mass transfer resistance in the aqueous phase. The characteristic thickness of the diffusion boundary layer in the artificial membrane system was determined from the permeability of weak organic acids under variable stirring intensity. After the optimal stirring intensity was determined for the desired diffusion characteristics, the absorption/elimination behavior of the artificial membrane system was evaluated using effective membrane permeabilities and elimination rates of 23 selected simple aromatic chemicals and compared with literature values of absorption and elimination rates for small fish.

5.2. MATERIALS AND METHODS

5.2.1. Chemicals

Twenty-three simple aromatic chemicals, phenol, aniline, four nitroanilines (2-nitroaniline (2NA), 3-nitroaniline (3NA), 4-nitroaniline (4NA) and 2,4-dinitroaniline (24DNA)), six chloroanilines (2-chloroaniline (2CA), 3-chloroaniline (3CA), 4-chloroaniline (4CA), 2,4-dichloroaniline (24DCA), 3,4-dichloroaniline (34DCA) and 2,3,5,6-tetrachloroaniline (2356TeCA)), bromobenzene and nine chlorobenzenes (chlorobenzene (CB), 1,3-dichlorobenzene (13DCB), 1,4-dichlorobenzene (14DCB),

1,2,3-trichlorobenzene (123TCB), 1,2,4-trichlorobenzene (124TCB), 1,3,5-trichlorobenzene (135TCB), 1,2,3,4-tetrachlorobenzene (1234TeCB), 1,2,4,5-tetrachlorobenzene (1245TeCB), pentachlorobenzene (PeCB) and hexachlorobenzene (HCB)), were chosen for the evaluation of the bioconcentration rate parameters, because they are stable and their uptake/elimination rates have been reported in the literature. Four organic acids, benzoic acid (BZA), 2,4-dinitrophenol (DNP), 2,4-dinitro-o-cresol (DNOC), 2,4-dichlorophenol (DCP) and 2,4,6-trichlorophenol (TCP), were used for the determination of the aqueous diffusion layer thickness. All of these chemicals were of high purity and obtained from Sigma-Aldrich Co. (St. Louis, MO, USA), Fluka (Milwaukee, WI, USA), or Fischer Scientific, Inc. (Pittsburgh, PA, USA). Acetonitrile and water were used as eluents for HPLC analysis. n-Hexane was used for extraction of lipid membranes and as the solvent for GC analysis. Polyvinylidene fluoride (PVDF) membrane filters (0.1 μm pore size, 125 μm thickness) were purchased from Millipore Co. (Billerica, MA, USA). 30 mM buffer solutions were prepared from phosphoric acid for pH 2.0-3.0, acetic acid for pH 3.8-5.6, potassium dihydrogen phosphate for pH 6.2-8.2, and anhydrous disodium tetraborate ($Na_2B_4O_7$) for pH 8.5-10.0. The ionic strength of each buffer solution was adjusted to 154 mM using NaCl. The lipid phase in this study was dodecane containing 1% (w/w) of a phosphatidylcholine lipid mixture. Although lipid membrane permeation is more likely to be dominated by the dodecane, the lipid mixture was comprised of 25% didocosahexaenoylphosphatidylcholine (DHA, 22:6, 22:6), 20% dioleoylphosphatidylcholine (DOPC, 18:1, 18:1), 15% stearoyldocosahexaenoylphosphatidylcholine (SDPC, 18:0, 22:6), 10% dipalmytoylphosphatidylcholine (DPPC, 16:0, 16:0) and 30% cholesterol, based on the general fatty acids composition of fish gill (Henderson and Tocher, 1987; Staurnes et al.,

1994). Chloroform solutions of all phosphatidylcholines were purchased from Avanti Polar Lipids (Albaster, AL, USA).

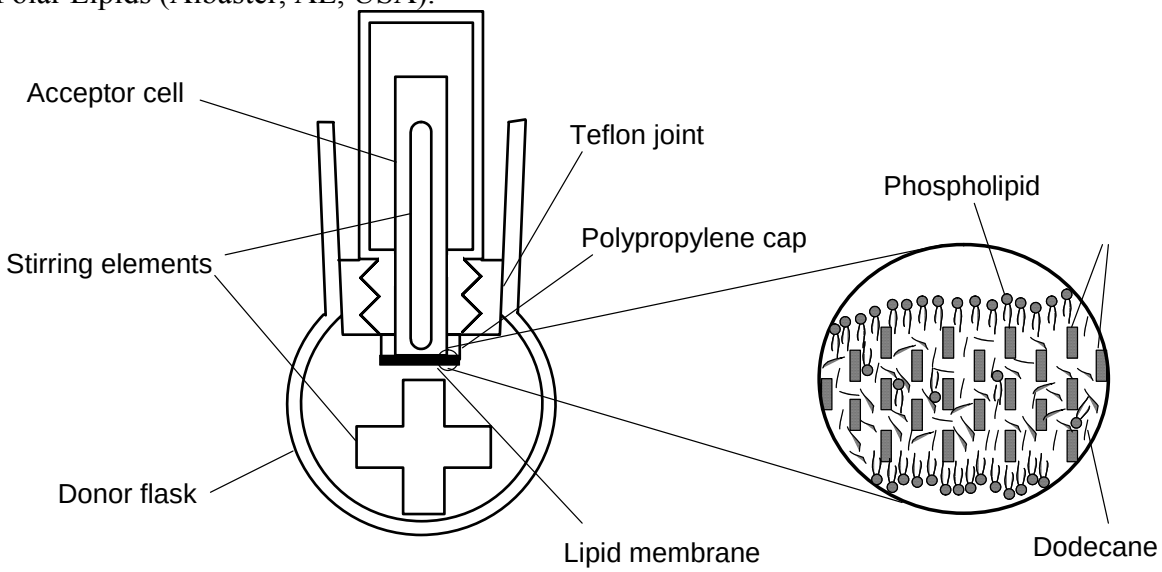

Figure 5.1: Schematic of the artificial membrane permeation reactor with suggested micro structure of filter supported lipid bilayers (reconstructed from Thompson et al., 1982).

5.2.2. Chemical analyses

For the determination of membrane permeability, aqueous samples of the donor and the acceptor cells of custom made experimental reactors shown in Figure 5.1 were analyzed using a Waters 2690 HPLC system equipped with a Waters 996 PDA detector (Milford, MA, USA) on C18 column (Waters Nova-Pak, 3.9×150 mm) at 40ºC. The HPLC flow rate was 1.5 ml/min, and the eluent was an isocratic composition of water and acetonitrile that varied depending on the polarity of the analyte mixture. The concentration of each compound was measured at its optimum absorption wavelength.

For the elimination experiments, concentrations of n-hexane extracts of lipid membranes were measured by GC-electron capture detector (ECD) using a HP6890 GC (Hewlett-Packard, Palo Alto, CA, USA) equipped with a 63Ni μECD. Recoveries of all

analytes ranged between 85~110%. One μl of extract was injected in a splitless mode onto a 30 m×0.25 mm DB1701 column (J&W Scientific, Folsom, CA, USA) with a 0.25 μm film thickness. Hydrogen was used as a carrier gas at a flow rate of 0.9 ml/min. Injector and detector temperatures were 250°C and 280°C, respectively. Column temperature varied depending on the analyte mixture.

5.2.3. Diffusion mass transfer model

A diffusion mass transfer model proposed by Gobas et al. (1986) was used to model bioconcentration and to evaluate the parallel artificial membrane system. In this model, molecules pass through a series of aqueous and lipid membrane barriers during transport between the ambient water and the storage compartments. This model is consistent with the hypothesis that the main uptake route of HOCs is passive diffusion through fish gill made of multiple layers of lipid membrane lamellas and water (Randall et al., 1998). For a simple two-compartment model with first-order rates, the bioconcentration model can be expressed as:

$$\frac{dC_f}{dt} = k_a C_w - k_e C_f \tag{5.1}$$

where C_w and C_f are the concentrations of the pollutant in water and fish, k_a is a first-order absorption rate constant (cm^3/g-h) and k_e is a first-order elimination rate constant (h^{-1}). The two rate parameters, k_a and k_e, can be determined by aqueous and membrane resistances as follows (Gobas et al., 1986; Sijm and van der Linde, 1995):

$$k_a = P\frac{A}{W} = \frac{1}{\frac{\delta_w}{D_w} + \frac{\delta_m}{K_m D_m}}\frac{A}{W} \tag{5.2}$$

$$k_e = \frac{1}{\frac{\delta_w}{D_w} + \frac{\delta_m}{K_m D_m}}\frac{1}{(1-\alpha)+\alpha K_m}\frac{A}{W} \tag{5.3}$$

where P is overall permeability (cm/h), δ_w and δ_m are the thickness of aqueous and membrane diffusion films (cm), respectively, D_w and D_m are diffusion coefficients in water and in the membrane (cm^2/h), α is the lipid content (-), K_m is lipid membrane-water partition coefficient (-), A is interface area (cm^2), and W is fish weight (g).

5.2.4. Evaluation of the literature bioconcentration rate constants

Twenty-three simple aromatic organic chemicals were selected for the evaluation of a diffusion mass transfer model and the performance of the artificial membrane system. Their bioconcentration mass transfer coefficients (often referred to as uptake and elimination rate constants) have been reported for small fish (0.1~5.0 g) by many authors (Banerjee et al., 1984; Bradbury et al., 1993; de Wolf and Lieder, 1998; de Wolf et al., 1994a, b; Ensenbach and Nagel, 1991; Kalsch et al., 1991; Könemann and van Leeuwen, 1980; Sijm and van der Linde, 1995; Smith et al., 1990; van Eck et al., 1997). Data on small fish were chosen in order to avoid significant allometric effects other than changes in surface to volume ratio. These uptake and elimination rate constants were normalized to that of a standard 1 g fish using an allometric relationship (Sijm et al., 1995):

$$\frac{A}{W} = \left(5.59 \pm 3.16\ \mathrm{cm^2 g^{-0.77}}\right) W^{-0.23} \qquad (5.4)$$

where A is surface area of permeation (cm^2) and W is weight of fish (g). Normalized absorption/elimination rates ($k_{a,\ norm}/k_{e,\ norm}$) can be calculated by substituting Equation 5.4 into Equation 5.2 and assuming that permeability (P) does not change significantly for the selected fish size.

$$k_{a,norm}\left(\text{or } k_{e,norm}\right) = k_a\left(\text{or } k_e\right) W^{0.23} \qquad (5.5)$$

Aqueous and membrane resistances were calculated from the diffusion mass transfer model described in Equation 5.2 with normalized uptake rate constants of the selected chemicals by a least square regression using K_{OW} as a surrogate for membrane-

water partition coefficient (K_m) in Equation 5.2. Median values of $k_{a,\ norm}$ were chosen when multiple data were available for a chemical.

5.2.5. Membrane permeability

Permeation experiments were carried out at 25°C in a custom made reactor (Figure 5.1). A 0.35 ml shell insert and a 5 ml volumetric flask were used as acceptor and donor cells, respectively. These two cells were separated by two sheets of PVDF membrane filter (0.1 μm pore size, 125 μm thickness, Millipore Co.) thermally attached to a polypropylene cap. The polypropylene surfaces were wrapped with Teflon tape to minimize surface contact. Aqueous buffer solution was filled in the acceptor cell. As soon as 5 μl of the dodecane/lipid solution described above was applied to the membrane filter, the acceptor cell was closed and attached to the donor cell that had been prefilled with buffer containing the chemical species. The reactor was stirred using a VP710C1 tumble stirrer (V&P Scientific, San Diego, CA, USA) to maximize vertical mixing. Incubation time varied from 10 min to 30 h, depending on the chemical's permeability and the stirring intensity. After incubation, the reactor was dissembled, and the solutions in both the donor and acceptor cells were analyzed by HPLC. Membrane resistance was measured using a HP 3466A digital multimeter (Hewlett-Packard, Palo Alto, CA, USA) with custom-made copper electrodes to insure that the membrane permeation was not due to unfilled pores or gaps in the membrane cap. Data were accepted when the electrical resistance across the membrane was greater than 50 kΩ.

The change in concentration of the acceptor solution with respect to time can be expressed as a simple differential equation using an effective permeability, P_{eff}.

$$\frac{dC_A}{dt} = \frac{P_{eff} A}{V_A}\left(C_D - C_A\right) \tag{5.6}$$

where C_A and C_D are the concentrations in the acceptor and the donor cells (mg/L), respectively, P_{eff} is the effective permeability (cm/s), A is the surface area of membrane permeation (0.124 cm^2), V_A is the volume of the acceptor cell (cm^3), and t is the incubation time (s). P_{eff} is obtained by solving Equation 5.6, assuming negligible membrane retention:

$$P_{eff} = -\frac{V_D V_A}{(V_D + V_A)At} \ln\left(1 - \frac{C_A}{C_{eq}^*}\right) \tag{5.7}$$

where C_{eq}^* is the theoretical equilibrium concentration that represents the concentration in donor and acceptor cell after equilibrium is reached, calculated using a mass balance equation that includes membrane retention. For more hydrophobic chemicals having membrane retention greater than 15% of the total mass, Equation 5.8 was used instead, assuming that membrane holding occurs within a short loading time, τ_{SS} (Avdeef, 2001).

$$P_{eff} = -\frac{V_D V_A}{(V_D + V_A)A(t - \tau_{SS})} \ln\left(1 - \frac{C_A}{C_{eq}^*}\right) \tag{5.8}$$

where P_{eff}, τ_{SS} and C_{eq}^* were estimated as best-fit parameters by plotting C_A versus t. Non-linear regression analyses were performed using SPSS for Windows (Ver 12.0; SPSS, Chicago, IL, USA).

5.2.6. Determining the thickness of diffusion layers

In the model artificial system, the overall resistance is assumed to be a sum of the artificial lipid membrane resistance and aqueous diffusion layer resistances on both sides of the membrane. Thus, the effective permeability, the inverse of the overall resistance, is written as:

$$\frac{1}{P_{eff}} = \frac{1}{P_{aq}} + \frac{1}{P_m} \tag{5.9}$$

where P_{aq} is the permeability of the aqueous diffusion layer including both sides (cm/h) and P_m is the permeability of the artificial lipid membrane (cm/h).

Since the artificial membrane is not permeable to ionized species, the membrane permeability, P_m, depends on the pH of the solution for an ionizable chemical. For a monoprotic weak acid, P_m is obtained by multiplying intrinsic membrane permeability, P_o, and the fraction of the unionized species (Gutknecht and Tosteson, 1973).

$$P_m = \frac{P_o}{10^{(pH-pK_a)}+1} \tag{5.10}$$

$$\frac{1}{P_{eff}} = \frac{1}{P_{aq}} + \frac{10^{(pH-pK_a)}+1}{P_o} \tag{5-11}$$

Both P_{aq} and P_o can be calculated by plotting P_{eff} versus pH when the pK_a of the acid is known. P_{aq} and P_o were determined for the selected organic acids at different stirring intensity using a non-linear least square regression. pK_a values obtained from the literature were corrected for the ionic strength of the solution, I, using the Davies equation for a monoprotic acid (Stumm and Morgan, 1995):

$$pK_a^{'} = pK_a - \left[\frac{A\sqrt{I}}{(1+I)} - 0.2I\right] \tag{5.12}$$

where $pK_a^{'}$ is $-\log_{10}$ of the ionic strength corrected mixed acidity constant, pK_a is $-\log_{10}$ of the infinite dilution equilibrium constant, and A is a constant that has a value of 0.5 at 25°C.

The thickness of the aqueous diffusion layer is calculated from the aqueous permeability and calculated diffusion coefficient using a molecular weight (D_{aq}, cm^2/h) (Schwarzenbach et al., 2003), as follows:

$$\delta_{aq} = \frac{D_{aq}}{P_{aq}} \tag{5.13}$$

$$D_{aq}(cm^2/h) = \frac{0.972}{M^{0.71}} \tag{5.14}$$

where δ_{aq} is the thickness of the aqueous diffusion layer (cm), D_{aq} is the aqueous diffusion coefficient of the acid (cm^2/h) and M is the molecular weight of a solute (g/mole).

5.2.7. Elimination rate constants

Elimination rate constants from the artificial membrane were measured for the thirteen most hydrophobic chemicals. The reactor used for the permeability experiments was modified to allow the aqueous buffer solution (pH 7.4, I = 154 mM) to flow through the donor cell. The experimental procedure was the same as that used in the permeability measurement, except that the 5 μl dodecane/lipid mixture applied to the PVDF membrane also contained the chemical species. The flow rate of approximately 1 ml/min was sufficient to ensure that the aqueous concentration in the donor cell was much smaller than the equilibrium concentration and reabsorption from the aqueous phase was negligible. After incubation, the PVDF membrane cap was dissembled and placed into a 10 ml vial containing 5 ml n-hexane. After shaking for 30 minutes, the species concentration in the n-hexane extract was measured using GC-ECD. The elimination rate constant was calculated using a first order rate expression:

$$C_M(t) = C_{M,0} \exp(-k_e t) \tag{5.15}$$

where $C_M(t)$ is the membrane concentration after time t (mg/L), $C_{M,0}$ is the initial membrane concentration (mg/L), k_e is elimination rate constant (h^{-1}), and t is incubation time (h). k_e was calculated from regression of the linear form:

$$\ln\left(\frac{C_M(t)}{C_{M,0}}\right) = -k_e t \tag{5.16}$$

5.3. RESULTS

5.3.1. Evaluation of literature data

Figure 5-2 shows the relationship between $\log k_{a,norm}$ and $\log K_{OW}$. Consistent with the diffusion model, uptake rates increased with increasing hydrophobicity for $\log K_{OW}$ values less than 2 and then approached a plateau for more hydrophobic chemicals. Best-fit parameters were obtained by least square regression (Equation 5.17).

$$k_{u,norm}\ \left[\text{cm}^3/\text{g}\cdot\text{hr}\right] = \frac{K_{\text{OW}}}{3.570 + 0.0252K_{\text{OW}}} \tag{5.17}$$

From Equations 5-2 and 5-4, the corresponding membrane resistance (δ_m/D_m) and aqueous resistance (δ_w/D_w) were determined to be 20.0 h/cm and 0.141 h/cm, respectively. The corresponding δ_w is about 27 μm for a typical water pollutant (molecular weight of 250 g/mole) with a value of D_w of 0.019 cm^2/h calculated from Equation 5.13. Diffusion thickness of the membrane phase could not be determined because D_m was unknown. Aqueous phase resistance was also calculated from the average uptake rate constant of the most hydrophobic chemicals (i.e., chemicals with literature lipid normalized BCF greater than $10^{4.5}$) for which membrane resistance was assumed to be negligible. δ_w/D_w was calculated to be 0.114 h/cm, and the corresponding δ_w was 22 μm. The slight decrease in δ_w is due to a slight increase of $k_{a,\,norm}$ at log K_{OW} > 3 (Figure 5.2). However, this value is not significantly different from that value obtained by regression, which indicated the membrane resistance equals the aqueous resistance when log K_{OW} of the chemical is 2.15.

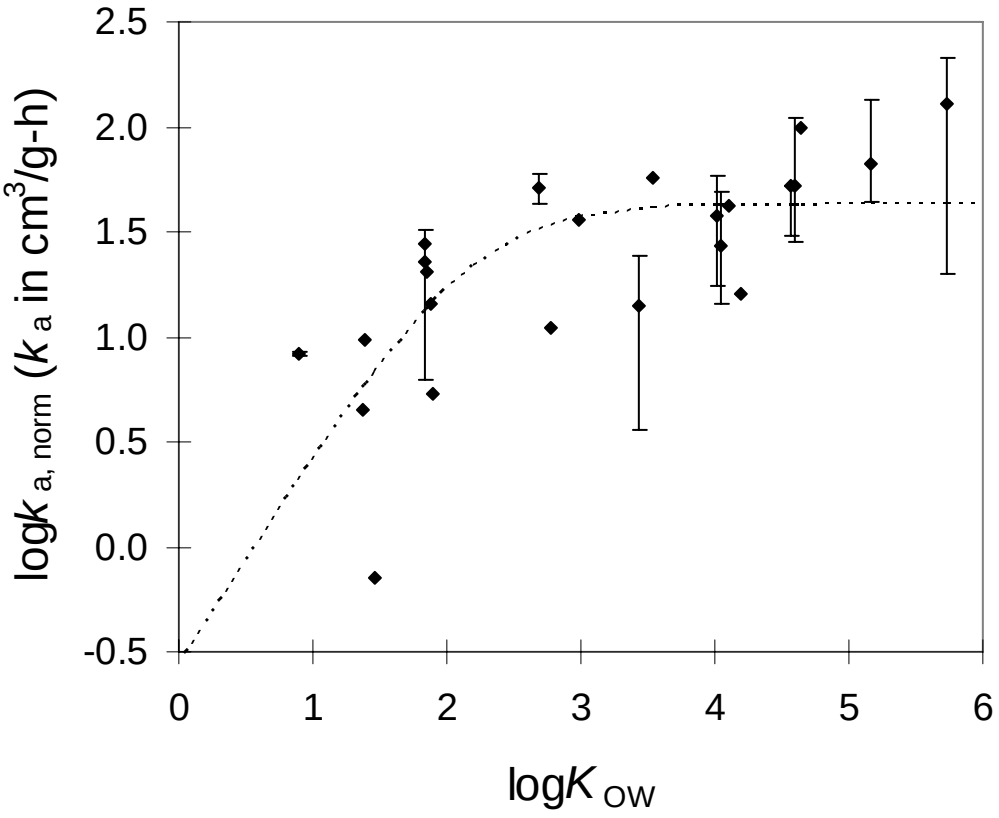

Figure 5.2: log$k_{a,\ norm}$ versus logK_{OW} for 23 selected simple aromatic chemicals. Broken line indicates the Equation 17. Median values of the uptake rate constant were chosen when there are multiple values for one chemical. The error bar denotes the range of literature values for one chemical when multiple values are available.

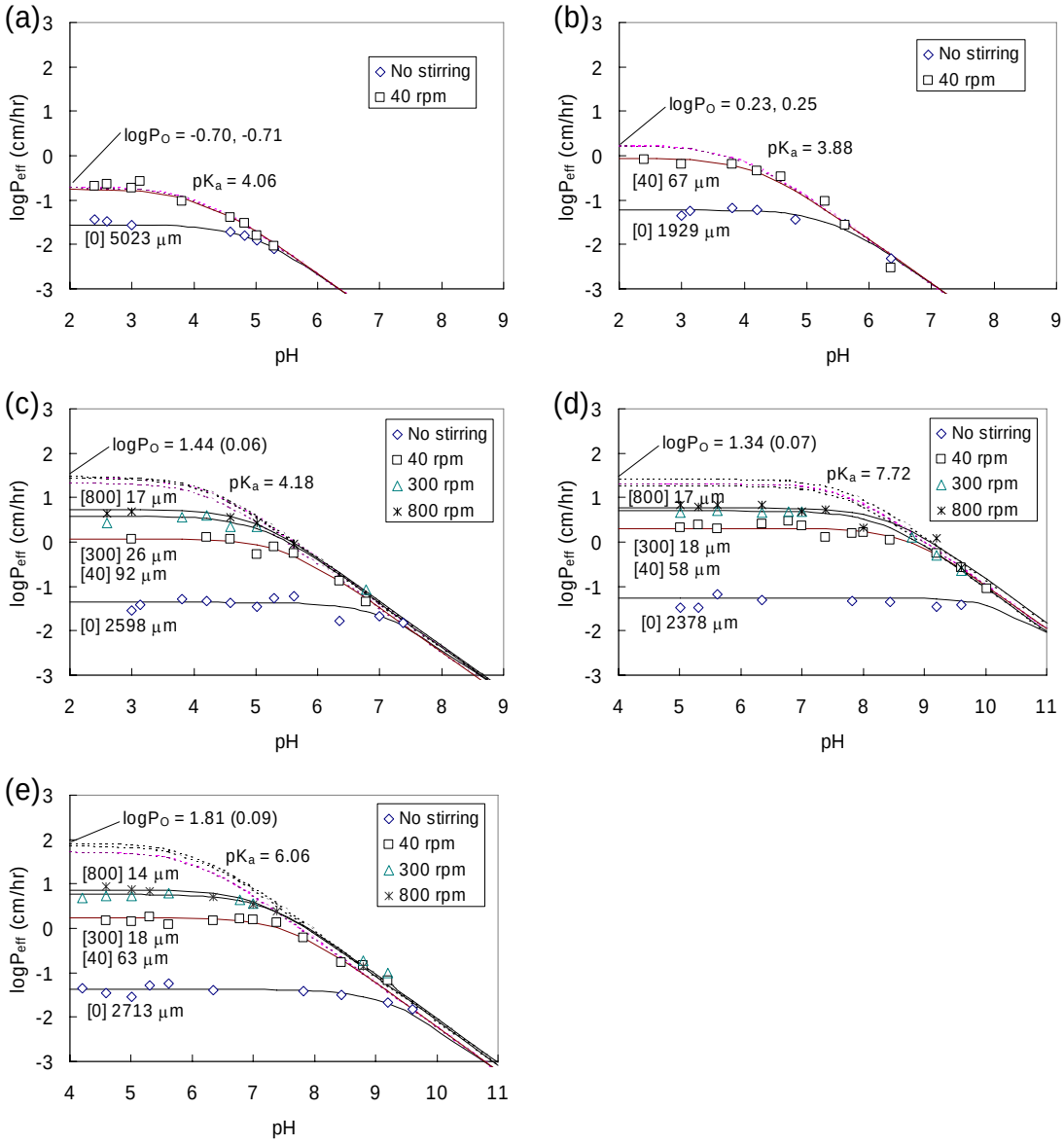

Figure 5.3: Log permeability (cm/h) versus pH plots for five standard acids, (a) benzoic acid (BZA), (b) 2,4-dinitrophenol (DNP), (c) 2,4-dinitro-o-cresol (DNOC), (d) 2,4-dichlorophenol (DCP) and (e) 2,4,6-trichlorophenol (TCP). The solid curves represent the best-fit of measured logP_{eff} vs. pH according to Equation 5.11. The estimated thickness of the aqueous diffusion layer is indicated in μm with the corresponding stirring speed in square bracket. The dashed curves are the calculated intrinsic permeability curves from Equation 5.10. The mean values of logP_O are indicated in the frames along with the estimated standard deviation in parentheses.

5.3.2. Determination of the thickness of the aqueous diffusion layer

Figure 5.3 presents the changes in effective permeability (P_{eff}) of five standard organic acids as a function of pH. P_{eff} is proportional to the fraction of the unionized species in the system, showing that P_{eff} did not change with increasing pH at values less than the pK_a and decreased with increasing pH with a slope of –1 for pH > pK_a. P_{eff}, depicted by solid lines, increased with increasing stirring speed unless it was limited by membrane diffusion, whereas membrane permeability (P_m), described in dashed lines, did not change regardless of the stirring speed. P_{eff} for benzoic acid (BZA) and 2,4-dinitrophenol (DNP) was close to P_m at 40 rpm, indicating that the overall permeation is limited by membrane diffusion at stirring speeds greater than 40 rpm. Thus, the corresponding thickness of aqueous diffusion layer (δ_w) could not be calculated when the resistance to permeation of solutes was dominated by membrane diffusion. For the other three acids, P_{eff} is at least one order of magnitude lower than P_m, indicating that the aqueous resistance dominates. Thus, δ_w was calculated for all stirring speeds for these acids. δ_w values were between 1900 and 5000 μm for unstirred experiments, between 58 and 92 μm at 40 rpm, between 18 and 26 μm at 300 rpm, and between 14 and 17 μm at 800 rpm. 300 rpm was chosen for permeability assays of the selected chemicals, because δ_w was close to that obtained in the previous section and the reactor was more stable at 300 rpm than at 800 rpm.

5.3.3. Artificial membrane permeability

The artificial membrane permeabilities (P_{eff}) of phenol, ten anilines, bromobenzene, and three chlorobenzenes are presented in Table 5.1. P_{eff} was calculated from measured aqueous concentrations in the donor and acceptor cells of the less hydrophobic chemicals, because their membrane retention was not significant (less than 15% by mass). P_{eff} was calculated from data collected in triplicate reactors for at least

three different incubation times. Because P_{eff} was not affected significantly by incubation time for these chemicals, all values were averaged and the standard deviation was calculated from all data. Equation 5.8 was used to obtain P_{eff} for the more hydrophobic chemicals, CB, BB, 13DCB, 14DCB. Their membrane retentions ranged from 47-83% by mass (Appendix C). Standard error in P_{eff} from the non-linear regression was used instead of the standard deviation (Table 5.1). P_{eff} generally increased with increasing chemical hydrophobicity (K_{OW}), and approached an upper limit value of approximately 7 cm/h, a value limited by aqueous diffusion resistance (Figure 5.3).

5.3.4. Elimination rate constant

Elimination rate constants of the 13 chemicals from the artificial membrane (Table 5.1) were calculated from membrane concentrations measured at different times using linear regression of $\ln(C_M(t)/C_{M,0})$ vs. t in Equation 5.16. Corresponding half lives of the chemicals in the membrane ranged from 10 min for the dichloroanilines to 5 days for hexachlorobenzene (HCB). The correlation coefficients, r^2, of the regression were greater than 0.9 for all the chemicals except HCB (Appendix C). Smaller correlation coefficients for HCB could be due to a relatively short incubation time.

Table 5.1: log K_{OW}, artificial membrane permeabilities and elimination rate constants, and literature absorption and elimination rate constants for selected chemicals.

		Experimental values		Median literature values[b]		
Chemicals	logK_{OW}[a]	Effective permeability, P_{eff} (cm/h)	Elimination rate constant, k_e (h^{-1})	Normalized uptake rate constant, $k_{a,\ norm}$ (cm^3/g-h)	Normalized elimination rate constant, $k_{e,\ norm}$ (h^{-1})	reference
Phenol	1.46	0.15±0.02	-	0.72	0.040	Ensenbach and Nagel, 1991
Aniline	0.90	1.05±0.18	-	8.29	4.06	Bradbury et al., 1993; Kalsch et al., 1991
2-Nitroaniline	1.85	0.94±0.24	-	20.3	2.50	Kalsch et al., 1991
3-Nitroanilne	1.37	0.26±0.05	-	4.47	0.54	Kalsch et al., 1991
4-Nitroaniline	1.39	0.083±0.008	-	9.78	2.20	Kalsch et al., 1991
2,4-Dinitroaniline	1.84	0.078±0.006	-	27.4	2.12	Kalsch et al., 1991
2-Chloroaniline	1.90	4.93±0.46	-	5.38	0.35	Kalsch et al., 1991
3-Chloroaniline	1.88	3.02±0.33	-	14.5	1.29	Kalsch et al., 1991
4-Chloroaniline	1.83	2.67±0.30	-	22.5	3.06	Bradbury et al., 1993; Kalsch et al., 1991; de Wolf et al., 1994b
2,4-Dichloroaniline	2.78	6.50±1.03	9.0	10.9	0.12	Kalsch et al., 1991
3,4-Dichloroaniline	2.69	3.70±0.93	12.7	51.4	1.59	Ensenbach and Nagel, 1991; Kalsch et al., 1991
2,3,5,6-Tetrachloroaniline	4.10	-	0.14	41.6	0.14	De Wolf et al., 1994a
Monochlorobenzene	2.84	6.82±1.79[c]	-	15.2	0.30	De Wolf and Lieder, 1998
Bromobenzene	2.99	5.60±1.90[c]	0.90	36.1	0.21	De Wolf and Lieder, 1998
1,3-Dichlorobenzene	3.53	7.95±5.60[c]	0.26	57.3	0.086	De Wolf and Lieder, 1998
1,4-Dichlorobenzene	3.44	5.92±3.32[c]	0.26	14.0	0.38	Könemann and van Leeuwen, 1980; Smith et al., 1990
1,2,3-Trichlorobenzene	4.05	-	0.059	27.2	0.0095	Könemann and van Leeuwen, 1980; Sijm and van der Linde, 1995
1,2,4-Trichlorobenzene	4.02	-	0.087	37.9	0.023	Smith et al., 1990; van Eck et al., 1997
1,3,5-Trichlorobenzene	4.19	-	0.11	16.1	0.28	Könemann and van Leeuwen, 1980
1,2,3,4-Tetrachlorobenzene	4.60	-	0.024	51.8	0.0098	Banerjee et al., 1984; Könemann and van Leeuwen, 1980
1,2,4,5-Tetrachlorobenzene	4.64	-	0.031	98.7	0.017	Smith et al., 1990
Pentachlorobenzene	5.17	-	0.012	66.1	0.0114	Banerjee et al., 1984; Könemann and van Leeuwen, 1980; Sijm and van der Linde, 1995
Hexachlorobenzene	5.73	-	0.0054	129.2	0.0004	Könemann and van Leeuwen, 1980; Sijm and van der Linde, 1995

a. logK_{OW} values are suggested experimental values from KOWWIN program (US Environmental Protection Agency, 2000),

b. median values are used when multiple data are available for a chemical,, c. standard error obtained from non-linear regression analyses.

5.4. DISCUSSION

5.4.1. Diffusion mass transfer model

According to the diffusion model described above, the uptake rate constant ($\log k_a$) should increase with increasing membrane/water partition coefficient ($\log K_m$) with a slope of unity for less hydrophobic chemicals and reach an upper limit as aqueous resistance dominates. Although some of the observed results deviate from that expected (Figure 5.2), the relationship between normalized uptake rate constants ($k_{a,\,norm}$) and K_{OW} as a surrogate for K_m shows the general trend predicted by the diffusion mass transfer model. Quality of fit is better for the more hydrophobic chemicals and conversely, less hydrophobic chemicals deviate more from the relationship. This tendency suggests that transport of less hydrophobic chemicals is not solely due to passive permeation processes, as assumed in the diffusion model.

Previous studies showed that uptake rate constants increase with $\log K_{OW}$ and are independent of $\log K_{OW}$ for $\log K_{OW}$ between 3 and 6 (Chaisuksant et al., 1997; Gobas et al., 1986; Hawker and Connell, 1988). The break point for dependence on $\log K_{OW}$ was estimated in the literature to be $\log K_{OW} \approx 3$ (Gobas et al., 1986; Hawker and Connell, 1988), while the regression results in this study indicated it to be less than 3. This may be due to the greater deviation from the suggested relationship, especially for less hydrophobic chemicals. Hawker and Connell (1988) developed an empirical curvilinear relationship between k_a and K_{OW} mostly using chlorobenzenes:

$$k_a = \frac{0.048 K_{OW}}{0.00142 K_{OW} + 12.01} \qquad (5.18)$$

According to their relationship, the aqueous phase resistance equals the membrane phase resistance at $\log K_{OW}=3.8$. Hawker and Connell did not analyze many compounds with lower hydrophobicity, as needed to verify the linearly increase and unit

slope. Thus, membrane resistance was determined from the slight variation in k_a for moderately hydrophobic chemicals. Although the ratio of aqueous resistance to membrane resistance in Equation 5.18 is different from that in this study (Equation 5.17), their maximum value of k_a (33.8 cm^3/g-h) is very close to that obtained in this study, 39.7 cm^3/g-h. This suggests that the mass transfer of highly hydrophobic chemicals is limited by aqueous diffusion.

5.4.2. Determination of the thickness of the aqueous diffusion layer

As proposed in previous research, most diffusion resistance for uptake of a chemical occurs in fish gill (Randall et al., 1998). Thus, the net aqueous diffusion layer for bioconcentration would be comprised of an external aqueous film, interlamellar aqueous layer, mucous layers, etc. The distance between two gill lamellae is approximately 20 μm for 1 g fish (Sijm and van der Linde, 1995; Sijm et al., 1994). From this value, Sijm and van der Linde (1995) assumed that the aqueous diffusion path length is 10% of the interlamellar distance and the viscosity of the solution is ten times that of pure water. The aqueous phase resistance using their assumption was equivalent to that for 20 μm of pure water (Sijm and van der Linde, 1995). In terms of mass transfer resistances, the thickness of the aqueous diffusion layer from the previous studies was consistent with 22~27 μm of pure water for 1 g fish analyzed from Figure 5.2. Thus, stirring intensity was optimized at 300 rpm to obtain a δ_w of 20.7±4.6 μm calculated from the pK_a-flux method using three acids, DNOC, DCP, and TCP.

The thickness of the membrane phase in the system was about 300 μm. With this membrane thickness, membrane permeation of less hydrophobic acids, BZA and DNP with log K_{OW} values less than 2.0, were limited by membrane diffusion whereas more hydrophobic acids with log K_{OW} greater than 2.0 were limited by aqueous diffusion at

300 rpm (Figure 5.3). These results are consistent with the critical log K_{OW} value obtained from Figure 5.2.

5.4.3. Comparison of uptake/elimination rate constants in fish with analogous parameters in the artificial membrane system

Artificial membrane permeability obtained either from Equation 5.7 and 5.8 could be related to the normalized absorption rate constant ($k_{a,\ norm}$) from the literature. Although diffusion resistances in both aqueous and membrane phases are affected by fish size, allometric effects on mass transfer resistances could be neglected when rate constants are obtained from a relatively narrow range of fish sizes, 0.1~5 g. Fish permeability (P) in Equation 5.2 should be comparable to the effective permeability obtained from the artificial membrane system, if two systems are not significantly different in terms of partitioning. Thus, $k_{a,\ norm}$ values are directly related to artificial membrane permeability (P_{eff}) from Equation 5.2 assuming $P_{eff} \approx P$. By taking logarithms of both sides of Equation 5.2 and using the surface-to-weight ratio (A/W) of 1 g fish of 5.59±3.16 cm^2/g (Sijm et al., 1995), Equation 5.19 is obtained.

$$\log k_{a,norm} = \log P_{eff} + \log(5.59 \pm 3.16) \quad (5.19)$$

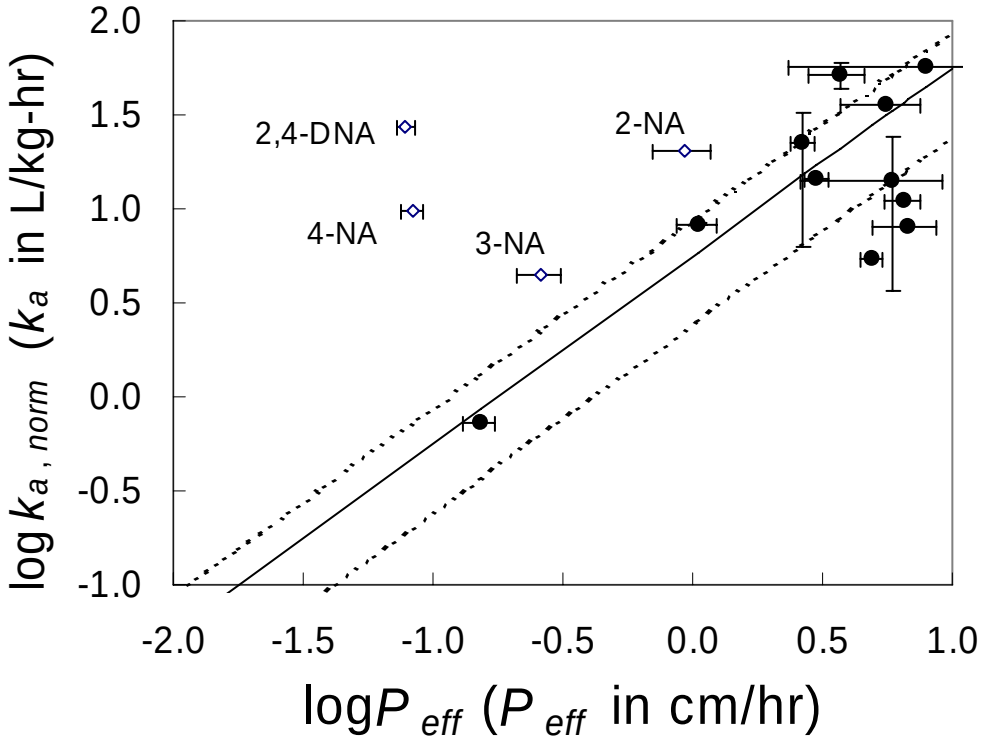

Figure 5.4: Relationship between normalized literature absorption rate constants ($k_{a,norm}$) and the artificial membrane permeability (P_{eff}). Solid line indicates the theoretical relationship shown in Equation 5.19. Dashed lines indicate one standard deviation of surface-to-weight ratio. Vertical error bars denote the range of literature values when multiple data are available for one chemical. Horizontal error bars denote standard deviation or standard error from non-linear regression.

Figure 5.4 represents the relationship between log$k_{a,\ norm}$ and logP_{eff} obtained from the artificial membrane system with the solid line representing Equation 5.19 and dashed lines indicating one standard deviation range of A/W. Seven chemicals fall within one standard deviation range of Equation 5.19, and the other chemicals were close to that theoretically expected, except for the nitroanilines. All nitroanilines are above Equation 19 indicating that the uptake rate of these chemicals in fish is much faster than expected based on the artificial membrane permeability. Substitution of nitro group enhances

delocalization of π electrons in the benzene ring and stabilizes the conjugate base (neutral anilines). The permanent dipole moment of aniline (1.53D) increases significantly by substitution of the nitro group. Dipole moments of 2NA and 4NA are 4.26D and 6.12D, respectively (Gaffar and Abu El-Fadl, 1989). Thus, the extremely low permeability of 24DNA and 4NA could be due to their strong dipole moments. In spite of their electrical properties, absorption rate constants of nitroanilines are similar to those of aniline and chloroanilines (Kalsch et al., 1991). Relatively high absorption rate constants by fish indicate that uptake of nitroanilines by fish may not be described by passive diffusion across a series of biological barriers. Contributions of other uptake mechanisms for less hydrophobic chemicals would increase $k_{a,\ norm}$ greater than expected from the passive diffusion model. This also makes it difficult to fit less hydrophobic chemicals in the linear region of Figure 5.2.

In the diffusion mass transfer model, the elimination rate constant can be obtained from permeability (P_{eff}), membrane/water partition coefficient (K_m) and a size-related factor (A/W). Since elimination of the chosen hydrophobic chemicals are limited by aqueous diffusion, elimination rate constants from the artificial membrane (k_e) should be related with that from fish assuming that the artificial membrane and fish have the same K_m for a chemical. Thus, a normalized elimination rate constant from fish ($k_{e,\ norm}$) can be expressed as:

$$k_{e,norm} = \frac{(A/W)_{fish}}{(A/W)_{AM}} \frac{\delta_{w,AM}}{\delta_{w,fish}} k_{e,AM} \tag{5.20}$$

Although the donor side thickness of the aqueous diffusion film could not be separated from the total thickness of the aqueous diffusion film using the pK_a-flux method, it is thought to be about 30~50% of the total thickness of the aqueous diffusion film. Estimates were between 9~11 μm for BB, 13DCB, and 14DCB using the changes in

concentration at the donor side and assuming that the absorption rate is solely limited by aqueous diffusion (see Appendix C). The outer surface area of the artificial membrane system was approximately 0.40 cm^2 and the applied volume of dodecane/lipid phase was 5 μl (3.78 mg). If a typical small fish contains 5% lipid content, the corresponding weight would be approximately 0.076 g and the value of $(A/W)_{AM}$ would equal 5.3 cm^2/g. Therefore, $k_{e,\ norm}$ is related to $k_{e,\ AM}$ as:

$$\log k_{e,norm} = \log k_{e,AM} - 0.4 \qquad (5.21)$$

Figure 5.5 represents the relationship between $\log k_{e,norm}$ and $\log k_{e,\ AM}$ with the solid line representing Equation 5.21. Deviations from the expected values are within 0.5 log units for most chemicals and at least within one order-of-magnitude for all chemicals except 24DCA. $\text{Log}k_{e,norm}$ of 24DCA was extremely small compared to other structurally similar compounds (Kalsch et al., 1991). The extraordinarily slow elimination rate of 24DCA could not be explained by passive diffusion processes.

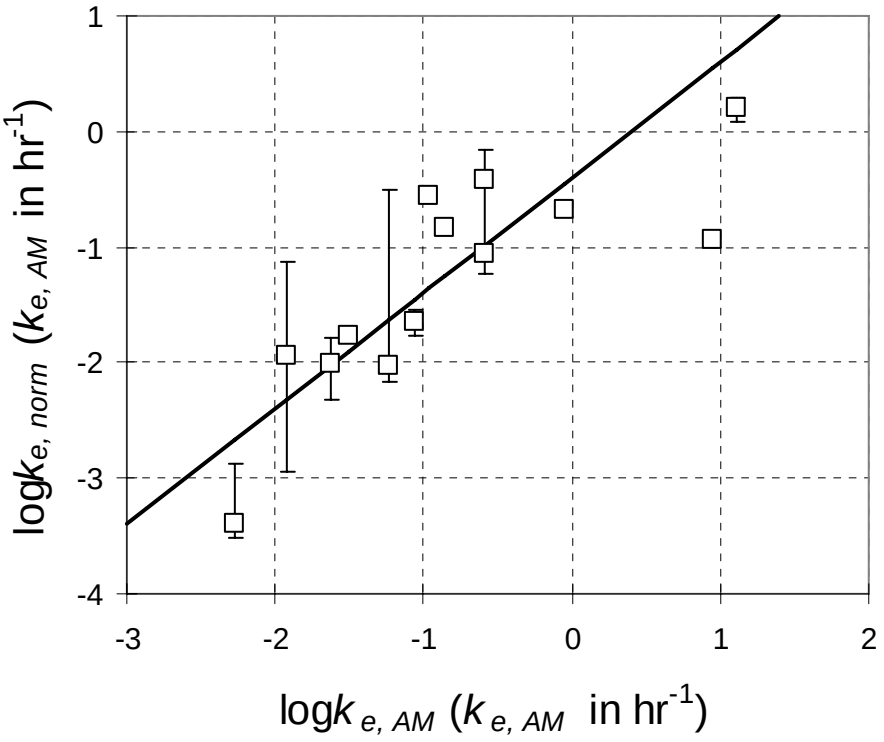

Figure 5.5: Relationship between normalized literature elimination rate constants (log$k_{e,norm}$) and the artificial membrane elimination rate constant (log$k_{e,\ AM}$). Solid line indicates the theoretical relationship shown in Equation 5.21. Vertical error bars denote the range of literature values when multiple data are available for one chemical.

5.4.4. Potential application of this study

The parallel artificial membrane system developed in this study showed great potential for mimicking passive uptake and elimination processes in aquatic animals. This system has great applicability, because it allows easy access to both aqueous solution sides of the membrane which correspond to the external aqueous environment and the internal aqueous solution in fish. More reliable risk prediction would be possible especially for non-narcotic pollutants, if highly sensitive chemical or biological sensors are placed in the acceptor phase of this parallel membrane system to evaluate specific toxicity. A combined system can emulate transport processes to target sites via passive diffusion and adverse toxic effects at cellular/molecular levels.

Chapter 6: Modeling Binding Equilibrium in a Competitive Estrogen Binding Assay

Although the free concentration is more significant in environmental chemistry and toxicology of receptor-mediated toxicants, few studies have been conducted to use it as a dose-metric. The relative binding affinity of three model endocrine disrupting chemicals, diethylstilbestrol (DES), ethylnylestradiol (EE2), and bisphenol A (BPA), were evaluated using a competitive enzyme-linked immunosorbant assay (ELISA) with human estrogen receptor α. After measuring the available receptors and the dissociation constant for 17β-estradiol, binding inhibition curves using the free concentration as a dose-metric were obtained (by assuming species equilibrium in the ELISA system) and compared to apparent inhibition curves generated using nominal concentration as a dose-metric. Because ligand binding to estrogen receptors may reduce its free concentration in the assay system, the differences between the two curves for free and nominal concentrations are more significant for stronger ligands. The ratio of the compound's concentration causing 50% inhibition (IC50) to the IC50 of DES, the positive control, was strongly affected by specific assay conditions unless it was calculated from estimated IC50 by modeling free concentration, indicating that free concentration is a better dose-metric for a competitive binding assay.

6.1. INTRODUCTION

The presence of estrogenic endocrine disrupting chemicals (EDCs) has been of significant concern for decades. Estrogenic potential of suspected EDCs and extracts prepared from environmental samples has been evaluated by various in vitro (e.g., Koda et al., 2002; Kuiper et al., 1997, 1998; Nishikawa et al., 1999; Ohno et al., 2002; Routledge and Sumpter, 1996; Soto et al., 1995) and in vivo (e.g., Allen et al., 1999; Hemmer et al., 2002; vom Saal et al., 1997) methods. Competitive binding to estrogen receptors is one of the most popular endpoints during the initial screening stage because ligand binding to the receptors is the initial step for most hormonal actions. Competitive binding assays applying fluorescence polarization (Ohno et al., 2002), enzyme-linked immunosorbant assays (ELISA) (Koda et al., 2002; Morohoshi et al., 2005), and using bacterial magnetic particles (Yoshino et al., 2005) have been developed to replace conventional assays using radio labeled compounds.

It is generally accepted that the free concentration is the driving force for modes of toxic action and the environmental fate of aquatic pollutants (Heringa et al., 2004; Reichenberg and Mayer, 2006). Unfortunately, the free concentration is rarely used as a dose-metric for conventional in vitro screening methods including competitive receptor binding assays. For example, Heringa et al. (2004) have shown that significant underestimation of the estrogenic potential of highly hydrophobic EDCs, such as alkylphenols, may be caused by their binding to serum proteins, surfaces of plastic labwares, etc. Although no serum proteins are added in typical competitive receptor binding assays, binding of EDCs to estrogen receptors may significantly reduce the free concentrations in the solution, especially for strong ligands. This variability in the

proportionality between free and nominal concentrations may cause inconsistency in results obtained from different assay conditions.

Consequently, competitive binding to human estrogen receptor α (hER-α) was conducted for three model EDCs, diethylstilbestrol, ethynylestradiol, and bisphenol A. A competitive hER-α binding assay detecting released estrogen by ELISA was used because it is high-throughput and does not require expensive experimental devices. An equilibrium binding model was used to estimate the free concentrations of EDCs in the given assay condition under the assumption that equilibrium is achieved rapidly. Effects of receptor concentration on the inhibition curves and corresponding concentration causing 50% inhibition (IC50) were also evaluated.

6.2. MATERIALS AND METHODS

6.2.1. Materials

Three model endocrine disrupting chemicals were selected to evaluate the effects of binding affinity on the inhibition curves. Diethylstilbestrol (DES) and 17α-ethynylestradiol (EE2) were chosen as examples of the strong ligands and bisphenol A (BPA) was chosen as a model weak ligand. All chemicals were of high purity. DES and EE2 were purchased from Sigma Chemical Co. (St. Louis, MO, USA). 17β-estradiol (E2) and BPA were purchased from Aldrich Chemical Co. (Milwaukee, WI, USA).

For an artificial lipid membrane permeation system, dodecane containing 0.5% (w/w) palmitoyloleoylphosphatidylcholine (POPC, C18:1, 16:0) was chosen for a model lipid membrane supported by a polyvinylidene fluoride (PVDF) filter (0.45 μm pore size; Millipore, Billerica, MA, USA). A chloroform solution of POPC was purchased from Avanti Polar Lipids (Albaster, AL, USA).

Human estrogen receptor α (hER-α) was purchased from PanVera (Madison, WI, USA). Aqueous estradiol not bound to hER-α was detected using an enzyme-linked immunosorbant assay (ELISA) kit for the detection of 17β-estradiol (Neogen Corp., Lexington, KY, USA).

6.2.2. Competitive estrogen receptor binding assay

Relative binding affinity and inhibition curves of three selected estrogenic chemicals were obtained using a competitive estrogen receptor binding assay in the absence of radio-labeled compounds. The assay was performed using a procedure described in literature (summarized as depicted in Figure 6.1; for details, see Koda et al., 2002; Morohoshi et al., 2005) with slight modifications. In brief, 25 μL of chemical solutions containing endocrine disrupting chemicals (EDCs) were incubated for 1 h with receptor (1/50 dilution from the solution provided by the manufacturer, 15 μL) and a 17β-estradiol (E2) solution (7.2 nM, 25 μL). A custom-made Teflon® well plate was used as the reaction plate to minimize any possible interactions with surface material. To detect E2 concentrations not bound to hER-α, 50 μL of the reaction solution was transferred to an antibody plate coated with estradiol antibody and incubated with an equal amount of estradiol-horseradish peroxidase (E2-HRP) obtained from Neogen for 1 h. After the plate was cleaned three times using a washing solution (50 mM disodiumphosphate, 150 mM NaCl, 0.05% Tween 20, 200 μL), 150 μL of a substrate solution (3,3',5,5'-tetramethylbenzidine) was added and the antibody plate was further incubated for 30 min at 25°C. The absorbance of each well was measured at 650 nm using a Synergy™ HT multi-detection microplate reader (BIO-TEK Instruments, Inc., Winooski, VT, USA). The measured absorbance was normalized by the absorbance from the blank sample (buffer+E2-HRP). Reaction solution incubated with excess diethylstilbestrol (500 nM) was used as a positive control. Inhibition in color

development (I) was calculated from I= ([B]-[S])/ ([B]-[P]), where [B], [S], and [P] are normalized absorbance (A/A0) for the negative control (buffer and 7.2 nM E2), the EDC solution, and the positive control (500 nM DES + 7.2 nM E2), respectively.

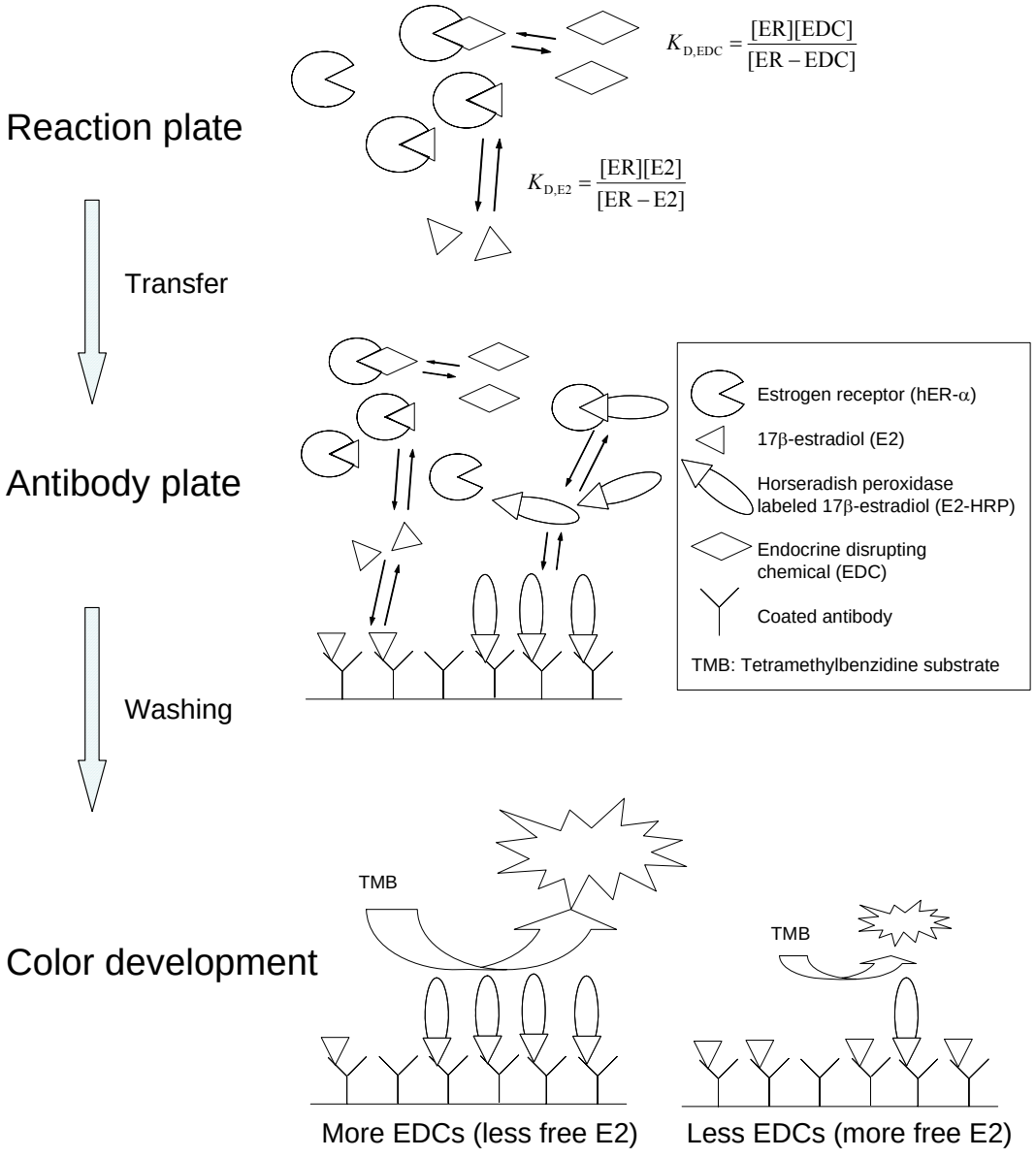

Figure 6.1: Principle of the competitive receptor binding assay using an enzyme-linked immunosorbant assay for the detection of free estrogens. (reconstructed from Koda et al., 2002).

6.2.3. Equilibrium binding model

Because ligand-receptor binding and antigen-antibody binding are thought to be very fast reactions, it is reasonable to assume that all chemical species are in equilibrium for both the reaction and the antibody plates. Thus, competitive binding in the reaction plate can be expressed by two equilibrium binding reactions:

E2 + ER $\Leftrightarrow$ ER-E2 $\qquad K_{\mathrm{D,E2}} = \dfrac{\mathrm{free[ER]\,free[E2]}}{\mathrm{[ER-E2]}}$ (6.1)

EDC + ER $\Leftrightarrow$ ER-EDC $\qquad K_{\mathrm{D,EDC}} = \dfrac{\mathrm{free[ER]\,free[EDC]}}{\mathrm{[ER-EDC]}}$ (6.2)

Mass balance equations for E2, EDC, and ER in the antibody plate are

$$\mathrm{total[E2] = unbound[E2] + [ER\text{-}E2] = free[E2] + [Ab\text{-}E2] + [ER\text{-}E2]} \tag{6.3}$$

$$\mathrm{total[EDC] = free[EDC] + [ER\text{-}EDC]} \tag{6.4}$$

$$\mathrm{total[ER] = free[ER] + [ER\text{-}E2] + [ER\text{-}EDC]} \tag{6.5}$$

where unbound[E2] represents any 17β-estradiol in a well of the antibody plate not bound to receptors (i.e., free and unbound to the antibody) and [Ab-E2] represents estradiol bound to the coated antibody. In the absence of any other competing ligands, unbound[E2] can be estimated from measured A/A0 by interpolation using two nearest A/A0 values from the standard curve. Under the assumtion that free[E2] is proportional to unbound[E2], equation 6.1 can be written using unbound[E2] instead of free[E2] with the modified dissociation constant, $K'_{\mathrm{D,E2}}$:

$$K'_{\mathrm{D,E2}} = \frac{\mathrm{free[ER]\,unbound[E2]}}{\mathrm{[ER-E2]}} \tag{6.6}$$

Plugging equation 6.3 into 6.6 and rearranging, one finds

$$\frac{\mathrm{[ER-E2]}}{\mathrm{unbound[E2]}} = \frac{1}{K'_{\mathrm{D,E2}}}\left(\mathrm{total[ER]} - \mathrm{[ER-E2]}\right) \tag{6.7}$$

Thus, the modified dissociation constant and total amount of active hER-α can be obtained by plotting [ER-E2]/unbound[E2] vs. [ER-E2].

In the presence of competing ligands, unbound[E2] can be calculated from EDC dose, either total[EDC] or free[EDC] with the estimated $K_{D,EDC}$ by solving equations 6.2 through 6.6 (see Appendix C for a more detailed derivation). Corresponding A/A0 and inhibition in color development (I) were calculated from unbound[E2]. Relative binding affinity (RBA) is calculated as a ratio of $K'_{D,E2}$ over $K_{D,EDC}$.

6.2.4. Experiment using an artificial membrane system

The competitive estrogen binding assay was coupled with a parallel artificial membrane system using a custom-made reactor at 25°C. Detailed description of the system has been presented in our earlier work (Kwon et al., 2006b). In short, an acceptor (0.35 ml shell insert) and a donor (5 ml volumetric flask) were separated by a polyvinyledene fluoride (PVDF) membrane filter (0.45 μm pore size, 125 μm thickness, Millipore, Milford, MA, USA). The acceptor cell was filled with 60 μl of receptor solution for measuring inhibition or aqueous buffer solution for measuring permeation rate. Permeation rates for DES and BPA were determined. As soon as 3 μl of the dodecane containing 0.5% (w/w) palmitoyloleoylphosphatidylcholine (POPC, C18:1, 16:0) solution was applied to the membrane filter, the acceptor cell was closed and attached to the flow-through donor cell that had been prefilled with buffer containing the chemical species. The donor cell was stirred using a VP710C1 tumble stirrer (V&P Scientific, San Diego, CA, USA) at 300 rpm for rapid mixing of the donor solution. The acceptor cell was not stirred because preliminary experiments showed that the binding activity of receptors significantly decreased with stirring. After incubation, both the acceptor and donor solutions were analyzed using a Waters 2690 HPLC system equipped

with a Waters 996 PDA detector (Milford, MA, USA) on C18 column (Waters Nova-Pak, 3.9×150 mm) at 40ºC for the determination of membrane permeation rate.

6.3. RESULTS AND DISCUSSION

6.3.1. Determination of the dissociation constant and active ER concentration

Figure 6.2 shows a typical standard curve without estrogen receptors or EDCs and normalized absorbance values (A/A0) measured after incubation in the reaction plate with hER-α. Horizontal differences between two series represent 17β-estradiol (E2) bound to the receptor, [ER-E2]. The dissociation constant for E2 from hER-α and the active concentration of hER-α (total[ER]) were determined using a Scatchard plot ([ER-E2]/unbound[E2] vs. [ER-E2]; Figure 6.3). From the slope and the intercept of the regression described in equation 6.7, $K'_{D,E2}$ was determined to be 0.92 nM and the active receptor concentration was 3.84 nM. The measured $K'_{D,E2}$ in this study is in good agreement with literature K_D values, typically reported to between 0.1 and 2.0 nM, obtained using various techniques (e.g., Kuiper et al., 1997, 1998; Matthews et al., 2000; Ohno et al., 2002; Rich et al., 2002; Usami et al., 2002; Yoshino et al., 2005), although $K'_{D,E2}$ may overestimate the dissociation constant because unbound[E2] used in equation 6.6 is greater than free[E2]. The measured active receptor concentration is slightly less than the value calculated by the manufacturer using a dilution factor, 4.6 nM. This could be due to denaturation of the receptor during the preparation steps.

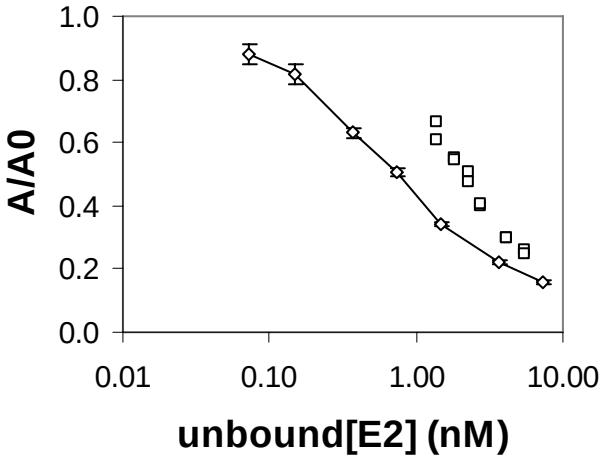

Figure 6.2: A typical standard curve (◇) and measured normalized absorbance, A/A0 (□) in the presence of hER-α. Error bars denote standard deviations.

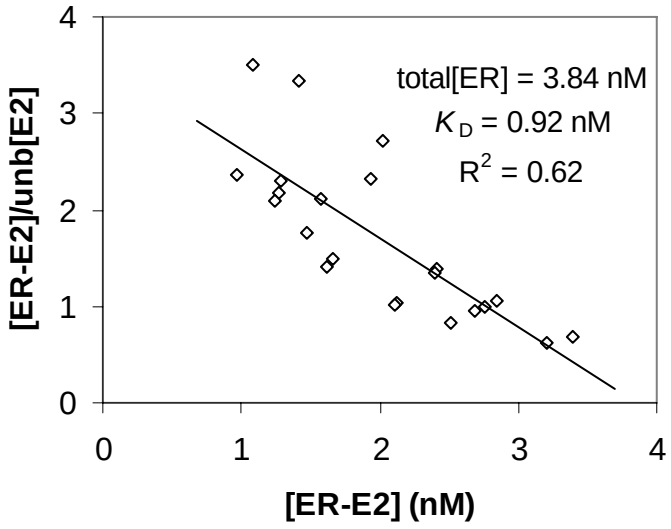

Figure 6.3: Scatchard plot ([ER-E2]/unb[E2] vs. [ER-E2]) for 17β-estradiol (E2) binding to human estrogen receptor α (hER-α).

6.3.2. Competitive estrogen receptor binding assay

Figure 6.4 shows inhibition curves for DES, EE2, and BPA obtained from the receptor and E2 concentrations described above. Solid lines are theoretical inhibition curves obtained using a least-square method. The estimated relative absorbance (A/A0) was calculated from the unbound[E2] concentration which is determined by dissociation constants for the EDCs as described in equation 6.2 through 6.6. Dissociation constants for DES, EE2, and BPA, obtained as a best-fit parameter, were 0.86, 3.0, and 1130 nM, respectively. Inhibition curves calculated using the free concentration of the EDC as a dose-metric were also presented (as dotted lines) in Figure 6.4. As can be seen from Figure 6.4, the discrepancy between the two inhibition curves strongly depends on the binding affinity of an EDC to hER-α, because binding of a strong ligand to the receptor significantly lowers the free concentration of the ligand in the assay system. Table 6.1 shows IC50 values of EDCs. The ratio, $IC50_{DES}/IC50_{EDC}$ for EE2 and BPA using apparent IC50 values are 0.46 and 0.0015, respectively. These values are significantly greater than the ratios of the relative binding affinity for EE2 and BPA to that for DES. If $IC50/IC50_{DES}$ values are calculated from the free concentration inhibition curves, they are equal to the ratio of dissociation constants. As can be seen in Table 6.1, overestimation of the binding affinity is expected especially for weaker ligands, if the relative binding affinity is simply normalized by the apparent IC50 of DES, as reported in literature (Koda et al., 2002; Morohoshi et al., 2005).

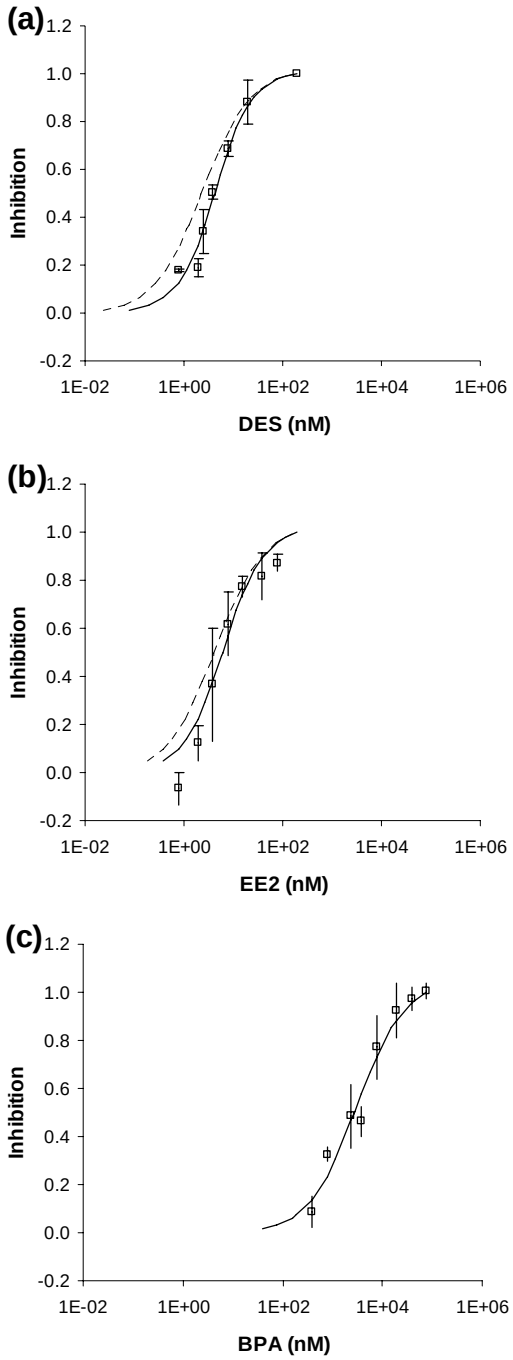

Figure 6.4: Inhibition curves for (a) diethylstilbestrol (DES), (b) ethynylestradiol (EE2), and (c) bisphenol A (BPA). Theoretical inhibition curves are shown in solid lines using nominal concentration as a dose-metric and in dotted lines using free concentration as a dose-metric. Error bars denote the standard deviation in inhibition from at least three independent measurements.

Table 6.1: IC50 values calculated using nominal and free concentration

	IC50 (nM)		$IC50_{DES}$/IC50	
	Apparent	Free	Apparent	Free
Diethylstilbestrol (DES)	4.2	2.3	1	1
Ethynylestradiol (EE2)	6.0	4.1	0.70	0.56
Bisphenol A (BPA)	2570	2570	0.0016	0.00094

6.3.3. Prediction of inhibition curves using an equilibrium model

Although dissociation constants are unchanged at a given experimental temperature, apparent IC50 values obtained from the experimental inhibition curve depend on specific assay conditions, including receptor and E2 concentration. More receptors or more E2 in the reaction plate should increase measured IC50 values determined from the experimental inhibition curve. Figure 6.5 shows the inhibition values obtained using a 7.7 nM receptor concentration to check the validity of the equilibrium binding model. Dotted lines and solid lines represent the estimated inhibition curves from Figure 6.4 and predicted inhibition curves using the same parameter values except for the receptor concentration, respectively. The experimental values agree well with the predicted inhibition, indicating that the chemistry of competitive binding in the ELISA system can be described by the equilibrium binding model. In addition, the effects of receptor concentration on IC50 are greater for stronger ligands.

The increased sensitivity of detecting inhibition with decreasing receptor and estradiol concentration in Koda et al. (2002) can be explained quantitatively as presented in this study. However, as can be seen in Table 6.1, $IC50_{DES}$/IC50 may depend on the assay condition, unless free concentration IC50 or estimated dissociation constants are

used. Figure 6.6 shows predicted changes in apparent $IC50_{DES}/IC50$ using BPA as an example weak ligand. Apparent $IC50_{DES}/IC50_{BPA}$ increases with increasing receptor concentration because the inhibition curve for a stronger ligand is shifted more to the right than that for a weak ligand. This supports the hypothesis that more reliable results for relative binding affinity can be obtained from estimated dissociation constants rather than apparent IC50 values.

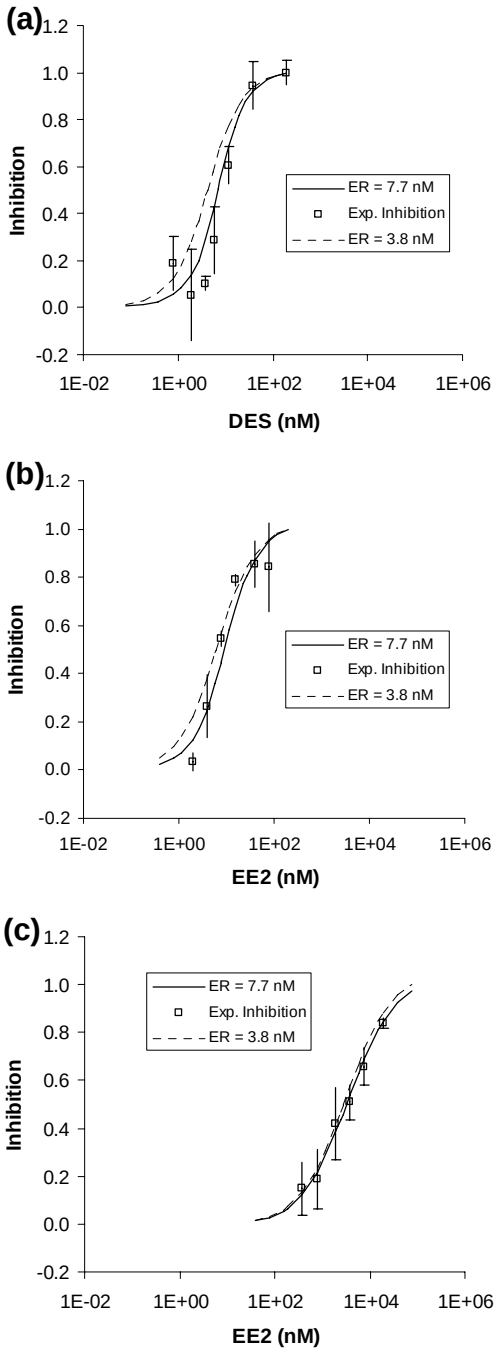

Figure 6.5: Estimated inhibition curves for (a) diethylstilbestrol (DES), (b) ethynylestradiol (EE2), and (c) bisphenol A (BPA) with experimental inhibition results. Estimated inhibition curves with receptor concentration of 7.7 nM are represented in solid lines. Dotted lines indicate the inhibition curves from Figure 6.4.

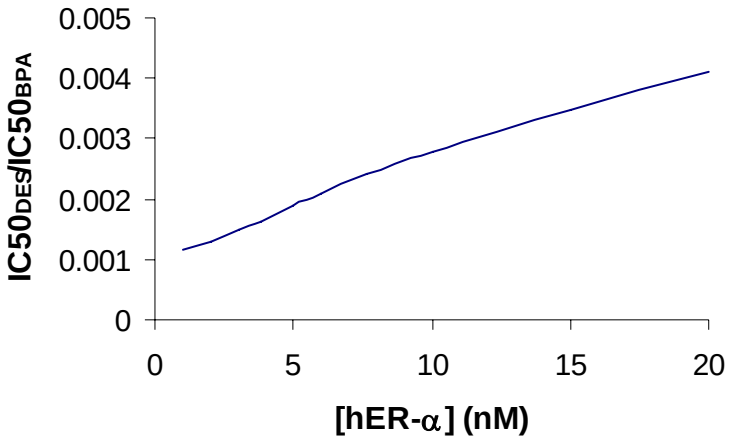

Figure 6.6: The effects of receptor concentration on the apparent IC50DES/IC50 using bisphenol A as an example ligand.

6.3.4. Receptor binding assay using the artificial membrane system

Figure 6.7 shows the change in acceptor concentration with respect to time of exposure. DES permeates the membrane faster than BPA probably due to its higher lipid membrane partition coefficient. Although stirring effectively decreases the thickness of the diffusion film on the donor side, the rate of membrane permeation is likely determined by aqueous diffusion on the acceptor side. The incubation time required to obtain an apparent equilibrium, typically C_A/C_{in} greater than 0.95, was longer than 24 h. However, the binding activity of the receptor solution could not be reasonably maintained for 24 h for the experimental conditions. Thus, it was not possible to obtain experimental inhibition curves using free concentration as a dose-metric. Furthermore, receptor solutions incubated in the acceptor cell for a relatively short time (1-8 h) did not significantly bind to E2 after incubating this solution with the standard concentration of E2, 2.77 nM. The significant reduction of binding capacity of the receptor was probably

due to either sorption of the receptor to the lipid membrane or denaturation. In order to show the effects of free concentration in the competitive binding ELISA linked to an exposure to EDCs through the parallel artificial membrane system, a stable ER binding domain may be attached to a solid phase (e.g., Kim et al., 2004). If this binding domain is not susceptible to the shear stress caused by mixing the acceptor solution, the system could be ideal for the evaluation of real-time estrogen receptor binding because the parallel artificial membrane system can be optimized to mimic passive transfer of organic chemicals in fish by stirring both the donor and the acceptor (Kwon et al., 2006b).

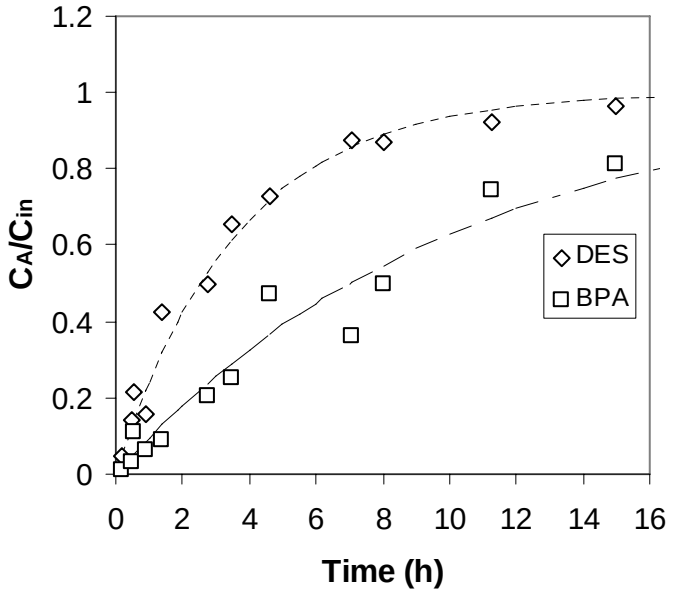

Figure 6.7: Concentration of chemicals in the acceptor cell with respect to time of exposure for diethylstilbestrol (DES) and bisphenol A (BPA). Broken lines represent estimated using best-fit values of first-order uptake rate constant.

6.3.4. Implications to endocrine disruption in aquatic animals

The competitive receptor binding assay has been typically used to evaluate relative binding affinity (RBA) to receptors (e.g., Koda et al., 2002; Kuiper et al., 1997, 1998; Ohno et al., 2002). However, an RBA value obtained from a specific assay condition may not be consistent with values obtained using different conditions due to depletion of strong ligands by binding to the receptors, unless dissociation constants (or free concentration) are used. Because free concentration is the driving force for the fate of aquatic pollutants, better prediction of RBA in terms of aquatic toxicology can be obtained from models incorporating measured dissociation constants.

Endocrine disruption in wildlife is the result of several very complicated processes as described in Chapter 2. However, ligand binding to the hormone receptor is the initial step for the hormone action. Although many potential estrogenic EDCs have been evaluated by their binding affinity to different estrogen receptors isolated from different species (e.g., Lutz and Kloas, 1999; Matthews et al., 2000; Menuet et al., 2002), little is known about the relationship between the amount of the activated receptors from foreign ligands and the various endpoints for the detection of estrogenicity. Because the toxicity of receptor mediated toxicant at the species level may not be evaluated by simply combining bioconcentration rates and in vitro toxicity endpoints (Verhaar et al., 1992, 1999), further investigation is need to fill the gaps among different in vitro and in vivo assays. Free concentration as evaluated in this study would be critical to explain the differences in responses.

Chapter 7: Conclusions and Recommendations for Future Research

7.1. CONCLUSIONS

This research provided a mechanistic insight for biopartitioning between water and lipid membranes and a practical tool for assessing the environmental exposure to aqueous pollutants. Chapter 3 and Chapter 4 provided the theoretical background for why K_{OW} cannot be directly correlated with lipid membrane-water partition coefficients (K_{lipw}). Hydrophobic interactions evaluated from octanol/water systems were not appropriate for estimating K_{lipw} for the selected endocrine disrupting chemicals (EDCs) having a relatively large molar liquid volume (MLV) and containing polar functional groups. Correlations that include MLV and polar surface area (PSA) reduce the predicted value of log K_{lipw}, suggesting that lipid membranes are less favorable than 1-octanol for a hydrophobic solute because of the changes in membrane fluidity and the amount of cholesterol in the lipid bilayer. These results suggested that K_{OW} alone has limited potential for estimating K_{lipw} and MLV or PSA may be used as additional descriptors for the prediction. In addition, K_{lipw} values vary up to two orders of magnitude due to the changes in membrane fluidity and the amount of cholesterol in the lipid bilayer. A careful choice of the lipid components is necessary to evaluate bioconcentration of these compounds. The observed discrepancy between K_{OW} and K_{lipw} may be due to the highly organized structure of lipid bilayers. Partitioning into lipid bilayers can be driven by negative enthalpy change or positive entropy change. Experimental results showed that the entropy contribution is much more significant for partitioning into more structurally organized saturated liposomes than into unsaturated liposomes. It is proposed that an entropy-driven partitioning process makes it different from 1-octanol/water system especially for more saturated lipid bilayer membranes. Differences in thermodynamic

constants in partitioning within different types of lipid membrane partly explain the inter- or intra-species variation of bioconcentration factors (BCFs) even though they are normalized by total lipid mass, including all different classes of membrane and non-membrane lipids.

Chapter 5 and Chapter 6 present the development and a potential application of a parallel artificial lipid membrane system for environmental exposure assessment. In this physical model system, a membrane filter-supported lipid bilayer separates two aqueous phases that represent the external and internal aqueous environments of fish. The thickness of the aqueous mass transfer boundary layer was carefully adjusted to mimic bioconcentration rate parameters in small fish. For the selected twenty-three simple aromatic hydrocarbons, literature absorption/elimination rates fall closely into the range predicted from measured membrane permeabilities and elimination rates of the selected chemicals determined using the physical model system. Because the artificial membrane system can be used to control freely available concentration of toxicants in the acceptor cell, it can be linked to existing in vitro toxicity assays for better assessment of the effects of receptor-mediated toxicants. However, this system has not yet been successfully coupled with estrogen receptor assays in the acceptor cell due to the lack of stability of the receptor solution under the experimental condition. Equilibrium modeling showed that the relative binding affinity of strong ligands may be underestimated if nominal concentration is used. This implies that the free concentration is a better dose-metric, and the artificial membrane device will be useful to control freely available concentrations of aquatic pollutants.

7.2. RECOMMENDATIONS FOR FUTURE RESEARCH

7.2.1. Predicting biopartitioning

Attempts have been made to predict bioaccumulation/bioconcentration of anthropogenic chemicals in aquatic organisms using simple parameters for decades. Although there have been noticeable successes in predicting biopartitioning from water and bulk organic solvent equilibrium partition coefficients (e.g., K_{OW}), the applicability of K_{OW} is in doubt for a wide range of chemicals. The results presented in Chapter 3 and 4 provide possible mechanistic insights to the non-linear relationship between log K_{OW} and bio-partitioning as well as the theoretical basis. The recommended direction of future investigation is presented, as follows.

1. In this study, K_{OW}, MLV, PSA are used to relate K_{OW} and K_{lipw} to evaluate hydrophobic interactions (e.g., van der Waals interaction), solute size effects, and polar interactions (e.g., hydrogen bonding), respectively (Chapter 3). However, those parameters are not completely independent from each other and the actual contributions of each may be masked. Effects of those parameters could be scrutinized by carefully selecting a large set of structurally different model compounds. Theoretical improvement of the relationship could be made by using quantum mechanical descriptors (Vaes et al., 1998).
2. Phosphatidylcholine lipid membrane vesicles are more representative models for biological membranes than surfactant micelles or bulk organic solvents. However, real biomembranes have diverse headgroups and contain significant amount of sugars and membrane proteins (Alberts et al., 2002). Although membrane permeation and equilibrium partitioning of hydrophobic organic chemicals are thought to be determined by fatty acid tails, little is known about

the roles of headgroups, membrane proteins and other components. Their contribution should be assessed as they may be important for certain chemicals.

3. In this study, K_{lipw} values varied within two-orders of magnitude for certain chemicals depending on the membrane fluidity and cholesterol content. Although the choice of the model lipid components in this study was somewhat extreme, the results imply that there should be an intrinsic variance of bioconcentration factors (BCFs) in aquatic organisms even if they are completely determined by equilibrium partitioning. Species-to-species variation of lipid-normalized BCF (LBCF) could be explained by the lipid compositions of the organism. A greater LBCF is expected for an organism containing more non-membrane lipids, more unsaturated fatty acids, and less cholesterol. Similarly, the internal distribution of hydrophobic organic chemicals may be explained by the lipid compositions of an organ, although it depends on physiological processes.
4. Unlike 1-octanol/water partitioning model (Chiou et al., 1985; Sangster, 1989), the activity of moderately hydrophobic EDCs in lipid membranes is very significant. To validate the model proposed in Chapter 4, investigation of the association of sorbed chemicals within different regions of the lipid membranes at the molecular level is required. Perhaps NMR could be used to identify specific interactions between the partitioning atoms and lipid molecules and confirm preferred orientations and locations within the membranes.
5. Although regulatory standards for hydrophobic water pollutants should be based on their fate in the environment and in the body, it is difficult to determine a precise value causing an impact because there are large variations among experimental BCFs. Thus, the development of mathematical models or simple

physical models for predicting a whole-body BCF in a tiered risk assessment approach is needed (de Wolf et al., 2006).

7.2.2. Refining the parallel artificial membrane system

Although it requires improvements, the parallel artificial membrane system developed in this study showed great potential for mimicking passive uptake and elimination of water pollutants in fish (Chapter 5). A modification of the system was proposed in Chapter 6 by placing estrogen receptors in the acceptor cell which conceptually represents internal cellular environment. The following are recommended directions for future research toward extending the applicability of the system for ionizable or metabolizable chemicals (Escher and Kwon, 2006) and linking the system for ecotoxicological risk assessment.

1. For ionized compounds, common BCF models assume that the charged species do not contribute to the overall BCF but experimental evidence refutes this assumption (Saarikoski et al., 1986). Actual bioconcentration is higher than anticipated from these models. Very recently a comprehensive model of bioconcentration of ionizable organic compounds has been developed (Erickson, 2006a) that describes bioconcentration as a series of passive diffusion processes of the neutral species followed by re-equilibration of the acid-base equilibrium so that a net uptake of charged molecules is possible. Because CO_2 transfer at the fish gill is proposed to significantly affect uptake of ionizable chemicals by changing internal pH (Erickson et al., 2006a, b), the permeability of ionizable chemicals could be evaluated at various pH values. The acceptor cell may be saturated with CO_2 and the optimized CO_2 concentration gradient (or pH gradient) may be pursued to validate the applicability of this system for ionizable chemicals. Schematic design of this modification is described in Figure 7.1.

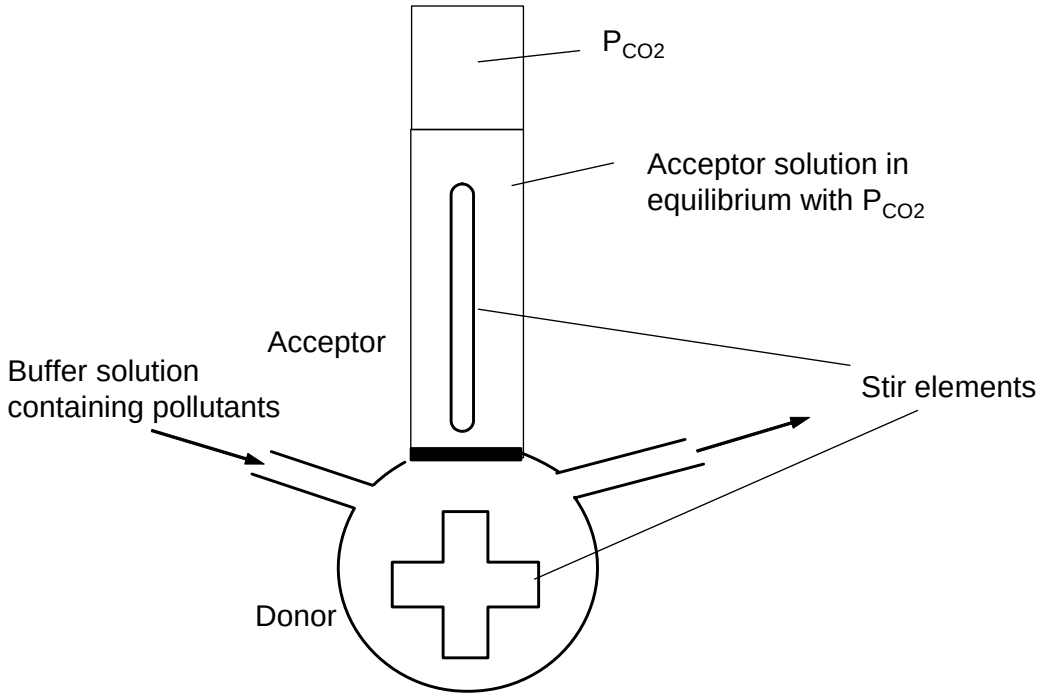

Figure 7.1: A conceptual design of the modified parallel artificial membrane reactors for the evaluation of pH gradient.

2. Bioconcentration is a comprehensive process including absorption, distribution, metabolism, and excretion (ADME). Although metabolism decreases the BCF, this is not taken into account in existing bioconcentration models. Thus, an alternative in-vitro test method and prediction model for bioconcentration in fish must take into account these limitations and find solutions for them. Metabolic degradation rate will be evaluated by adding an enzyme mixture. Initially the metabolic degradation rate could be evaluated using a simple enzymatic batch reactor system. With separate measurement of the degradation rate and the effective permeability, bioconcentration kinetics in fish will be modeled using passive membrane permeation rate and metabolic deactivation rate. The

estimation from the two separate experiments could be evaluated by linking the enzymatic batch reactor to the artificial membrane system as conceptually described in Figure 7.2.

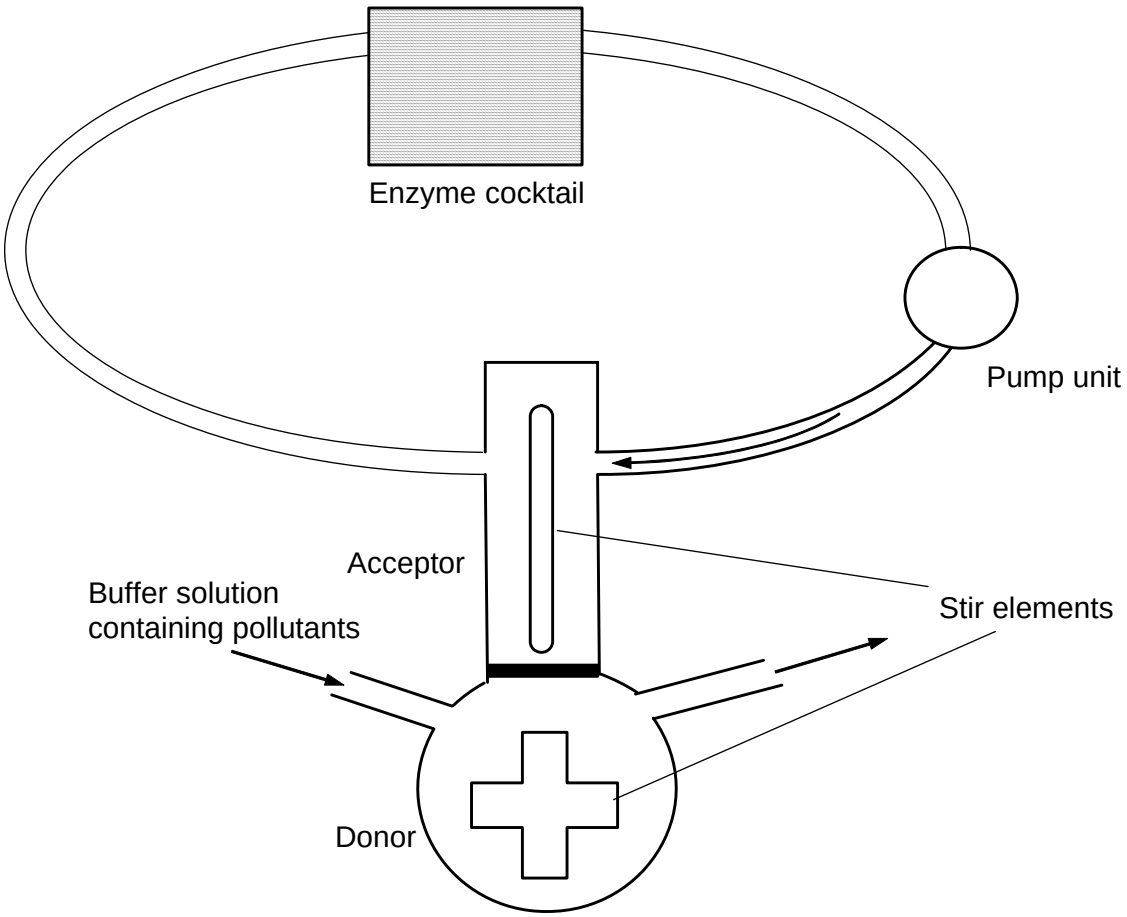

Figure 7.2: A conceptual design of the modified parallel artificial membrane reactors for the evaluation of metabolic degradation.

3. The parallel artificial membrane system used in this study was not very suitable for high-throughput screening, although it shows promise for wide applicability.

Adapting the system to make it compatible with a standard 96 well plate format would be desirable.

4. The lipid membrane phase used in this study is mostly comprised of a non-polar organic solvent, *n*-dodecane. Although it is generally thought that solute permeation through a series of cellular membranes is primarily determined by the diffusion in the aqueous boundary layer and in the hydrophobic core of the lipid bilayer, large amounts of dodecane in the membrane makes the system significantly different from natural membranes. Immobilized liposomes in a glass wool filter (or other supports) may solve this problem. To model paracellular diffusion, defined as solute transfer through tight junctions, immobilized liposomes may be used after being reinforced by an artificial cytoskeleton (e.g., actin filaments).
5. In Chapter 6, it was proposed that a competitive receptor binding assay may be better interpreted by using freely available concentration as a dose-metric. However, the experimental evidence was not clearly provided by the present study. The major drawback was stabilizing the binding affinity of the estrogen receptor in the acceptor cell. In addition, estrogen receptors seem to aggregate easily by stirring, although stirring both the donor and the acceptor cell is desired to more closely mimic aquatic organisms. If it is difficult to maintain the activity of the receptor solution during the incubation time, a ligand binding domain covalently attached to a solid surface may be used instead (Nesatyy et al., 2006).
6. Because the toxicity of many emerging environmental pollutants is not simply determined by the baseline toxicity (e.g., Escher and Hermens, 2002), similar experiments linking bioavailability to toxicity assays can be done for receptor-

mediated toxicants other than estrogenic EDCs. In addition, the system is also applicable for reactive toxicants (e.g., those causing oxidative damage in DNA).

Appendix A. Supplemental Data for Chapter 3

Table A.1: Sorption coefficients of the selected EDCs into DPPC liposomes.

Chemical	C_o (mg/L)	C_{ref} (mg/L)	C_w (mg/L)	R (%)	m (mg/L)	Fraction sorbed (%)	K_{lipw} (L/Kg-lipid)
Diethylstilbestrol	1.759	0.828±0.009	0.595±0.015	94.1	23.65	28.2	$1.66(\pm0.15)\times10^{4}$
Meso-Hexestrol	2.185	1.056±0.027	0.868±0.040	96.7	23.65	17.8	$9.23(\pm2.37)\times10^{3}$
Dienestrol	0.808	0.333±0.017	0.087±0.018	82.5	181.1	74.0	$1.63(\pm0.41)\times10^{4}$
4-Phenylphenol	1.873	0.939±0.006	0.790±0.009	100.2	421.5	15.8	$4.47(\pm0.33)\times10^{2}$
4-*sec*-Butylphenol	2.183	1.140±0.022	1.068±0.040	104.4	1029	6.3	$6.63(\pm3.78)\times10^{1}$
4-*tert*-Amylphenol	2.063	1.016±0.032	0.799±0.032	98.4	897.5	21.4	$3.04(\pm0.56)\times10^{2}$
Butyl-4-hydroxybenzoate	2.290	1.023±0.033	0.908±0.019	89.3	421.5	11.2	$2.99(\pm0.57)\times10^{2}$
Benzyl-4-hydroxybenzoate	1.898	0.949±0.017	0.794±0.015	100.0	421.5	16.4	$4.67(\pm0.53)\times10^{2}$
4,4'-Dihidroxybenzophenone	4.210	1.996±0.047	1.817±0.039	94.8	1818	9.0	$5.44(\pm1.31)\times10^{1}$
Progesterone	2.006	0.894±0.025	0.809±0.037	89.1	421.5	9.5	$2.53(\pm1.19)\times10^{1}$

Table A.2: Sorption coefficients of the selected EDCs into DPPC/cholesterol liposomes.

Chemical	C_o (mg/L)	C_{ref} (mg/L)	C_w (mg/L)	R (%)	m (mg/L)	Fraction sorbed (%)	K_{lipw} (L/Kg-lipid)
Diethylstilbestrol	1.994	0.900±0.014	0.829±0.032	90.3	524.3	7.9	$1.67(\pm0.83)\times10^{2}$
Meso-Hexestrol	2.155	1.026±0.021	0.962±0.023	95.2	524.3	6.2	$1.28(\pm0.48)\times10^{2}$
Dienestrol	0.808	0.333±0.017	0.139±0.007	82.5	966.8	58.4	$1.45(\pm0.12)\times10^{3}$
4-Phenylphenol	1.873	0.939±0.006	0.618±0.006	100.2	1087	34.2	$4.77(\pm0.13)\times10^{2}$
4-*tert*-Amylphenol	2.063	1.016±0.032	0.960±0.026	98.4	1755	5.4	$3.32(\pm1.66)\times10^{1}$
Butyl-4-hydroxybenzoate	2.141	1.052±0.026	0.881±0.042	98.2	1087	16.3	$1.80(\pm0.52)\times10^{2}$
Benzyl-4-hydroxybenzoate	2.068	1.020±0.018	0.793±0.027	98.6	1087	22.2	$2.63(\pm0.40)\times10^{2}$
Progesterone	2.006	0.894±0.025	0.842±0.032	89.1	524.3	5.8	$1.19(\pm0.75)\times10^{1}$

Table A.3: Sorption coefficients of the selected EDCs into POPC liposomes

Chemical	C_o (mg/L)	C_{ref} (mg/L)	C_w (mg/L)	R (%)	m (mg/L)	Fraction sorbed (%)	K_{lipw} (L/Kg-lipid)
Diethylstilbestrol	1.947	0.910±0.035	0.183±0.019	92.6	41.43	79.9	$9.61(\pm1.18)\times10^4$
Meso-Hexestrol	2.185	1.056±0.027	0.619±0.033	96.7	18.58	41.4	$3.82(\pm0.49)\times10^4$
Dienestrol	0.808	0.333±0.017	0.045±0.006	82.5	22.96	86.5	$2.84(\pm0.40)\times10^5$
4-Phenylphenol	1.873	0.939±0.006	0.387±0.011	100.2	293.2	58.8	$4.87(\pm0.23)\times10^3$
4-sec-Butylphenol	2.183	1.140±0.022	0.913±0.008	104.4	171.0	19.9	$1.45(\pm0.07)\times10^3$
4-tert-Armylphenol	2.063	1.016±0.032	0.547±0.021	98.4	213.7	21.4	$4.01(\pm0.33)\times10^3$
Butyl-4-hydroxybenzoate	2.290	1.023±0.033	0.506±0.020	89.3	293.2	50.5	$3.49(\pm0.27)\times10^3$
Benzyl-4-hydroxybenzoate	1.898	0.949±0.017	0.313±0.003	100.0	293.2	67.0	$6.93(\pm0.09)\times10^3$
4,4'Dihydroxybenzophenone	4.210	1.996±0.047	1.227±0.010	94.8	1241	38.5	$5.05(\pm0.11)\times10^2$
Diethylphthalate	5.184	2.449±0.099	2.283±0.059	94.5	1241	6.8	$5.93(\pm2.20)\times10^1$
Progesterone	2.006	0.894±0.025	0.678±0.041	89.1	171.0	24.2	$1.89(\pm0.49)\times10^3$

Appendix B. Supplemental Data for Chapter 4

Table B.1: Liposome-water partition coefficients (K_{lipw}s) for the selected EDCs obtained at 5 different temperatures using dioleoylphosphatidylcholine (DOPC) and dimyristoylphosphatidylcholine (DMPC), and distearylphosphatidylcholine (DSPC) liposomes.

		K_{lipw}s ($\times 10^3$)		
Chemicals	Temperature	DOPC	DMPC	DSPC
17β-Estradiol	11°C	1.49 (0.14)	0.40 (0.05)	0.12 (0.05)
	22°C	1.88 (0.69)	1.38 (0.31)	0.25 (0.05)
	25°C		1.96 (0.51)	
	30°C	1.85	1.89	0.23
	37°C	1.48 (0.14)	1.93 (0.25)	0.26 (0.10)
Diethylstilbestrol	11°C	73.8 (18.1)	29.9 (1.0)	5.40 (1.58)
	22°C	55.8 (12.1)	52.3 (12.8)	4.97 (1.22)
	25°C		44.9 (15.9)	
	30°C	53.4 (0.73)	85.2 (11.2)	4.84 (0.41)
	37°C	24.8	46.6 (3.9)	4.06 (0.50)
Bisphenol A	11°C	5.35 (0.97)	3.71 (0.30)	1.66 (0.03)
	22°C	4.35 (1.41)	4.17 (0.82)	1.22
	25°C		7.59 (0.44)	
	30°C	6.08 (0.50)	10.39 (0.57)	0.69 (0.12)
	37°C	3.17 (0.32)	6.27 (1.84)	0.36 (0.15)
p-*n*-Nonylphenol	11°C	615 (74)	1461 (332)	411 (91)
	22°C	705 (224)	1133 (135)	419 (79)
	25°C		1697 (1137)	
	30°C	393 (160)	1544 (254)	457 (181)
	37°C	437	723 (104)	418

Values in parentheses are standard deviation of triplicate analyses. Average values are used when duplicates are used without standard deviation.

Table B.2: Enthalpies (ΔH) and entropies (ΔS) of partitioning for 17β-estradiol, diethylstilbestrol, bisphenol A, and *p*-*n*-nonylphenol between water and three synthetic membrane vesicles, dioleoylphosphatidylcholine (DOPC) and distearylphosphatidylcholine (DSPC).

	$K_{lipw, DOPC}$			$K_{lipw, DSPC}$		
Chemicals	ΔH (kJ/mole)	$T\Delta S$* (kJ/mole)	r^2	ΔH (kJ/mole)	$T\Delta S$* (kJ/mole)	r^2
17β-Estradiol	0.7 (6.1)	18.9 (6.0)	0.01	22.0 (9.3)	34.9 (9.2)	0.74
Diethylstilbestrol	-26.8 (10.4)	-0.1 (10.3)	0.77	-7.2 (2.2)	13.7 (2.2)	0.84
Bisphenol A	-9.6 (11.3)	11.1 (11.2)	0.27	-42.1(8.7)	-25.2 (8.6)	0.92
p-*n*-Nonylphenol	-13.1 (8.8)	19.3 (8.8)	0.52	1.3 (2.0)	33.1 (2.0)	0.44

*Entropy contribution ($T\Delta S$) to the free energy change (ΔG) calculated at 22°C. Values in parentheses are standard errors of the regression.

Table B.3: Liposome-water partition coefficients (K_{lipw}s) for the selected EDCs obtained at 4 different temperatures using dioleoylphosphatidylcholine (DOPC) and dipalmytoylphosphatidylcholine (DPPC) with various cholesterol contents.

		K_{lipw}s ($\times 10^3$)					
		DOPC with cholesterol			DPPC with cholesterol		
Chemicals	Temperature	15%*	30%	50%	15%	30%	55%
Diethylstilbestrol	11°C	75.0	59.9	29.0	8.44 (1.22)	2.05 (0.03)	
	22°C	37.5 (7.4)	24.7 (5.9)	19.0 (4.2)	7.24 (3.94)	2.45 (0.95)	
	30°C	44.6 (7.1)	27.3 (1.6)	18.7 (2.0)	5.48 (0.60)	1.63 (0.33)	
	37°C	28.7 (4.2)	21.8 (2.4)	12.5 (0.8)	3.41 (0.35)	1.60 (0.14)	
Meso-Hexestrol	11°C	28.8 (6.0)	15.8 (0.3)	7.66 (0.54)	1.95 (0.21)	0.41 (0.06)	
	22°C	18.5 (2.4)	10.1 (1.9)	4.89 (3.04)	3.62 (1.11)	1.18 (0.09)	
	30°C	15.9 (2.0)	7.42 (1.08)	4.38 (0.53)	2.33 (0.09)	0.39 (0.04)	
	37°C	7.89	5.89 (0.49)	3.78 (0.79)	1.81 (0.58)	0.83 (0.28)	
p-tert-octylphenol	11°C	368 (16)	310	278 (25)	320 (35)	306 (34)	213 (32)
	22°C	244 (20)	293 (25)	336 (63)	132 (24)	171 (53)	138 (9)
	30°C	231 (27)	186 (9)	252 (32)	163 (22)	130 (7)	135 (11)
	37°C	136	98.4 (19.5)	134 (18)	126 (24)	84.0 (9.0)	104 (22)

*Mole fraction of cholesterol in the lipid bilayers. Values in parentheses are standard deviation of triplicate analyses. Average values are used when duplicates are used without standard deviation.

Table B.4: Enthalpies (ΔH) and entropies (ΔS) of partitioning for diethylstilbestrol, meso-hexestrol, and *p-tert*-octylphenol between water and dioleoylphosphatidylcholine (DOPC) with various cholesterol contents.

	$K_{lipw,\ DOPC/cholesterol\ (85/15)}$			$K_{lipw,\ DOPC/cholesterol\ (70/30)}$			$K_{lipw,\ DOPC/cholesterol\ (50/50)}$		
Chemicals	ΔH (kJ/mole)	$T\Delta S$* (kJ/mole)	r^2	ΔH (kJ/mole)	$T\Delta S$* (kJ/mole)	r^2	ΔH (kJ/mole)	$T\Delta S$* (kJ/mole)	r^2
Diethylstilbestrol	-23.7 (8.5)	2.7 (8.4)	0.80	-26.5 (9.8)	-0.9 (9.7)	0.79	-21.5 (4.6)	2.8 (4.6)	0.91
meso-Hexestrol	-33.4 (7.9)	-9.4 (7.8)	0.90	-28.0 (0.4)	-5.4 (0.4)	1.00	-19.5 (2.9)	1.6 (2.9)	0.96
p-tert-Octylphenol	-25.5 (6.0)	5.1 (6.0)	0.90	-31.2 (10.9)	-0.9 (10.8)	0.80	-18.9 (12.9)	11.7 (12.8)	0.52

*Entropy contribution ($T\Delta S$) to the free energy change (ΔG) calculated at 22°C. Values in parentheses are standard errors of the regression.

Table B.5: Enthalpies (ΔH) and entropies (ΔS) of partitioning for diethylstilbestrol, meso-hexestrol, and *p-tert*-octylphenol between water and dipalmitoylphosphatidylcholine (DPPC) with various cholesterol contents.

	$K_{lipw,\ DPPC/cholesterol\ (85/15)}$			$K_{lipw,\ DPPC/cholesterol\ (70/30)}$			$K_{lipw,\ DPPC/cholesterol\ (45/55)}$		
Chemicals	ΔH (kJ/mole)	$T\Delta S$* (kJ/mole)	r^2	ΔH (kJ/mole)	$T\Delta S$* (kJ/mole)	r^2	ΔH (kJ/mole)	$T\Delta S$* (kJ/mole)	r^2
Diethylstilbestrol	-24.4 (6.6)	-2.9 (6.5)	0.87	-9.0 (6.9)	9.6 (6.9)	0.46			
meso-Hexestrol	0.6 (5.5)	19.2 (5.5)	0.01	13.4 (13.3)	28.7 (13.2)	0.34			
p-tert-Octylphenol	-23.5 (11.0)	6.3 (10.9)	0.70	-35.2 (2.6)	-5.6 (2.5)	0.99	-18.7 (3.6)	10.6 (3.5)	0.93

*Entropy contribution ($T\Delta S$) to the free energy change (ΔG) calculated at 22°C. Values in parentheses are standard errors of the regression.

Appendix C. Supplemental Data for Chapter 5

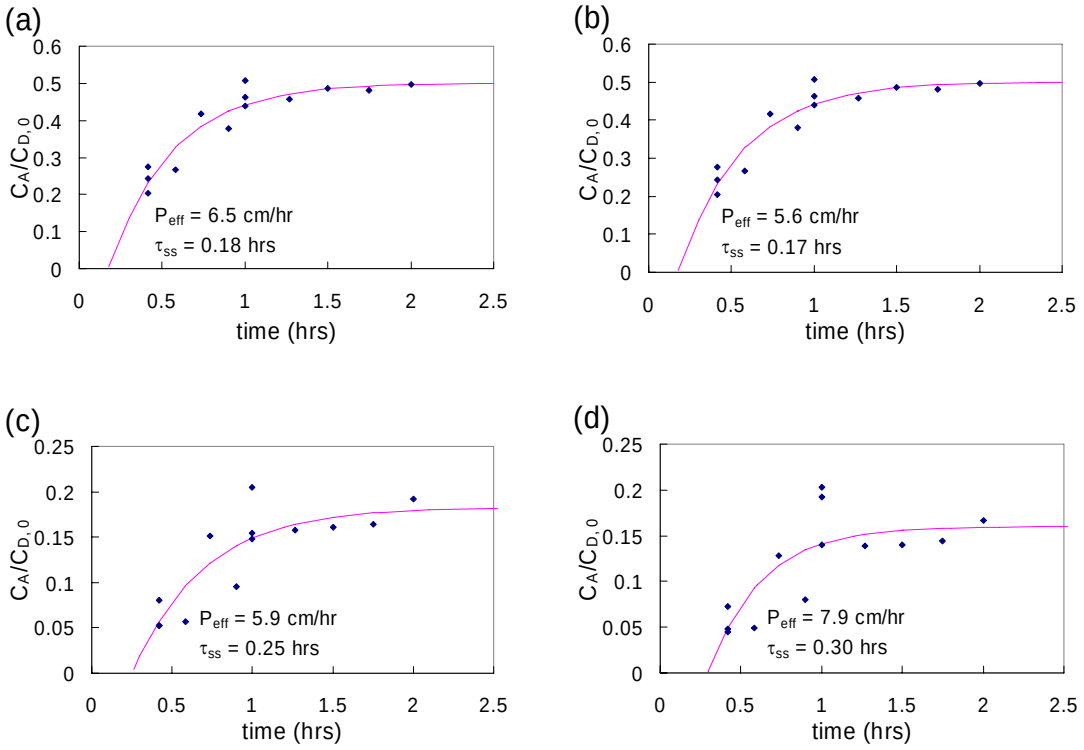

Figure B.1: Determination of the effective membrane permeability by non-linear regression using Equation 5.8 for (a) CB, (b) BB, (c) 14DCB, (d) 13DCB.

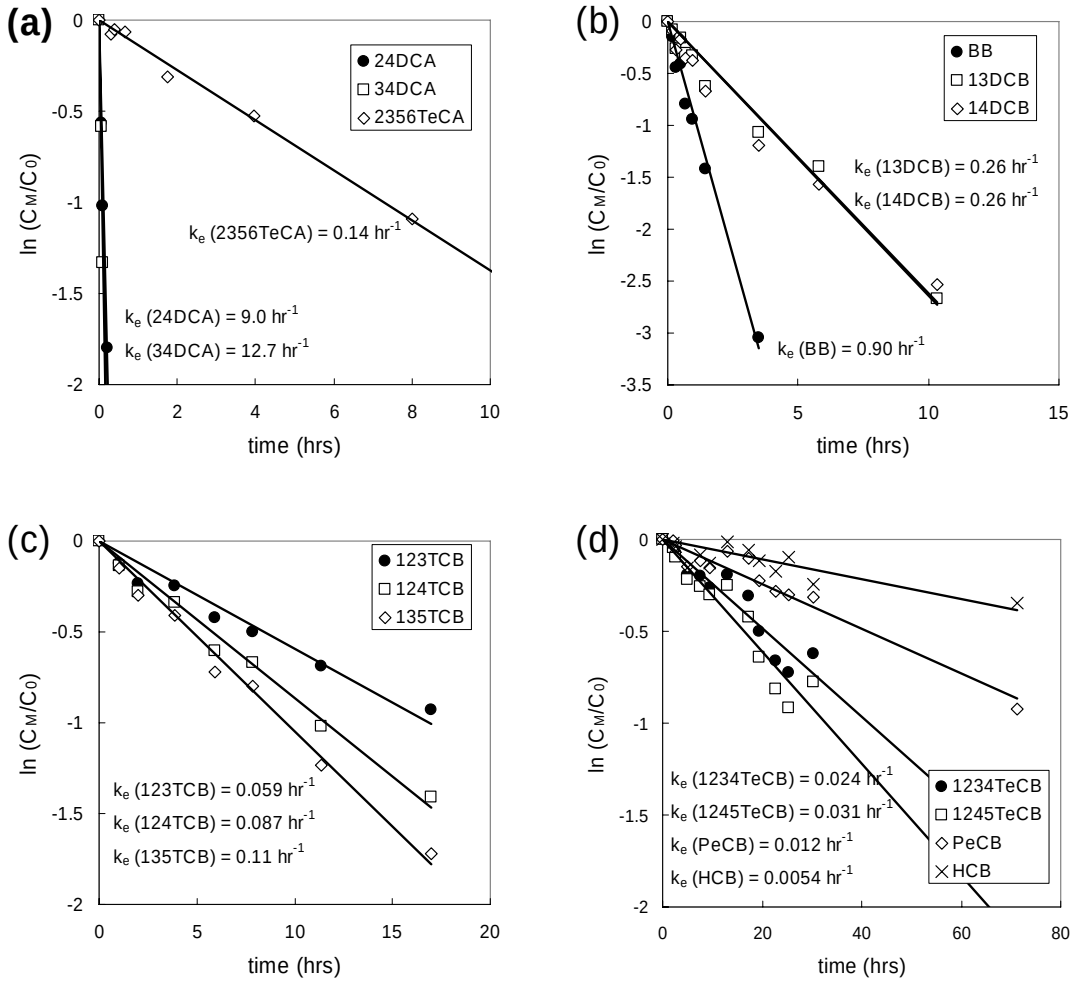

Figure B.2: Determination of first-order elimination rate constant from the artificial membrane system for (a) 24DCA, 34DCA, and 2356TeCA, (b) BB, 13DCB, 14DCB, (c) 123TCB, 124TCB, and 135TCB, and (d) 1234TeCB, 1245TeCB, PeCB, and HCB.

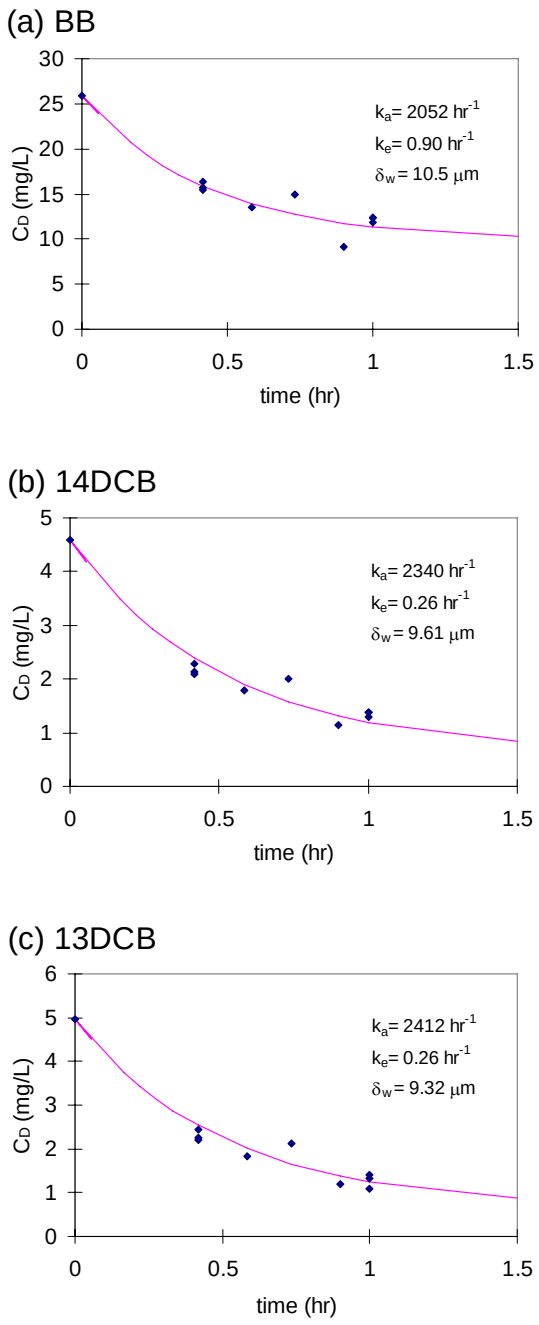

Figure B.3: Estimation of the donor side thickness of diffusion film. Best fit parameter, k_a, was obtained from measured elimination rate constants. δ_w was calculated from equation 5.2 assuming that this process is solely limited by aqueous diffusion.

Appendix D. Analytical Solutions for Chapter 6

At the equilibrium binding condition, there are five equations (eq. 6.2-6.6, repeated below) with five unknowns.

EDC + ER $\Leftrightarrow$ ER-EDC $\qquad K_{\mathrm{D,EDC}} = \dfrac{\mathrm{free[ER]\,free[EDC]}}{\mathrm{[ER-EDC]}}$ (6.2)

$$\mathrm{total[E2] = unbound[E2] + [ER\text{-}E2] = free[E2] + [Ab\text{-}E2] + [ER\text{-}E2]} \quad (6.3)$$

$$\mathrm{total[EDC] = free[EDC] + [ER\text{-}EDC]} \quad (6.4)$$

$$\mathrm{total[ER] = free[ER] + [ER\text{-}E2] + [ER\text{-}EDC]} \quad (6.5)$$

$$K'_{\mathrm{D,E2}} = \frac{\mathrm{free[ER]\,unbound[E2]}}{\mathrm{[ER-E2]}} \quad (6.6)$$

If $K'_{\mathrm{D,E2}}$ and $K_{\mathrm{D,EDC}}$ are not identical, a cubic equation for unbound[E2] is obtained by substituting relationships for free[ER], free[EDC], and [ER-EDC] based on unbound[E2] and known total concentrations as follows:

$$\mathrm{unbound[E2]}^3 + p\ \mathrm{unbound[E2]}^2 + q\ \mathrm{unbound[E2]} + r = 0 \quad (C.1)$$

where

$$p = -\frac{\left[K'_{\mathrm{D,E2}}\left(\mathrm{tot[EDC]-tot[ER]+2tot[E2]}-K'_{\mathrm{D,E2}}\right)+K_{\mathrm{D,EDC}}\left(\mathrm{tot[ER]-tot[E2]}+K'_{\mathrm{D,E2}}\right)\right]}{K'_{\mathrm{D,E2}}-K_{\mathrm{D,EDC}}},$$

$$q = -\frac{K'_{\mathrm{D,E2}}\,\mathrm{tot[E2]}\left(\mathrm{tot[EDC]-tot[ER]+tot[E2]}-2K'_{\mathrm{D,E2}}+K_{\mathrm{D,EDC}}\right)}{K'_{\mathrm{D,E2}}-K_{\mathrm{D,EDC}}}, \text{ and}$$

$$r = -\frac{{K'_{\mathrm{D,E2}}}^2\,\mathrm{tot[E2]}^2}{K'_{\mathrm{D,E2}}-K_{\mathrm{D,EDC}}}.$$

This cubic equation may be reduced to the form,

$$x^3+ax+b=0 \quad (C.2)$$

by substitution of the variable $x-\dfrac{p}{3}$ for the unbound[E2]. Here

$$a=\frac{1}{3}\left(3q-p^2\right) \text{ and } b=\frac{1}{27}\left(2p^3-9pq+27r\right).$$

Equation C.2 can be solved by transforming it to the trigometric identity (Shelby, 1969)

$$4\cos^3\theta - 3\cos\theta - \cos(3\theta) = 0 \tag{C.3}$$

Let $x = m\cos\theta$, then

$$x^3 + ax + b = 4\cos^3\theta - 3\cos\theta - \cos(3\theta) = 0 \tag{C.4}$$

where $m = 2\sqrt{-\frac{a}{3}}$ and $\cos(3\theta) = \frac{3b}{am}$.

Any solution θ_1 which satisfies $\cos(3\theta) = \frac{3b}{am}$ will also have the solutions $\theta_1 + \frac{2\pi}{3}$ and $\theta_1 + \frac{4\pi}{3}$.

Therefore, the roots of the cubic equations, $x^3+ax+b=0$ are $2\sqrt{-\frac{a}{3}}\cos\theta_1$, $2\sqrt{-\frac{a}{3}}\cos\left(\theta_1 + \frac{2\pi}{3}\right)$, $2\sqrt{-\frac{a}{3}}\cos\left(\theta_1 + \frac{4\pi}{3}\right)$.

In the case that $K_{\mathrm{D,EDC}}$ equals to $K'_{\mathrm{D,E2}}$, unbound[E2] can be solved by a quadratic equation

$$\text{unbound[E2]}^2 + s\ \text{unbound[E2]} + t = 0 \tag{C.5}$$

where $s = -\frac{\text{tot[E2]}\left(\text{tot[EDC]} - \text{tot[ER]} + \text{tot[E2]} - K'_{\mathrm{D,E2}}\right)}{\text{tot[EDC]} + \text{tot[E2]}}$ and $t = -\frac{K'_{\mathrm{D,E2}}\text{tot[E2]}^2}{\text{tot[EDC]} + \text{tot[E2]}}$.

Bibliography

Aerni HS, Kobler B, Rutishauser BV, Wettstein FE, Fischer R, Giger W, Hungerbühler A, Marazuela MD, Peter A, Schönenberger R, Vögeli AC, Suter MJF, Eggen RIL. 2004. Combined biological and chemical assessment of estrogenic activities in wastewater treatment plant effluents. *Anal Bioanal Chem* 378:688-696.

Ahel M, Giger W. 1993. Aqueous solubility of alkylphenols and alkylphenol polyethoxylates. *Chemosphere* 26:1461-1470.

Ahel M, Giger W, Schaffner C. 1994. Behavior of alkylphenol polyethoxylate surfactants in the aquatic environment. I. occurrence and transportation in rivers. *Wat Res* 28:1131-1142

Alberts B, Johnson A, Lewis J, Raff M, Roberts K, Walter P. 2002. Molecular *Biology of the Cell*, 4th eds., Garland Science, NewYork, NY, USA.

Allen Y, Mathiessen P, Haworth S, Thain JE, Feist S. 1999. A survey of the estrogenic activity in the UK estuarine and coastal waters and its effects on gonadal development of the flounder (Platichthys flesus). *Environ Toxicol Chem* 18:1791-1800.

Alzieu C. 1991. Environmental problems caused by TBT in France – assessment, regulations, prospects. *Mar Environ Res* 32:7-17.

Avdeef A. 2005. The rise of PAMPA. *Expert Opinion on Drug Metabolism and Toxicology* 1:325-342.

Avdeef A. 2001. Physicochemical profiling (solubility, permeability and charge state). *Curr Topics Med Chem* 1:277-351.

Ávila CM, Martinez F. 2003. Thermodynamics of partitioning of benzocaine in some organic solvent/buffer and liposome systems. *Chem Pharm Bull* 51:237-240.

Bahadur NP, Shiu WY, Boocock DGB, Mackay D. 1997. Temperature dependence of octanol-water partition coefficient for selected chlorobenzenes. *J Chem Eng Data* 42:685-688.

Banerjee S, Sugatt RH, O'Grady DP. 1984. A simple method for determining bioconcentration parameters of hydrophobic compounds. *Environ Sci Technol* 18:79-81.

Barber MC, Suárez LA, Lassiter RR. 1988. Modeling bioconcentration of nonpolar organic pollutants by fish. *Environ Toxicol Chem* 7:545-558.

Barnhoorn IEJ, Borman MS, Pieterse GM, van Vuren JHJ. 2004. Histological evidence of intersex in feral sharptooth catfish (*Clarias gariepinus*) from an estrogen-polluted water source in Gauteng, South Africa. *Environ Toxicol* 19:603-608.

Barron MG, Schultz IR, Hayton WL. 1989. Presystemic branchial metabolism limits di-ethylhexyl phthalate accumulation in fish. *Toxicol Appl Pharmacol* 15:49-57.

Bergen BJ, Nelson WG, Quinn JG, Jayaraman S. 2001. Relationships among total lipid, lipid classes, and polychlorinated biphenyl concentrations in two indigenous populations of ribbed mussels (*Geukensia Demissa*) over an annual cycle. *Environ Toxicol Chem* 20:575-581.

Birkett JB, Lester JN. 2003. Endocrine Disrupters in Wastewater and Sludge Treatment Processes, CRC Press, Boca Raton, FL.

Blair RM, Fang H, Branham WS, Hass BS, Dial SL, Moland CL, Tong W, Shi L, Perkins R, Sheehan DM. 2000. The estrogen receptor relative binding affinities of 188 natural and xenochemicals: Structural diversity of ligands. *Toxicol Sci* 54:138-153.

Bolger R, Wiese TE, Ervin K, Nestich S, Checovich W. 1998. Rapid screening of environmental chemicals for estrogen receptor binding capacity. *Environ Health Perspect* 106:551-557.

Briggs GG. 1981. Theoretical and experimental relationships between soil adsorption, octanol-water partition coefficients, water solubilities, bioconcentration factors, and the parachor. *J Agric Food Chem* 29:1050-1059.

Burnham KP, Anderson DR. 2002. *Model Selection and Multimodel Inference: A Practical Information-theoretic Approach*. Springer-Verlag, New York, NY, USA.

Bradbury SP, Dady JM, Fitzsimmons PN, Voit MM, Hammermeister DE, Erickson RJ. 1993. Toxicokinetics and metabolism of aniline and 4-chloroaniline in medaka (*Oryzias latipes*). *Toxicol Appl Pharm* 118:205-214.

Cantor RS. 2001. Bilayer partition coefficients of alkanols: Predicted effects of varying lipid composition. *J Phys Chem B* 105:7550-7553.

Chaisuksant Y, Yu Q, Connell DW. 1997. Bioconcentration of bromo- and chlorobenzenes by fish (*Gambusia affinis*). *Water Res* 31:61-68.

Chen JY, Penco S, Ostrowski J, Balaguer P, Pons M, Starrett JE, Reczek P, Chambon P, Gronemeyer H. 1995. RAR-specific agonist/antagonist which dissoziate transactivation ans AP1 transrepression inhibit anchorage-independent cell proliferation. *EMBO J* 14:1187-1197.

Chiou CT, Porter PE, Schmedding DW. 1983. Partition equilibria of non-ionic organic compounds between soil organic matter and water. *Environ Sci Technol* 17:227-231.

Clark DE. 1999. Rapid calculation of polar molecular surface area and its application to the prediction of transport phenomena. 1. Prediction of intestinal absorption. *J Pharm Res* 88:807-814.

Colborn T, Dumanoski D, Myers JP. 1996. *Our Stolen Future*, Dutten, NY.

Czuczwa JM, Hites RA. 1984. Environmental fate of combustion-generated polychlorinated dioxins and furans. *Environ Sci Technol* 18:444-450.

Dachs J, Vanry DA, Eisenreich SJ. 1999. Occurrence of estrogenic nonylphenols in the urban and coastal atmosphere of the lower Hudson river estuary. *Environ Sci Technol* 33:2676-2679.

Davies RP, Dobbs AJ. 1984. The prediction of bioconcentration in fish. *Water Res* 18:1253-1262.

De Wit CA. 2002. An overview of brominated flame retardants in the environment. *Chemosphere.* 46:583-624.

De Wolf W, Lieder P. 1998. A novel method to determine uptake and elimination kinetics of volatile chemicals in fish. *Chemosphere* 36:1713-1724.

De Wolf W, Comber M, Douben P, Gimeno S, Holt M, Léonard M, Lillicrap A, Sijm D, van Egmond R, Weisbrod A, Whale G. 2006. Animal use replacement, reduction and refinement: development of an integrated testing strategy for bioconcentration of chemicals in fish. *Integr Environ Assess Manag* (Accepted).

De Wolf W, Yedema ESE, Hermens JLM. 1994. Bioconcentration kinetics of chlorinated anilines in guppy, *Poecilia reticulata*. *Chemosphere* 28:159-167.

De Wolf W, Mast B, Yedema ESE, Seinen W, Hermens JLM. 1994. Kinetics of 4-chloroanilines in guppy, *Poecilia reticulata. Aquatic Toxicol* 28:65-78.

Diamond JM, Katz Y. 1974. Interpretation of nonelectrolyte partition coefficients between dimyristoyl lecithin and water. *J Membr Biol* 17:121-154.

Dulfer WJ, Govers HAJ. 1995. Membrane-water partitioning of polychlorinated biphenyls in small unilamellar vesicles of four saturated phosphatidylcholines. *Environ Sci Technol* 29:2548-2554.

Dulfer WJ, Bakker MW, Govers MAJ. 1995. Micellar solubility and micelle/water partitioning of polychlorinated biphenyls in solution of sodium dodecyl sulfate. *Environ Sci Technol* 29:985-992.

Edwards K, Almgren M. 1992. Surfactant-induced leakage and structural change of lecithin vesicles: effect of surfactnat headgroup size. *Langmuir* 8:824-832.

Ellington JJ, Floyd TL. 1996. *Octanol/water Partition Coefficients for Eight Phthalate Esters*. EPA/600/S-96/006. U.S. Environmental Protection Agency, Athens, GA.

Ensenbach U, Nagel R. 1991. Toxicokinetics of xenobiotics in zebrafish-Comparison between tap and river water. *Comp Biochem Physiol C* 100:49-53.

Erickson RJ, McKim JM. 1990. A model for exchange of organic chemicals at fish gills: flow and diffusion limitations. *Aquat Toxicol* 18:175-198.

Erickson RJ, McKim JM, Lien GJ, Hoffman AD, Batterman SL. 2006a. Uptake and elimination of ionizable organic chemicals at fish gills: I. Model formulation, parameteriation, and behavior. *Environ Toxicol Chem* 25:1512-1521.

Erickson RJ, McKim JM, Lien GJ, Hoffman AD, Batterman SL. 2006b. Uptake and elimination of ionizable organic chemicals at fish gills: II. Observed and predicted effects of pH, alkalinity, and chemical properties. *Environ Toxicol Chem* 25:1522-1532.

Ertl P, Rohde B, Selzer P. 2000. Fast calculation of molecular polar surface area as a sum of fragment-based contributions and its application to the prediction of drug transport properties. *J Med Chem* 43:3714-3717.

Escher BI, Hermens JLM. 2004. Internal exposure: linking bioavailability to effects. *Environ Sci Technol* 38:455A-462A

Escher BI, Hermens JLM. 2002. Modes of action in ecotoxicology: their role in body burdens, species sensitivity, QSARs, and mixture effects. *Environ Sci Technol* 36:4201-4217.

Escher BI, Kwon JH. 2006. *Development of an in-vitro system for modeling bioaccumulation of neutral, ionizable, and metabolically active organic pollutants in fish*. Research proposal accepted by 3R (Reduction, refinement and replacement of animal testing).

Escher BI, Schwarzenbach RP. 1996. Partitioning of substituted phenols in liposome-water, biomembrane-water, and octanol-water systems. *Environ Sci Technol* 30:260-270.

Escher BI, Schwarzenbach RP, Westall JC. 2000. Evaluation of liposome-water partitioning of organic acids and bases. 1. Development of a sorption model. *Environ Sci Technol* 34:3954-3961.

Ewald G, Larsson P. 1994. Partitioning of ^{14}C-labelled 2,2',4,4'-tetrachlorobiphenyl between water and fish lipids. *Environ Toxicol Chem* 13:1577-1580.

Feher M, Sourial E, Schmidt JMA. 2000. simple model for the prediction of blood-brain partitioning. *Int J Pharm* 201:239-247.

Freidig AP, Garicano EA, Busser FJM, Hermens JLM. 1998. Estimating impact of humic acid on bioavailability and bioaccumulation of hydrophobic chemicals in guppies using kinetic solid-phase extraction. *Environ Toxicol Chem* 17:998-1004.

Gaffar MA, Abu El-Fadl A. 1989. Investigation of the pyroelectric and piezoelectric properties of triglycine sulphate single crystals containing organic molecules. *J Phys – Condens Matter* 1:8991-8999.

Gennis RB. *Biomembrane – Molecular Structure and Function*. Springer-Verlag, New York, NY, USA.

Giesy JP, Ludwig J, Tiilitt D. 1994. Deformities in birds of the Great Lakes region. Assigning casualty. *Environ Sci Technol.* 28:128A-135A.

Gobas FAPC, Morrison HA. 2000. Bioconcentration and biomagnification in the aquatic environment, In R. S. Boethling and D. Mackay eds. *Handbook of Property Estimation Methods for Chemicals – Environmental and Health Sciences*, CRC Press, Boca Raton, FL.

Gobas FAPC, Opperhuizen A, Hutzinger O. 1986. Bioconcentration of hydrophobic chemicals in fish: relationship with membrane permeation. *Environ Toxicol Chem* 5:637-646.

Gobas FAPC, Lahittete JM, Garofalo G., Shiu WY, Mackay D. 1988. A novel method for measuring membrane-water partition coefficients of hydrophobic organic chemicals: Comparison with 1-octanol-water partitioning. *J Pharm Sci* 77:265-272.

Golden GA, Rubin RT, Mason RP. 1998. Steroid hormones partition to distinct sites in a model membrane bilayer: Direct demonstration by small-angle X-ray diffraction. *Biochim Biophys Acta* 1368:161-166.

Guha S, Jaffé PR, Peters CA. 1998. Bioavailability of mixture of PAHs partitioned into the micellar phase of nonionic surfactants. *Environ Sci Technol* 32:2317-2324.

Guillette LJJ, Gross TS, Masson GR, Matter JM, Percival HF, Woodward AR. 1994. Developmental abnormalities of the gonad and the abnormal sex hormone concentrations in juvenile alligators from contaminated and control lakes in Florida. *Environ Health Perspect* 102:680-688.

Gupta C. 2000. Reproductive malformation of the male offspring following maternal exposure to estrogenic chemicals. *Proc Soc Exp Biol Med* 224:61-68.

Gutendorf B, Westendorf J. 2001. Comparison of an array of in vitro assays for the assessment of the estrogenic potential of natural and synthetic estrogens, phytoestrogens and xenoestrogens. *Toxicology* 166:79-89.

Gutknecht J, Tosteson DC. 1973. Diffusion of weak acids through lipid bilayer membranes: Effects of chemical reactions in the aqueous unstirred layers. *Science* 182:1258-1261.

Hansch C, Leo A. 1979. *Substituent Constants for Correlation Analysis in Chemistry and Biology*. John Wiley, New York, NY, USA.

Hansch C, Leo A. 1995. *Exploring QSAR – Fundamentals and Applications in Chemistry and Biology*. ACS Professional Reference Book. American Chemical Society, Washington DC.

Hansch C, Leo A, Hoekman D. 1995. *Exploring QSAR – Hydrophobic, Electronic and Steric Constants*. ACS Professional Reference Book. American Chemical Society, Washington DC.

Hanselman TA, Graetz DA, Wilkie AC. 2003. Manure-borne estrogens as potential environmental contaminants: A review. *Environ Sci Technol* 37:5471-5478.

Hawker DW, Connell DW. 1985. Relationships between partition coefficient, uptake rate constant, clearance rate constant and time to equilibrium for bioaccumulation. *Chemosphere* 14:1205-1219.

Hawker DW, Connell DW. 1988. Influence of partition coefficient of lipophilic compounds on bioconcentration kinetics with fish. *Water Res* 22:701-707.

Hayton WL, Barron MG. 1990. Rate-limiting barriers to xenobiotic uptake by the gill. *Environ Toxicol Chem* 9:151-157.

Hazel JR. 1995. Thermal adaptation in biological membranes: is homeoviscous adaptation the explanation?. *Annu Rev Physiol* 57:19-42.

Hemmer MJ, Bowman CJ, Hemmer BL, Friedman SD, Marcovish D, Kroll KJ, Denslow ND. 2002. Vitellogenin mRNA regulation and plasma clearance in male

sheephead minnows, (*Cyprinodon variegates*) after cessation of exposure to 17β-estradiol and *p*-nonylphenol. *Aquat Toxicol* 58:99-112.

Henderson JR, Tocher DR. 1987. The lipid composition and biochemistry of freshwater fish. *Prog Lipid Res* 26:281-347.

Heringa MB, Schreurs RHMM, Busser F, van der Saag P, van der Burg B, Hermens JLM. 2004. Toward more useful in vitro toxicity data with measured free concentrations. *Environ Sci Technol* 38:6263-6270.

Hope MJ, Bally MB, Webb G, Cullis PR. 1985. Production of large unilamellar vesicles by a rapid extrusion procedure. Characterization of size distribution, trapped volume and ability to maintain a membrane potential. *Biochim Biophys Acta* 812:55-65.

Howard PH, Banerjee S, Robrillard KH. 1985. Measurement of water solubilities, octanol water partition-coefficients and vapor pressures of commercial phthalate esters. *Environ Toxicol Chem* 4:653-661.

Huckins JN, Tubergen MW, Manuweera GK. 1990. Semipermeable membrane devices containing model lipid: A new approach to monitoring the bioavailability of lipophillic contaminants and estimating their bioconcentration potential. *Chemosphere* 20:533-552.

Huckins JN, Manuweera GK, Petty JD, Mackay D, Lebo J. 1993. A. Lipid-containing semipermeable membrane device for monitoring organic contaminants in water. *Environ Sci Technol* 27:2489-2496.

Jabusch TW, Swackhamer DL. 2005. Partitioning of polychlorinated biphenyls in octanol/water, triolein/water, and membrane/water systems. *Chemosphere* 60:1270-1278.

Jacobsohn MK, Bauder S, Pine SR, Jacobsohn GM. 1994. Cholesterol limits estrogen uptake by liposomes and erythrocyte membranes. *Biochim Biophys Acta* 1195:131-140.

Jain MK. 1988. *Introduction to Biological Membrane*, John Wiley, New York, NY, USA.

James MO, Tong Z, Rowland-Faux L, Venugopal CS, Kleinow KM. 2001. Intestinal bioavailability and biotransformation of 3-hydroxybenzo(a)pyrene in an isolated perfused preparation from channel catfish, *Ictalurus punctatus*. *Drug Metab Dispos* 29:721-728.

Kalsch W, Urich K. 1991. Uptake, elimination, and bioconcentration of ten anilines in zebrafish (*Brachydanio rerio*). *Chemosphere* 22:351-363.

Kansy M, Senner F, Gubernator K. 1998. Physicochemical high throughput screening: parallel artificial membrane permeation assay in the description of passive absorption processes. *J Med Chem* 41:1007-1010.

Karickhoff SW, Brown DS, Scott TA. 1979. Sorption of hydrophobic pollutants on natural sediments. *Water Res* 13:241-248.

Katz Y, Diamond JM. 1974. Thermodynamic constants for nonelectrolyte partition between dimyristoyl lecithin and water. *J Mem Biol* 17:101-120.

Kawanishi M, Takamura-Enya T, Ermawati R, Shimohara C, Sakamoto M, Matsukawa K, Matsuda T, Murahashi T, Matsui S, Wakabayashi K, Watanabe T, Tashiro Y, Yagi T. 2004. Detection of genistein as an estrogenic contaminant of river water in Osaka. *Environ Sci Technol* 38:6424-6429.

Khim J, Kannan K, Villeneuve DL, Koh C, Giesy JP. 1999. Characterization and distribution of trace organic contaminants in sediment from Masan Bay, Korea. 1. Instrumental analysis. *Environ Sci Technol* 33:4199-4205.

Kim SH, Tamrazi A, Carlson KE, Daniels JR, Lee IY, Katzenellenbogen JA. 2004. Estrogen receptor microarrays: subtype-selective ligand binding. *J Am Chem Soc* 126 :4754-4755.

Kleinow KM, James MO, Tong Z, Venugopalan CS. 1998. Bioavailability and biotransformation of benzo(a)pyrene in an isolated perfused in situ catfish intestinal preparation. *Environ Health Persp* 106:155-166.

Koda T, Soya Y, Negish H, Shiraishi F, Morita M. 2002. Improvement of a sensitive enzym-linked immunosorbent assay for screening estrogen receptor binding activity. *Environ Toxicol Chem* 21:2536-2541.

Koelmans AA, Jiménez CS. 1994. Temperature dependency of chlorobenzene bioaccumulation in phytoplankton. *Chemosphere* 28:2041-2048.

Konstantinou IK, Albanis TA. 2004. Worldwide occurrence and effects of antifouling paint booster biocides in the aquatic environment: a review. *Environ Int* 30:235-248.

Könemann H, van Leeuwen K. 1980. Toxicokinetics in fish: accumulation and elimination of six chlorobenzenes by guppies. *Chemosphere* 9:3-19.

Kuch HM, Ballschmitter K. 2001. Determination of endocrine-disrupting phenolic compounds and estrogens in surface and drinking water by HRGC-(NCI)-MS in the picogram per liter range. *Environ Sci Technol* 35:3001-3006.

Kuiper GGJM, Lemmen JG, Carlsson B, Corton JC, Safe SH, van der Saag PT, ven der Burg B, Gustafsson JÅ. 1998. Interaction of estrogenic chemicals and phytoestrogens with estrogen receptor β. *Endocrinology* 139:4252-4263.

Kuiper GGJM, Carlsson B, Grandien K Enmark E, Häggblad J, Nilsson S, Gustafsson JÅ. 1997. Comparison of the ligand binding specifity and transcript tissue distribution of estrogen receptors α and β. *Endocrinology* 138:863-870.

Kwon JH, Katz LE, Liljestrand HM. 2006a. Use of a parallel artificial membrane system to evaluate passive absorption and elimination in small fish. *Environ Toxicol Chem* (In Press).

Kwon JH, Liljestrand HM, Katz LE. 2006b. Partitioning of moderately hydrophobic endocrine disrupters between water and synthetic membrane vesicles. *Environ Toxicol Chem* (In Press).

Lagerquist C, Beigi F, Karlén A, Lennernäs H, Lundahl P. 2001. Effects of cholesterol and model transmembrane proteins on drug partitioning into lipid bilayers as analysed by immobilized-liposome chromatography. *J Pharm Pharmacol* 53:1477-1487.

Lee Y, Lee DS, Kim SK, Kim YK, Kim DW. 2004. Use of the relative concentration to evaluate a multimedia model for PAHs in the absence of emission estimates. *Environ Sci Technol* 38:1079-1088.

Liu XY, Yang Q, Kamo N, Miyake J. 2001. Effect of liposome type and membrane fluidity on drug-membrane partitioning analyzed by immobilized liposome chromatography. *J Chromatogr A* 913:123-131.

Lutz I, Kloas W. 1999. Amphibians as a model to stuy endocrine disruptors: I. environmental pollution and estrogen receptor binding. *Sci Tot Environ* 225:49-57.

Lye CM, Frid CLJ, Gill ME, Cooper DW, Jones DM. 1999. Estrogenic alkylphenols in fish tissues, sediments, and water from the U.K. Tye and Ties estuaries. *Environ Sci Technol* 33:1009-1014

Mackay D. 1982. Correlation of bioconcentration factors. *Environ Sci Technol* 16:274-278.

Matthews J, Celius T, Halgren R, Zacharewski T. 2000. Differential estrogen receptor binding of estrogenic substances: a species comparison. *J Steroid Biochem Mol Biol* 74:223-234.

McCarty LS, Mackay D. 1993. Enhancing ecotoxicological modeling and assessment. *Environ Sci Technol* 27:1719-1728.

Menuet A, Pellegrini E, Anglade I, Blaise O, Laudet V, Kah O, Pakdel F. Molecular characterization of three estrogen receptor forms in zebrafish: binding characteristics, transactivation properties, and tissue distributions. *Biol Reprod* 66:1881-1892.

Meyer H. 1899. Welcher eigenshaft der anaesthetica bedingt ihre narkotische wirkung?. *Arch Exp Pathol Pharmacol* 42:109–118.

Meylan WM, Howard PH. 1995. Atom fragment contribution method for estimating octanol-water partition coefficients. *J Pharm Sci* 84:83-92.

Miller MM, Wasik SP, Huang GL, Shiu WY, Mackay D. 1985. Relationships between octanol–water partition coefficients and aqueous solubility. *Environ Sci Technol* 19:522–529.

Miyashita M, Shimada T, Miyagawa H, Akamatsu M. 2005. Surface plasmon resonance-based immunoassay for 17β-estradiol and its application to the measurement of estrogen receptor-binding activity. *Anal Bioanal Chem* 381:667-673.

Morohoshi K, Yamamoto H, Kamata R, Shiraishi F, Koda T, Morita M. 2005. Estrogenic activity of 37 components of commercial sunscreen lotions evaluated by in vitro assays. *Toxicol in Vitro* 19:457-469.

Mueller P, Rudin DO, Ti Tien H, Westcott WC. 1962. Reconstitution of cell membrane structures in vitro and its transformation into an excitable system. *Nature* 194:979-980.

Mueller P, Chien TF, Rudy B. 1983. Formation and properties of cell-size lipid bilayer vesicles. *Biophys J* 44:375-381.

Mueller SO. 2002. Overview of in vitro tools to assess the estrogenic and antiestrogenic activity of phytoestrogens. *J Chromatogr B* 777:155-165.

Mu X, LeBlanc G. 2004. Synergistic interaction of endocrine-disrupting chemicals: model development using an ecdysone receptor antagonist and a hormone synthesis inhibitor. *Environ Toxicol Chem* 23:1085-1091.

Muir D, Braune B, de March B, Borstrom R, Wagemann R, Lockhart L, Hargrave B, Bright D, Addison R, Payne J, Reimer K. 1999. Spatial and temporal trends and effects of contaminants in the Canadian Artic marine ecosystem: a review. *Sci Tot Environ* 230:83-144.

Murdoch FE, Meier DA, Furlow JD, Grunwald KAA, Gorski J. 1990. Estrogen receptor binding to a DNA response element in vitro is not dependent upon estradiol. *Biochemistry* 29:8377-8385.

Murk AJ, Boudewijin TJ, Meininger PL, Bosveld ATC, Rossaert G, Ysebaert T, Meire P, Dirksen S. 1996. Effects of polyhalogenated aromatic hydrocarbons and related contaminants on common tern reproduction: Integration of biological, biochemical and chemical data. *Arch Environ Contam Toxicol* 31:128-140.

Nakada N, Nyunoya H, Nakamura M, Hara A, Iguchi T, Takada H. 2004. Identification of estrogenic compounds in wastewater effluent. *Environ Toxicol Chem* 23:2807-2815.

Neely WB. 1979. Estimating rate constants for the uptake and clearance of chemicals by fish. *Environ Sci Technol* 13:1506-1510.

Neely WB, Branson DR, Blau GE. 1974. Partition coefficient to measure bioconcentration potential of organic chemicals in fish. *Environ Sci Technol* 8:1113-1115.

Nesatyy VJ, Ammann AA, Rutishauser BV, Suter MJF. 2006. Effect of cadmium on the interaction of 17β-estradiol with the rainbow trout estrogen receptor. *Environ Sci Technol* 40:1358-1363.

New RRC. 1990. *Liposomes: a practical approach*. Oxford University Press, New York, NY.

Nikov GN, Hopkins NE, Boue S, Alworth WL. 2000. Interactions of dietary estrogens with human estrogen receptors and the effect on estrogen receptor-estrogen response element complex formation. *Environ Health Perspect* 108:867-872.

Nishikawa J, Saito K, Goto J, Dakeyama F, Matsuo M, Nishihara T. 1999. New screening methods for chemicals with hormonal activities using interaction of nuclear hormone receptor with coactivator. *Toxicol Appl Pharm* 154:76-83.

Niu SL, Litman BJ. 2002. Determination of membrane cholesterol partition coefficient using a lipid vesicle-cyclodextrin binary system: Effect of phospholipid acyl chain unsaturation and headgroup composition. *Biophys J* 83:3408-3415.

Nolan M, Jobling S, Brighty G, Sumpter JP, Tyler CR. 2001. A historical description of intersexuality in the roach. *J Fish Biol* 58:160-176.

Organization for Economic Co-Ordination and Development (OECD). 1996. Test guideline 305. Bioaccumulation: Flow-through Fish Test, Guidelines for Testing Chemicals, TG 305.

Ohno K, Fukushima T, Santa T, Waizumi N, Tokuyama H, Maeda M, Imai K. 2002. Estrogen receptor binding assay method for endocrine disruptors using fluorescence polarization. *Anal Chem* 74:4391-4396.

Oliver BG, Niimi AJ. 1985. Bioconcentration factors of some halogenated organics for rainbow trout: limitations in their use for prediction of environmental residues. *Environ Sci Technol* 19:842-849.

Opperhuizen A. 1991. Bioconcentration and biomagnification: Is a distinction necessary?. In R. Nagel and R. Loskill eds. *Bioaccumulation in Aquatic Systems*, VCH Publishers Inc., New York, NY.

Opperhuizen A, Serné P, van der Steen JMD. 1988. Thermodynamics of fish/water and octan-1-ol/water partitioning of some chlorinated benzenes. *Environ Sci Technol* 22:286-292.

Palm K, Stenberg P, Luthman K, Artursson P. 1997. Polar molecular surface properties predict the intestinal absorption of drugs in humans. *Pharm Res* 14:568-571.

Pereira WE, Wade TL, Hostettler FD, Parchaso F. 1999. Accumulation of butyltins in sediments and lipid tissues of the Asian clam, *Potamocorbula amurensis*, near Mare Island Naval Shipyard, San Francisco Bay. *Mar Pollut Bull* 38:1005-1010.

Perrin DD, Dempsey B, Seheabt EP. 1977. *pKa Prediction for Organic Acids and Bases*. Chapman and Hall, London, UK.

Petty JD, Jones SB, Huckins JN, Cranor WL, Parris JT, McTague TB, Boyle TP. 2000. An approach for assessment of water quality using semipermeable membrane devices (SPMDs) and bioindicator tests. *Chemosphere* 41:311-321.

Pons M, Gagne D, Nicolas JC, Mehtali M. 1990. A new cellular model of response to estrogens: a bioluminescent test to characterize (anti)estrogens molecules. *BioTechniques* 9:450-459.

Pramauro E, Minero C, Saini G, Graglia R, Pelizzetti E. 1988. Partition equilibria of phenols between water and anionic micelles. *Anal Chim Acta* 212:171-180.

Randall DJ, Connell DW, Yang R, Wu SS. 1998. Concentrations of persistent lipophilic compounds in fish are determined by exchange across the gills, not through the food chain. *Chemosphere* 37:1263-1270.

Ratcliffe DA. 1967. Decrease in eggshell weight in certain birds of prey. *Nature* 215:208-210.

Reichenberg F, Mayer P. 2006. Two complimentary sides of bioavailability: accessibility and chemicalactivity of organic contaminants in sediments and soils. *Environ Toxicol Chem* 25:1239-1245.

Reid RC, Prausnitz JM, Sherwood TK. 1977. *The Properties of Gases and Liquids*, 3rd ed. McGraw Hill, New York, NY, USA.

Rich RL, Hoth LR, Geoghegan KF, Brown TA, LeMotte PK, Simons SP, Hensley P, Myszka DG. 2002. Kinetic analysis of estrogen receptor/ligand interactions. *Proc Natl Acad Sci USA* 99:8562-8567.

Robertson JC, Hazel JR. 1995. Cholesterol content of trout plasma membranes varies with acclimation temperature. *Am J Physiol* 38:R1113-R1119.

Rodgers-Gray TP, Jobling S, Morris S, Kelly C, Kirby S, Janbakhsh A, Harries JE, Waldock MJ, Sumpter JP, Tyler CR. 2001. Exposure of juvenile roach (Rutilus rutilus) to treated sewage effluent induces doe-dependent and persistent disruption in gonadal duct development. *Environ Sci Technol* 35:462-470.

Rowe ES, Zhang F, Leung TW, Parr JS, Guy PT. 1998. Thermodynamics of membrane partitioning for a series of n-alcohols determined by titration calorimetry: role of hydrophobic effects. *Biochemistry* 37:2430-2440.

Routledge EJ, Sumpter JP. 1996. Estrogenic activity of surfactants and some of their degradation products assessed using a recombinant yeast screen. *Environ Toxicol Chem* 15:241-248.

Routledge EJ, Sheanan D, Desbrow C, Brighty GC, Waldock M, Sumpter JP. 1998. Identification of estrogenic chemicals in STW effluent. 2. In vivo responses in trout and roach. *Environ Sci Technol* 32:1559-1565.

Rudel RA, Melly SJ, Geno PW, Sun G, Brody JG. 1998. Identification of alkylphenols and other estrogenic phenolic compounds in wastewater, septage, and groundwater on Cape Cod, Massachusetts. *Environ Sci Technol* 32:861-869.

Rutishauser BV, Pesonen M, Escher BI, Ackermann GE, Aerni HR, Suter MJF, Eggen RIL. 2004. Comparative analysis of estrogenic activity in sewage treatment plant effluents involving three in vitro assays and chemical analysis of steroids. *Environ Toxicol Chem* 23:857-864.

Saarikoski J, Lindström R, Tyynelä M, Viluksela M. 1986. Factors affecting the absorption of phenolics and carboxylic acids in the guppy (Poecilia reticulata). *Ecotoxicol Environ Safety* 11:158-173.

Sangster, J. 1989. Octanol-water partition coefficients of simple organic compounds. *J Phys Chem Ref Data* 18:1111-1120.

Scheidt HA, Pampel A, Nissler L, Gebhardt R, Huster D. 2004. Investigation of the membrane localization and distribution of flavonoids by high-resolution magic angle spinning NMR spectroscopy. *Biochim Biophys Acta* 1663:97-107.

Schwarzenbach RP, Gschwend PM, Imboden DM. 2003. Environmental Organic Chemistry, second edition, John Wiley & Sons, Inc. New York, NY, USA.

Selby SM. 1969. *CRC Standard Methematical Tables*, 17th edition, The Chemical Rubber Co., Cleveland, OH, USA.

Shao B, Hu JY, Yang M, An W, Tao S. 2005. Nonylphenol and nonylphenol ethoxylates in river water, drinking water, and fish tissues in the area of Chongqing, China. *Arch Environ Contam Toxicol* 48:467-473.

Seelig J, Ganz P. 1993. Nonclassical hydrophobic effect in membrane binding equilibria. Biochemistry 30:9354-9359.

Sijm DTHM, van der Linde A. 1995. Size-dependent bioconcentration kinetics of hydrophobic organic chemicals in fish based on diffusive mass transfer and allometric relationships. *Environ Sci Technol* 29:2769-2777.

Sijm DTHM, Pärt P, Opperhuizen A. 1993. The influence of temperature on the uptake rate constants of hydrophobic compounds determined by the isolated perfused gills of rainbow trout (*Oncorhynchus mykiss*). *Aquat Tox* 25:1-14.

Sijm DTHM, Verberne ME, Pärt P, Opperhuizen A. 1994. Experimentally determined blood and water-flow limitations for uptake of hydrophobic compounds using perfused gills of rainbow trout (*Oncorhynchus Mikiss*) – allometric applications. *Aquat Toxicol* 30:325-341.

Sijm DTHM, Verberne ME, de Jonge WJ, Pärt P, Opperhuizen A. 1995. Allometry in the uptake of hydrophobic chemicals determined in vivo and in isolated perfused gills. *Toxicol Appl Pharm* 131:130-135.

Singer SJ, Nicholson GL. 1972. The fluid mosaic model of the structure of cell membranes. *Science* 175:720-731.

Smejtek P, Blochel A, Wang S. 1996. Hydrophobicity and sorption of chlorophenolates to lipid membranes. *Chemosphere* 33:177-201.

Smith NR, Hansch C, Ames MM. 1975. Selection of reference partitioning system for drug design work. *J Pharm Sci* 64:599-606.

Smith AD, Bharath A, Mallard C, Orr D, McCarty LS, Ozburn GW. 1990. Bioconcentration kinetics of some chlorinated benzenes and chlorinated phenols in American flagfish, Jordanella floridae. *Chemosphere* 20:379-386.

Snyder SA, Keith TL, Verbrugge DA, Snyder EM, Gross TS, Kannan K, Giesy JP. 1999. Analytical methods for detection of selected estrogenic compounds in aqueous mixtures. *Environ Sci Technol* 33:2814-2820.

Soto AM, Sonnenschein C, Chung KL, Fernandez MF, Olea N, Serrano F. 1995. The E-screen assay as a tool to identify estrogens: An update on estrogenic environmental pollutants. *Environ Health Persp* 103(Supp 7):113-122.

Södergren A. 1987. Solvent-filled dialysis membranes simulate uptake of pollutants by aquatic organisms. *Environ Sci Technol* 21:855-859.

Staples CA, Peterson DR, Parkerton TF, Adams WJ. 1997. The environmental fate of phthalate esters: A literature review. *Chemosphere* 35:667-749.

Staurnes M, Rainuzzo JR, Sigholt T, Jørgensen L. 1994. Acclimation of Atlantic cod (Gadus morhua) to cold water: stress response, osmoregulation, gill lipid composition and gill Na-K-ATPase activity. *Comp Biochem Physiol* 109A:413-421.

Steinmetz R, Brown NG, Allen DL, Bigsby RM, Ben-Jonathan N. 1997. The environmental estrogen bisphenol a stimulates prolactin release in vitro and in vivo. *Endocrinology* 138:1780-1786.

Stumm W, Morgan JJ. 1995. Aquatic Chemistry – chemical equilibria and rates in natural waters. John Wiley & Sons, Inc. New York.

Subramanian AN, Tanabe S, Tatsukawa R, Saito S, Myazaki N. 1987. Reductions in the testosterone levels by PCBs and DDE in Dall's porpoises of Northwestern Noth Pacific. *Mar Pollut Bull* 18:643-646.

Sugano K, Nabuchi Y, Machida M, Aso Y. 2003. Prediction of human intestinal permeability using artificial membrane permeability. *Int J Pharm* 257:245-251.

Swackhamer DL, Skoglund RS. 1993. Bioaccumulation of PCBs by algae: kinetics versus equilibrium. *Environ Toxicol Chem* 12:831-838.

Takegami S, Kitamura K, Kitade T, Kawamura K. 2003. Thermodynamics of partitioning of phenothiazine drugs between phosphatidylcholine bilayer vesicles and water studied by second-derivative spectrophotometry. *Chem Pharm Bull* 51:1056-1059.

Tanford CH. 1980. *The Hydrophobic Effect: Formation of Micelles and Biological Membranes*. 2nd ed., John Wiley & Sons, New York, NY, USA.

Thompson M, Krull UJ, Worsfold PJ. 1980. The structure and electrochemical properties of a polymer-supported lipid biosensor. *Anal Chim Acta* 117:133-145.

Thompson M, Lennox RB, McClelland RA. 1982. Structure and electrochemical properties of microfiltration filter-lipid membrane systems. *Anal Chem* 54:76-81.

Tolls J, Sijm DTHM. 1995. A preliminary evaluation of the relationship between bioconcentration and hydrophobicity for surfactants. *Environ Toxicol Chem* 14:1675-1685.

Tremblay L, Kohl SD, Rice JA, Gagné JP. 2005. Effects of temperature, salinity, and dissolved humic substances on the sorption of polycyclic aromatic hydrocarbons to estuarine particles. *Mar Chem* 96:21-34.

U.S. Environmental Protection Agency. 2000. *EPI Suite™*, Ver 3.11. Washington, DC.

U.S. Environmental Protection Agency. 1998. *Endocrine Disrupter Screening and Testing Advisory Committee (EDSTAC) Final Report*.

Usami M, Mitsunaga K, Ohno Y. 2002. Estrogen receptor binding assay of chemicals with surface plasmon resonance biosensor. *J Steroid Biochem Mol Biol* 81:47-55.

Vaes WHJ, Ramos EU, Hamwijk C, van Holsteijn I, Blaauboer BJ, Seinen W, Verhaar HJM, Hermens JLM. 1997. Solid phase microextraction as a tool to determine membrane/water partition coefficients and bioavailable concentrations in in vitro systems. *Chem Res Toxicol* 10:1067-1072.

Vaes WHJ, Ramos EU, Verhaar HJM, Cramer CJ, Hermens JLM. 1998. Understanding and estimating membrane/water partition coefficients: Approaches to derive quantitative structure property relationships. *Chem Res Toxicol* 11:847-854.

Van Eck JMC, Koelmans AA, Deneer JW. 1997. Uptake and elimination of 1,2,4-trichlorobenzene in the guppy (*Poecilia reticulata*) at sublethal and lethal aqueous concentrations. *Chemosphere* 34:2259-2270.

Van Wezel AP, Opperhuizen A. 1995. Thermodynamics of partitioning of a series of chlorobenzenes to fish storage lipids, in comparison to partitioning to phospholipids. *Chemosphere* 31:3605-3615.

Van Wezel AP, Cornelissen G., van Miltenburg JK, Opperhuizen A. 1996. Membrane burdens of chlorinated benzenes lower the main phase transition temperature in dipalmitoyl-phosphatidylcholine vesicles: Implications for toxicity by narcotic chemicals. *Environ Toxicol Chem* 15:203-212.

Vasiluk L, Pinto LJ, Moore MM. 2005. Oral bioavailability of glyphosate: studies using two intestinal cell lines. *Environ Toxicol Chem* 24:153-160.

Veber DF, Johnson SR, Cheng HY, Smith BR, Ward KW, Kopple KD. 2002. Molecular properties that influence the oral bioavailability of drug candidates. *J Med Chem* 45:2615-2623.

Veith GD, Macek KJ, Petrocelli SR, Carroll J. 1980. An evaluation of using partition coefficients and water solubility to estimated bioconcentration factors for organic

chemicals in fish. In *Aquatic Toxicology*, ASTM STP707, J. G. Eaton, P. R. Parrish, and A. C. Hendricks, Eds., American Society for Testing and Materials, pp. 116-129.

Verbruggen EMJ, Vaes WHJ, Parkerton TF, Hermens JLM. 2000. Polyacrylate-coated SPME fibers as a tool to simulate body residues and target concentrations of complex organic mixtures for estimation of baseline toxicity. *Environ Sci Technol* 34:324-331.

Verhaar HJM, de Wolf W, Dyer S, Lefierse KCHM, Seinen W, Hermens JLM. 1999. An LC_{50} vs time model for the aquatic toxicity of reactive and receptor mediated compounds. Consequences for bioconcentration kinetics and risk assessment. *Environ Sci Technol* 33:758-763.

Verhaar HJM, van Leeuwen CJ, Hermens JLM. 1992. Classifying environmental pollutants. 1. Structure activity-relationships for prediction of aquatic toxicity. *Chemosphere* 25:471-491.

Verweij F, Booij K, Satumalay K, van der Molen N, van der Oost R. 2004. Assessment of bioavailable PAH, PCB and OCP concentrations in water, using semipermeable membrane devices (SPMDs), sediments and caged carp. *Chemosphere* 54:1675-1689.

Vom Saal FS, Timms BG, Montano MM, Palanza P, Thayer KA, Nagel SC, Dhar MD, Ganjam VK, Parmigiani S, Welshons WV. 1997. Prostate enlargement in mice due to fetal exposure to low doses of estradiol or diethylstilbestrol and opposite effects at high doses. *Proc Natl Acad Sci USA* 94:2056-2061.

Vrana B, Popp P, Paschke A, Schuurmann G. 2001. Membrane-enclosed sorptive coating. An integrative passive sampler for monitoring organic contaminants in water. *Anal Chem* 73:5191-5200.

Walter A, Gutknecht J. 1986. Permeability of small nonelectrolytes through lipid bilayer membranes. *J Mem Biol* 90:207-217.

Wenk MR, Fahr A, Reszka R, Seelig J. 1996. Paclitaxel partitioning into lipid bilayers. *J Pharm Sci* 85:228-231.

Wimley WC, White SH. 1993. Membrane partitioning: Distinguishing bilayer effects from the hydrophobic effect. *Biochemistry* 32:6307-6312.

Wohnsland F, Faller B. 2001. High-throughput permeability pH profile and high-throughput alkane/water log P with artificial membranes. *J Med Chem* 44:923-930.

Woodrow BN, Dorsey JG. 1997. Thermodynamics of micelle-water partitioning in micellar electrokinetic chromatography: comparisons with 1-octanol-water partitioning and biopartitioning. *Environ Sci Technol* 31:2812-2820.

Yalkowsky SH. 1999. *Solubility and Solubilization in Aqueous Media*. American Chemical Society, Washington DC.

Yalkowsky SH, Dannenfelser RM. 1992. *AQUASOL Database of Aqueous Solubility*, Ver 5. College of Phamacy, University of Arizona, Tucson, AZ, USA.

Yamamoto Y, Liljestrand HM. 2004. Partitioning of selected estrogenic compounds between synthetic membrane vesicles and water: Effects of lipid components. *Environ Sci Technol* 38:1139-1147.

Yang Q, Liu XY, Umetani K, Ikehara T, Miyauchi S, Kamo N, Jin T, Miyake J. 2000. Membrane partitioning and translocation of hydrophobic phosphonium homologues: Thermodynamic analysis by immobilized liposome chromatography. *J Phys Chem B* 104:7528-7534.

Yang R, Brauner C, Thurston V, Neuman J, Randall DJ. 2000. Relationship between toxicant transfer processes and fish oxygen consumption. *Aquat Toxicol* 48:95-108.

Yoshino T, Kato F, Takeyama H, Nakai M, Yakabe Y, Matsunaga T. 2005. Development of a novel method for screening of estrogenic compounds using nano-sized bacterial magnetic particles displaying estrogen receptor. *Anal Chim Acta* 532:105-111.

Zacharewski TR, Meek MD, Clemons JH, Wu ZF, Fielden MR, Matthews JB. 1998. Examination of the in vitro and in vivo estrogenic activities of eight commercial phthalate esters. *Toxicol Sci* 46:282-293.

Zhu C, Jiang L, Chen TM, Hwang KK. 2002. A comparative study of artificial membrane permeability assay for high throughput profiling of drug absorption potential. *Eur J Med Chem* 37:399-407.

Vita

Jung-Hwan Kwon was born in Seoul, Korea on January 2, 1974, the first son of Koo-Won Kwon and Hae-Young Lee. After completing his work at Kang-Seo High School, Seoul, Korea, he entered Seoul National University, Seoul, Korea, in March 1992. He received both Bachelor of Science in Chemistry and Master of Science in Urban Planning from Seoul National University in February 1996 and February 1998, respectively. After mandatory service for Korean Army from January 1998 to March 2000, he worked for Korea Research Institute of Chemical Technology as a research scientist from May 2000 to August 2002. He married Hea-Jin Cho on November 17, 2000. In August 2002, he entered the Graduate School of The University of Texas at Austin. On 24 January 2004, he was admitted to candidacy.

Permanent address: 101-1512, Dongbo 3-Cha APT, Poongdukchun-dong, Suji-gu, Yongin-si, Kyounggi-do, 448-170, Republic of Korea

This dissertation was typed by Jung-Hwan Kwon.